ELSEVIER

Biochimica et Biophysica Acta 1367 (1998) 1–62

BIOCHIMICA ET BIOPHYSICA ACTA

BBA

Review

Chlamydomonas genetics, a tool for the study of bioenergetic pathways

Michael Hippler [1], Kevin Redding [1], Jean-David Rochaix *

Departments of Molecular Biology and Plant Biology, University of Geneva, 30 Quai Ernest Ansermet, 1211 Geneva-4, Switzerland

Received 23 March 1998; revised 3 July 1998; accepted 16 July 1998

Keywords: Photosynthesis; Chloroplast; Bioenergetics; Mutant analysis; Thylakoid complex; (*Chlamydomonas*)

Contents

Abbreviations: ATP, adenosine tri-phoshate; ADP, adenosine di-phosphate; CABP, 2-carboxyarabinitol-1,5-bisphosphate; Chl, chlorophyll; cyt, cytochrome; DAS, decay-associated spectrum; DBMIB, 2,5-dibromo-3-methyl-6-isopropyl-*p*-benzoquinone; DCMU, 3-(3,4-dichlorophenyl)-1,1-dimethylurea; DNP-INT, dinitrophenylether of iodonitrothymol; DPC, diphenyl carbazide; DPCIP, dichlorophenol indophenol; EDC, *N*-ethyl-3-(3-diaminopropyl)carbodiimide; E_m, redox midpoint potential; ENDOR, electron nuclear double resonance; EPR, electron paramagnetic resonance; ESEEM, electron spin echo envelope modulation; FNR, ferredoxin:$NADP^+$ reductase; FTIR, Fourier transform infrared difference spectrum; LHC, light-harvesting complex; OEC, oxygen evolving complex; NAD, nicotinamide dinucleotide; NQNO, 2-*n*-4-hydroxyquinoline-*N*-oxide; 3-PGA, 3-phosphoglycerate; P_{700}, primary electron donor in PSI; P_{680}, primary electron donor in PSII; PSI, photosystem I; PSII, photosystem II; PQ, plastoquinone; RC, reaction center; SDS-PAGE, sodium dodecyl sulfate-polyacrylamide gel; SHAM, salicylhydroxamic acid; SQ, semiquinone; TMD, transmembrane domain; Tnt, Tentoxin; UHDBT, undecylhydoxydioxobenzothiozol

* Corresponding author. Fax: +41 (22) 702-6868; E-mail: jean-david.rochaix@molbio.unige.ch

[1] Both authors contributed equally to this review.

PII: S0005-2728(98)00136-4

1. Introduction

The genetic analysis of chloroplast function of the green unicellular alga *Chlamydomonas reinhardtii* started over 40 years ago when Sager discovered that, during crosses, certain traits were transmitted uniparentally from the mating-type (+), but not from the mating-type (−) parent to the progeny [1]. She also found that in rare cases the 'uniparental' traits of both parents could be inherited and that they could recombine with each other, a property which was used for constructing a genetic map of these markers [2]. Later, they were shown to be encoded by the chloroplast genome [3,4]. Levine was the first to recognize the potential of *C. reinhardtii* for a genetic dissection of photosynthesis [5]. Together with

his coworkers he isolated numerous mutants deficient in photosynthetic activity and found that most mutations were located within the nuclear genome [6]. Some of these mutants are still being studied today. This analysis provided genetic support for the linear Z-scheme of photosynthesis and led to the identification of new components of the photosynthetic electron transfer chain, such as the Rieske protein of the cytochrome b_6f complex [7].

In recent years, the powerful techniques of molecular genetics and the establishment of methods for nuclear [8–10] and chloroplast transformation [11] in *C. reinhardtii* have greatly increased the potential of this system for analyzing bioenergetic processes. Studies with *C. reinhardtii* have led to significant advances in our understanding of the assembly of photosynthetic complexes and of the structure–function relationship of their components. Here we review the progress achieved in these areas during recent years. Several earlier reviews have appeared on some of these topics [12–15].

2. Basic features of *Chlamydomonas*

2.1. Growth properties

An important feature of *C. reinhardtii* is that photosynthetic function is dispensable provided a carbon source such as acetate is added to the growth medium. The cells can therefore be grown under three different regimes: on acetate medium with light (mixotrophic growth), on acetate medium without light (heterotrophic growth) and with CO_2 as unique carbon source in the light (phototrophic growth). These growth properties allow one to screen for acetate-requiring mutants, many of which are affected in photosynthetic activity.

2.2. Isolation of photosynthetic mutants and genetic analysis

C. reinhardtii is a heterothallic alga. Cells of both mating-types (+) and (−) can be grown vegetatively. When vegetative cells are starved for nitrogen, they differentiate into gametes. Gametes of opposite mating-type fuse to form zygotes which undergo meiosis and ultimately produce a tetrad of four haploid progeny cells. It is also possible to produce stable vegetative diploids which are useful for establishing whether a mutation is dominant or recessive (for details see [16]).

As land plants, *C. reinhardtii* contains three distinct genetic systems located in the nucleus, chloroplast and mitochondria. Mutations in each of these genomes can be distinguished because they are transmitted in different ways to the offspring. Nuclear genes follow a typical Mendelian 2:2 segregation whereas chloroplast or mitochondrial mutations are predominantly inherited from the mating-type (+) or (−) parent, respectively (see [16]). Biparental zygotes are produced occasionally in which the chloroplast genomes of both parents are transmitted to the progeny. In this case, recombination between chloroplast markers is observed and has been used to construct a chloroplast genetic map (see [16]). Numerous nuclear and chloroplast photosynthetic mutants have been isolated, using as screens acetate requirement for growth or fluorescence analysis. This non-invasive method is based on the observation that mutants deficient in photosynthetic activity display altered fluorescence properties [17]. Thus, both high and low fluorescence mutants have been isolated. It is also possible to measure fluorescence transients on live cells which allows one to distinguish between PSII, PSI and cytochrome b_6f-deficient mutants. The recently developed fluorescence video imaging systems [18] have been particularly helpful for large scale screens of photosynthetic mutants [19].

2.3. Chloroplast biolistic transformation of *C. reinhardtii*

The pioneering work of Boynton et al. in 1988 [11], which established a method for chloroplast transformation, opened the door for extensive chloroplast gene manipulation. In this technique, tungsten particles are coated with DNA and bombarded onto cells with a particle gun. Once introduced into the chloroplast compartment, the transforming DNA is integrated into the chloroplast genome through homologous recombination. In principle, any chloroplast gene coding for an essential photosynthetic function can be used as selectable transformation marker, provided the host strain is deficient in the corresponding gene. Only few non-photosynthetic se-

lectable markers are available for plastid transformation in *C. reinhardtii*. They include alleles of the chloroplast ribosomal RNA genes conferring resistance to various antibiotics specific for 70S-type ribosomes [20]. However, the most useful selectable marker is the bacterial gene *aadA*, which encodes aminoglycoside adenyltransferase and confers resistance to spectinomycin and streptomycin when inserted into the chloroplast genome and fused to suitable chloroplast expression signals, such as a promoter and 5′ untranslated region [21]. The *aadA* gene has been used both as a selectable marker for gene disruption and for site-directed mutagenesis of several chloroplast genes (see [22]), and as reporter gene [23–25]. The glucuronidase gene has also been used successfully as a reporter gene [26].

Since the chloroplast genome is polyploid and is present in ca. 80 copies per cell, several subcloning steps are usually required after transformation until all copies contain the transforming DNA. This state is referred to as 'homoplasmic'. While homoplasmic disruptions of genes involved in photosynthesis can be achieved readily, this is not possible for plastid genes that are essential for cell survival. These essential genes include all those of the chloroplast gene expression system and some additional open reading frames whose function is not yet known.

Chloroplast DNA manipulations often involve at least two or more consecutive transformation events which could be performed readily if several independent selectable markers were available. However, attempts to develop other markers besides *aadA* have failed. As an alternative, two methods have been established for reusing the *aadA* marker [27]. In the first, the *aadA* expression cassette is flanked by two small repeats and introduced at a specific site into the chloroplast genome by transformation. Once the mutation is homoplasmic, the transformants are transferred to growth media lacking antibiotic. Under these conditions, recombination between the repeats leads to excision of the aadA casssette which can now be used for a second round of transformation. In the second strategy, cotransformation with a mutated chloroplast DNA fragment and a plasmid containing an essential chloroplast gene disrupted with the *aadA* cassette is performed. Once homoplasmicity of the mutation has occurred, the transformants are transferred to drug-free medium. Under these conditions, the *aadA* cassette is rapidly lost at the expense of the wild-type gene which is essential for cell survival.

2.4. Nuclear transformation

Nuclear transformation can be achieved readily in *C. reinhardtii* using as host nuclear mutants deficient in argininosuccinate lyase, nitrate reductase or PSII activity and the corresponding wild-type genes as transforming DNA [8–10]. The *CRY1* gene encoding ribosomal protein S14 isolated from a mutant strain of *C. reinhardtii* resistant to the eukaryotic translational inhibitors cryptopleurine and emetine can also be used as a dominant selectable marker in any *C. reinhardtii* strain [28]. Recently, a chimeric gene consisting of the coding sequence of the *ble* gene, conferring phleomycin-resistance, from *Streptoalloteichus hindustanus* was fused to the 5′ and 3′ untranslated regions of the nuclear *rbcS*2 gene and used successfully as another dominant selectable marker in *C. reinhardtii* [29]. The DNA can be introduced very efficiently by vortexing shortly cells and DNA in the presence of glass beads, provided a cell wall-deficient strain is used [30]. Another promising nuclear selectable transformation marker for *C. reinhardtii* is the aphVIII gene from *Streptomyces rimosus* which encodes aminoglycoside 3′-phosphotransferase and confers resistance to paromomycin [31].

During nuclear transformation in *C. reinhardtii*, the transforming DNA appears to integrate in most cases randomly into the nuclear genome. It has therefore been possible to use nuclear transformation as a tool for insertion mutagenesis in which the transformation vector functions as a tag [32]. This tag can be used to isolate the disrupted gene.

Attempts to perform targeted disruptions of nuclear genes of *C. reinhardtii* have met with limited success because of the low rate of homologous recombination and of the occurrence of frequent DNA rearrangements during integration of the transforming DNA into the nuclear genome. Nevertheless, targeted disruption of the NIT8 gene, involved in nitrate and nitrite assimilation, has been achieved [33]. Deletion of the *psaF* gene encoding the plastocyanin-docking protein of PSI was achieved by cotransforming an arginine-requiring strain with the *ARG* vector

and a plasmid in which the *psaF* gene was inactivated by three small deletions. Screening of the arginine prototrophic transformants for a PSI deficiency by fluorescence video imaging yielded one mutant in which the *psaF* gene and its surrounding region had been deleted [34]. It is not clear whether this event was mediated through homologous recombination. However, it shows that any nuclear gene which is important for photosynthetic activity can, in principle, be inactivated using similar approaches.

Because of the high rate of nuclear transformation, it has been possible to rescue nuclear mutants with cosmid libraries of *C. reinhardtii* [35,36]. As many interesting nuclear mutants affected in bioenergetic processes have been isolated in *C. reinhardtii*, this technology will prove very useful in the near future.

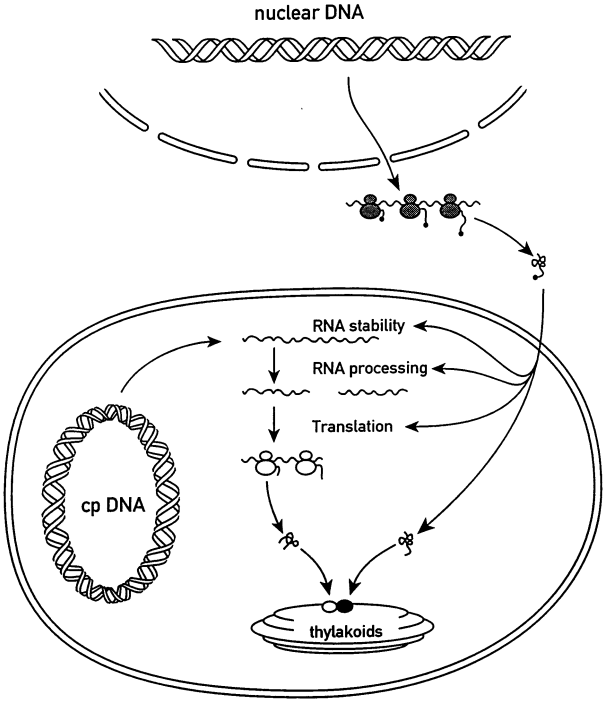

Fig. 1. Biosynthesis of the photosynthetic apparatus. The nucleus and chloroplast are shown in the upper and lower parts, respectively. Cytosolic 80S ribosomes and chloroplastic 70S ribosomes are represented by shaded and open double-ovals, respectively. The flow of genetic information from the nuclear and chloroplast genomes is symbolized with arrows, with the roles of nuclear-encoded factors in different steps of this process indicated.

3. Biosynthesis of the photosynthetic apparatus

It is now well established that the major photosynthetic complexes in algae and plants contain subunits, some of which are encoded by the chloroplast genome and translated on plastid 70S ribosomes. The other subunits are nuclear-encoded, translated as precursor proteins on 80S ribosomes and specifically imported into the plastids where they assemble with their chloroplast-encoded partners into functional complexes (Fig. 1). Analysis of numerous photosynthetic mutants has revealed that most of the mutations in *C. reinhardtii* affect chloroplast post-transcriptional steps (reviewed in [13–15]). Thus, mutants affected in chloroplast mRNA stability, in RNA processing, in RNA splicing and in translation have been identified. One surprising feature of this analysis in *C. reinhardtii* is that in most cases each of these mutations interferes with the expression of a single chloroplast gene. As an example, nuclear mutations affecting uniquely the stability or the translation of the *psbD* mRNA have been found [24,37]. Another remarkable feature is that for each post-transcriptional step in the synthesis of a given chloroplast-encoded component, several nuclear loci may be involved. An extreme example is the maturation of the *psaA* mRNA encoding one of the reaction center polypeptides of PSI which requires more than 14 nuclear loci [38]. The reason for this multiplicity of nuclear encoded factors involved in plastid post-transcriptional events may be due to specific requirements for the correct timing of the synthesis of the photosynthetic components or for their targeting to the thylakoid membrane.

4. Photosystem II

Photosystem II (PSII) uses the energy from photons of visible light to drive the oxidation of water and the reduction of plastoquinone. The core of PSII is known to be composed of a heterodimer of the related D1 and D2 proteins (they share 25% identity [39]; see Fig. 2A), each of which is predicted to contain 5 transmembrane α-helices (see Fig. 2B). This topological arrangement received experimental confirmation using the reaction of epitope-specific antibodies and proteases against thylakoid membranes

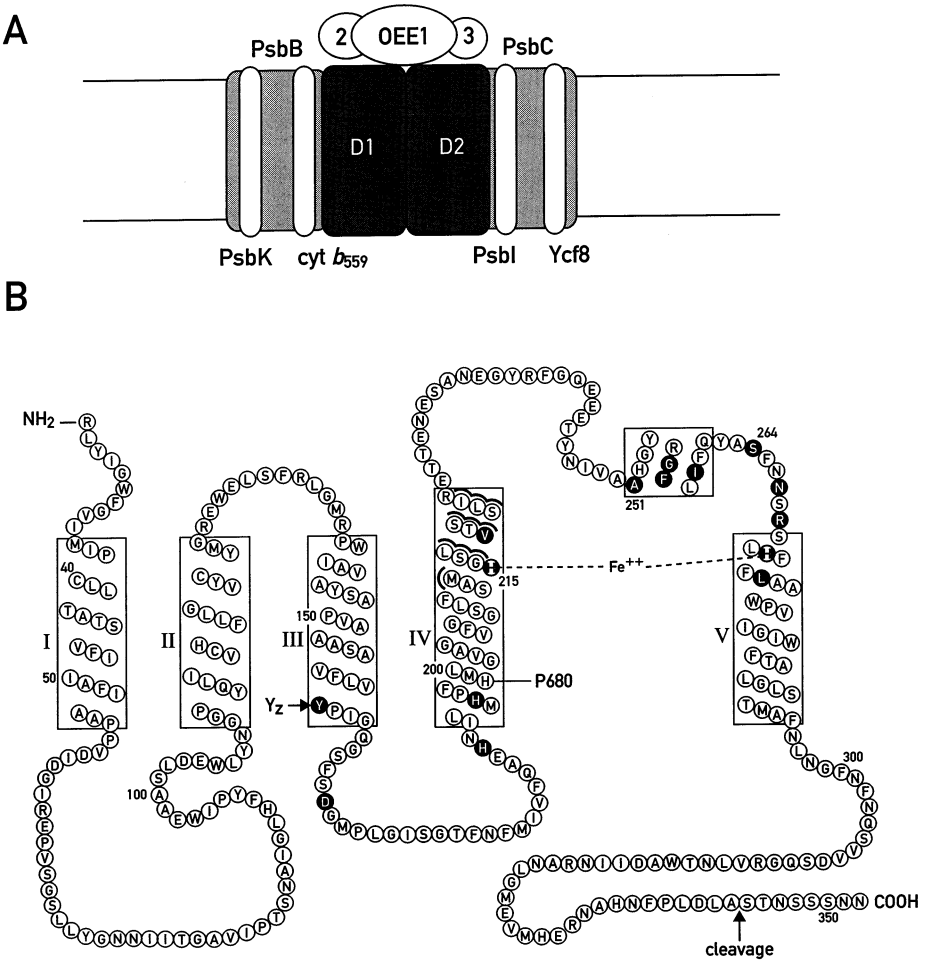

Fig. 2. (A) Schematic model of PSII. The D1 and D2 subunits form the core of PSII and bind all redox-active cofactors. The PsbB ('P5' or 'CP47') and PsbC ('P6' or 'CP43') subunits bind Chl *a* making up the core antenna. Cyt b_{559} is made up of two small, transmembrane subunits (α and β) that together bind two hemes. Also associated with PSII are various small subunits discussed in the text: PsbI, PsbK, and Ycf8 (note: not all small PSII subunits are included in this figure). On the lumenal side of the membrane are the extrinsic proteins required for maximal oxygen evolution: OEE1, OEE2, and OEE3. (B) Topological model of D1 from *C. reinhardtii*. Transmembrane α-helices are indicated as boxes and numbered I–V. The site of cleavage of the C-terminal extension is indicated. Residues that have been mutated in *C. reinhardtii* are indicated as blackened circles. Also shown are residues thought to be intimately associated with cofactors: Tyr^{161} serving as Y_Z, His^{198} serving as the axial ligand to one of the P_{680} chlorophylls, and the histidines (His^{215} and His^{272}) ligating the non-heme iron on the acceptor side.

of different topologies [40]. The D1 and D2 proteins were first identified by Chua and Bennoun [41] as 'diffuse bands 1 and 2' on an SDS polyacryalmide gel of ^{14}C-labeled thylakoid proteins. Although it had been proposed that D1 bound the secondary acceptor, Q_B [42], its role in primary charge separation was unclear until the isolation of a 'core PSII' complex from spinach [43]. This complex is able to perform primary charge separation between the primary donor, P_{680}, and the primary acceptor, Pheo, although it contains only D1, D2, and cyt b_{559}. Previous biochemical work with PSII from *C. reinhardtii* had implicated the CP47 protein as the site of primary charge separation [44]. The currently accepted model is that the D1 and D2 proteins bind the special pair of chlorophylls that are the primary donor, P_{680}, along with the primary acceptor, Pheo (a pheophytin *a*), secondary acceptor, Q_A (a plastoquinone) and the ultimate acceptor, Q_B (a plastoquinone). The heterodimer model is based upon the relatedness of

PSII to the purple bacterial reaction center (PbRC), whose structure has been solved [45,46]. As in the PbRC, charge separation followed by rapid transfer to the secondary acceptor results in the P_{680}^{+} Q_A^{-} state. This is followed by a slower transfer to Q_B. A subsequent charge separation and transfer with concomitant uptake of two protons results in the conversion of the Q_B quinone to quinol. This can then exchange with a plastoquinone to reset the acceptor side. An obvious difference between the PbRC and PSII is that the latter uses water, instead of a cytochrome, as its source of electrons. This stems from the fact that PSII is utilized in green plants to drive a linear electron transport chain involving the cyt b_6/f complex and PSI (see Section 5), while the PbRC is used to drive a cyclic electron transport pathway that allows the storage of energy by the creation of a transmembrane proton gradient. PSII has the addition of an oxygen evolving complex (OEC) that accomplishes the oxidation of water by means of a poorly understood process involving a cluster of four manganese atoms at the donor side. The Mn-cluster is protected by additional proteins at the lumenal side that have no counterpart in any other photosynthetic RC. A tyrosine residue (PsbA-Tyr^{161} in *Chlamydomonas*), known as Y_Z, serves as an intermediate between P_{680} and the OEC [47,48]. It is oxidized by P_{680}^{+} and then rereduced by the Mn-cluster, which stores the positive charges. The analogous tyrosine on D2 (Tyr^{160}), known as Y_D, is reduced very inefficiently by the Mn-cluster and is thus easily visualized by EPR as a long-lived radical in the dark. The four charge-storage states of the Mn-cluster are known as S0 (no charges stored), S1, S2, S3, and S4. After accumulation of four positive charges, the S4 state very rapidly decays to the S0 state with the concomitant release of one molecule of O_2. Thus, four charge separations are required for oxidation of two molecules of water, release of one molecule of dioxygen (and four protons in the lumenal space), and conversion of two molecules of plastoquinone to plastoquinol (with uptake of four protons from the stromal space).

4.1. Purification of the PSII complex

Diner and Wollman [49] were the first to report biochemical purification of PSII from *Chlamydomonas*. This preparation was unable, however, to evolve oxygen. Later, de Vitry et al. [50] improved upon this protocol by adding an ion-exchange step. They obtained a 440–510-kDa homogeneous particle, which should be a monomer (they estimated a contribution of 274 kDa from proteins, and the rest from lipids, detergent, and water). These PSII particles contained D1, D2, CP47, and CP43 in 1:1:1:1 stoichiometry. By N-terminal amino acid sequencing, they were also able to identify PsbE (cyt b_{559} a subunit), PsbM, PsbK, and a 6.1-kDa polypeptide. In addition, they observed two forms of phosphorylated PsbH. While unable to evolve O_2, the PSII particles did have significant $Y_Z \rightarrow Q_A$ activity, similar to such preparations from cyanobacteria and spinach.

Later, Bumann and Oesterhelt [51] purified PSII particles from *C. reinhardtiis* using the detergent dodecyl maltoside and anion exchange chromatography. They obtained a 230-kDa monodisperse particle with stoichiometry of 1 D1: 1 D2: 1 CP47: 1 CP43: 1 cyt b_{559}: 2 Pheo *a*: 40 ± 4 Chl. No LHC was detected, consistent with the high Chl *a*/*b* ratio (>12). These PSII particles exhibited high O_2 evolution rates. However, a higher activity using ferricyanide as an electron acceptor as compared with an artificial quinone (DCBQ), as well as only partial inhibition by DCMU, indicates some alteration of the Q_B site, as has been observed with other highly purified PSII preparations (e.g. K_m(DCBQ) = 84 ± 20 μM at pH 6.0, as compared to 92 ± 9 for spinach). All of these characteristics compare favorably with preparations from spinach, allowing one to do biochemical analysis of PSII in an organism tractable to genetic and molecular analysis.

Sugiura et al. [52] have recently taken advantage of the molecular biology to simplify purification of PSII from *Chlamydomonas*. After attaching a 'His-tag' (i.e. six consecutive histidine residues) to the C-terminus of D2, they found that they could purify PSII complexes in one step by passing detergent-solubilized thylakoid membranes over a Ni^{2+} affinity column. Elution with imidazole gave a very pure (Chl *a*/*b* ratio >14) and active (1030 μmol O_2 mg Chl^{-1} h^{-1}) preparation of PSII that appeared to contain all subunits. The short preparation time (4 h) of this procedure should help to advance the analysis of PSII.

4.2. Biophysical analysis of photosystem II

Rigby et al. [53] examined the dark-stable $Y_D^{+\bullet}$ radical in PSII isolated from spinach, *C. reinhardtii*, and a cyanobacterium (*Phormidium laminosum*) by electron-nuclear double resonance (ENDOR) spectroscopy. They were able to resolve eight hyperfine couplings, which they assigned to the tyrosine radical. The hyperfine couplings attributed to the tyrosine ring protons appear identical in all three species, but those arising from the β-proton differ noticeably. $Y_D^{+\bullet}$ from *C. reinhardtii* PSII exhibits larger couplings than that from spinach, resulting in a broader EPR spectrum (0.6 G), while Phormidium PSII has smaller couplings, resulting in a narrower EPR spectrum (0.8 G). This was interpreted in terms of a species-to-species variation in the orientation of the aromatic ring with relation to the β-methylene group.

4.3. Analysis of mutants deficient in photosystem II activity

4.3.1. Acceptor side

The first mutants obtained in PSII were those that rendered the complex resistant to various herbicides, such as DCMU or atrazine, which act by binding the Q_B site and blocking access to plastoquinone. The analysis of mutants affected in the acceptor side of PSII has thus been dominated by this class of mutants (all mutants discussed herein are mapped onto the topological representation in Fig. 2B). Erickson et al. [54,55] examined a set of six herbicide-resistant mutants of *Chlamydomonas*. They found that all of the mutations mapped to the *psbA* gene, which encodes the D1 protein. In fact, all of the changes giving rise to herbicide-resistance were located either in a small area of the loop between helices 4 and 5 or on the stromal side of these helices. Three of the six mutations mapped to a region predicted to be an extramembrane helix, in which one of the sites would be analogous to Trp^{250} (Phe^{255}) and the other to Ala^{258} (Ser^{264}) of the PbRC M subunit, both of which are involved in binding Q_A. Thus, by analogy, they would be predicted to be involved in binding Q_B in PSII. The mutations G256D and S264A resulted in the highest general resistance and much reduced $Q_A \rightarrow Q_B$ kinetics, while the others show only modest (2-fold at most) decreases in electron transfer.

Trebst and colleagues [56] examined the resistance of five different herbicide-resistant *C. reinhardtii* mutants (PsbA-V219I, A251V, F255Y, S264A, L275F) against a systematic battery of herbicides. They observed interesting trends with different mutants, and different herbicides. PsabA-F255Y is resistant to a very narrow range of inhibitors: only atrazine (and derivatives) and cyanoacrylate. Interestingly, the mutations in the fourth loop are cyanoacrylate resistant, but the ones in the helices (V219I and L275F) are not. Ioxynil displays a gradient in resistance from V219I (the highest) to L275F (supersensitive). None were resistant to the quinoline type inhibitors or to ketonitriles. Interestingly, while PsbA-S264A exhibits impressive resistance to urea and triazine derivatives, the corresponding mutation has little effect in land plants [57,58]. Przbilla et al. [59] made use of biolistic transformation to introduce double (S264A/N266T) and triple (I259S/S264A/N266T) mutants by virtue of S264A-mediated herbicide-resistance. While the N266T decreased resistance to atrazine and urea derivatives, it increases resistance to cyanoacrylate and phenmedipham; this is in contrast to the PsbA-N266T mutation in *Synechocystis* 6714, which resulted in increased resistance to metribuzin and ioxynil.

A more exhaustive analysis of residue Ala^{251} of the D1 subunit has been performed recently by Lardans et. al. [60,61]. While conversion of this residue to Gly, Cys, Ser, Val, Ile, Leu, or Pro allow PSII activity to some degree, mutation to Arg, Asp, Glu, Gln, or His do not. These latter were analyzed in more detail, and it was found that, although they accumulate various amounts of D1 polypeptide (15–75% the wild-type steady-state level), they are all incapable of oxygen evolution. Subsequent analysis by flash fluorometry indicated that electron transport between Q_A and Q_B is blocked in these mutants [60]. In fact, given the extremely high dissociation constant at Q_B measured in these mutants, it is likely that they do not normally have a quinone in the Q_B site [60]. Interestingly, some of these mutants exhibit novel forms of D1-related polypeptide. The PsbA-A251D,E,H,Q substitution mutants synthesize various amounts of a 33–34-kDa and a 24–25-kDa polypeptide (D1 is normally 32 kDa). That the 33–34-kDa form is not due to lack of C-terminal processing (see below) is evidenced by deletion of the C-terminal

extension in the context of the A251D mutation; the apparent molecular weight (33–34-kDa) is unchanged, indicating that processing occurs normally in the PsbA-A251D mutant. Although it cannot be excluded that the slower migration is due to phosphorylation of the mutant D1 polypeptides, it is striking that the 33–34-kDa forms of PsbA-A251H and PsbA-A251Q are approximately as stable as wild-type, while those of the PsbA-A251E and PsbA-A251D mutants are noticeably less stable. The 24–25-kDa form is unstable in all four mutants. Based on its size and its recognition by antibodies raised against N-terminal regions of D1, one can predict its C-terminus would be between residues 258–269 (i.e. near the end of loop 4, shortly after the mutation site). When solubilized with 1% lithium dodecyl sulfate, the 24–25-kDa form migrates at the position of the mature D1 (i.e. 32 kDa); 2% lithium dodecyl sulfate is required for adequate visualization of the 24–25-kDa form and, presumably, for disruption of its association with a 8–9-kDa polypeptide. Lardans et al. [61] concluded that this short form is not a degradation product of the 33–34-kDa form, as both forms are synthesized simultaneously and there is no observable chase of the longer to the shorter form, and instead proposed that the nascent D1 polypeptide is cleaved during translational pausing in loop 4 [62] and remains associated with a small polypeptide involved in PSII assembly. However, it seems equally likely that such a proteolytic cleavage could occur without necessarily disrupting further translation, and that the two parts of D1, although not covalently linked, could associate via hydrophobic interactions between transmembrane helices 3, 4, and 5 (note that helix 5 should be located between helices 3 and 4, based on analogy with the PbRC). Thus, it might be the loss of quinone at the Q_B site that makes this region of loop 4 more accessible to proteolytic attack. The 24–25-kDa polypeptide was not seen in the A251 substitution mutants that had Q_B quinone [60].

Lardans et al. [60] subsequently analyzed the phototrophic PsbA-Ala^{251} substitution mutants in more detail. The substitution of Ala^{251} with Cys has the smallest effect, and this mutant is completely photoautotrophic. Substitution with Gly, Pro, and to a lesser extent Ser, has the effect of somewhat slowing electron transfer between Q_A and Q_B as well as decreasing the efficiency of primary photochemical charge separation, but these mutants exhibit no significant defects in photosynthetic growth. Substitution with Ile, Leu, and to a lesser extent Val, more severely impairs Q_A to Q_B electron transfer, but these mutations do not affect primary charge separation. However, these mutants are noticeably impaired in photoautotrophic growth. As mentioned above, the PsbA-A251V mutant is herbicide-resistant. The PsbA-A251I mutant appears virtually identical to the PsbA-A251V mutant, while the PsbA-A251L mutation results in greater herbicide resistance and lower photosynthetic competence. These workers noticed a correlation between the bulkiness of the side chain at position 251 and the calculated plastoquinone dissociation constant at Q_B: the larger the volume of the side chain, the lower the occupancy of Q_B. This explains, perhaps, why occupation of this position with Gly, Ala, Ser, Cys, or Pro allows normal photoautotrophic growth, while Asp, Glu, Gln, His or Arg do not (reversion analysis of Arg, Gln, and His substitution mutants additionally indicates that substitution with Asn, Tyr, or Lys would also prohibit phototrophic growth [60]); conversion of Ala^{251} to Val, Ile, or Leu results in intermediate effects. It seems likely, however, that volume is not the only important variable, and that the chemical nature of the side chains also plays a role.

The non-heme iron (Fe^{2+}) of PSII is located between the quinone sites Q_A and Q_B. The bacterial RC2 has an analogous non-heme Fe in the same position [45,46], and the four histidines used to ligate it are conserved in D1 and D2 (Fig. 2B). However, the glutamate residue that serves as the fifth ligand in the bacterial RC2 is not conserved in PSII, where this role is thought to be performed by a bicarbonate ion (reviewed in [63]). This hypothesis would explain the effect of bicarbonate, and of its replacement by formate, upon kinetics of electron transfer from Q_A^- to Q_B/Q_B^-. Based on analogy with the *Rb. sphaeroides* RC structure, Hutchison et al. [64] hypothesized that Arg^{269} of D1 might be involved in binding the bicarbonate, and tested this idea by mutating it to Gly. The PsbA-R269G mutant is significantly perturbed in its function. Although the mutant complex is capable of accumulating to 60–80% the wild-type level, it does not have an associated tetramanganese complex, nor is it able to donate electrons to an artificial

acceptor (dichlorophenol indophenol (DPCIP)) in the presence of artificial donors that bypass the OEC (diphenyl carbazide (DPC) and hydroxylamine). It appears that approximately 30–50% of the mutant reaction centers are capable of charge separation, as the oxidized Y_D and reduced Q_A^- Fe^{2+} (formate-enhanced) EPR signals can be observed, albeit to a lower extent. As the *g*-values of both signals are unchanged, it is unlikely that the mutation causes large perturbations of the environments of either cofactor. Moreover, as formate still has an effect on Q_A^- to Q_B/Q_B^- electron transfer in the mutant, it would seem that PsbA-Arg^{269} is not required for binding bicarbonate [64]. However, loss of this large side chain has significant effects on both the acceptor and donor sides, indicating that structural changes can be transmitted from one side to the other.

4.3.2. Donor side

Most of the mutations made in the donor side affect either Y_Z or the oxygen evolving complex or both. Roffey et al. [65–67] constructed and characterized the PsbA-H190Y and PsbA-H190F mutants in *C. reinhardtii*. They saw a modest decrease of O_2 evolution in PsbA-H190Y, but no difference in P_{680}/Chl ratios. Fluorescence measurements suggest a reduction in the rate of electron transfer between Y_Z and Q_A. The PsbA-H190F mutant seems to lose the Mn-cluster, yet accumulates PSII to a level of 90%. This conclusion is supported by the lack of O_2 evolution, a 5-fold drop in the Mn/Chl ratio in washed PSII membranes, the observation of electron donation by DPC even before hydroxylamine treatment (DPC can bypass the OEC after it is removed), and the lack of 4-state cycling. These observations were rationalized by an EPR analysis [67]. The lineshapes of flash-induced $Y_Z^{+\bullet}$ and $Y_D^{+\bullet}$ are essentially unchanged in the PsbA-H190F,Y mutants. However, the yields of the $Y^{+\bullet}$ radicals are reduced by 85–90% in both mutants. It is surprising that these mutants can accumulate such high amounts of the PSII reaction center in the absence of the Mn-cluster; contrast this to the FuD44 mutant, where the complex does not accumulate in the absence of OEE33 (see below). Electron transfer is possible from Y_Z to Q_A in PSII from the mutants, and with DPC to reduce Y_Z, the maximum rate was 50% of wild-type using hydroxylamine-washed thylakoids (i.e. without the OEC). The low yield of $Y_D^{+\bullet}$ can be explained by the absence of the Mn-cluster (Y_D is usually oxidized by the S2 and S3 states). The low yield of $Y_Z^{+\bullet}$ could be due to a slower transfer from Y_Z to P_{680}^+. The high DPC→DCIP rate can be explained either by DPC pushing the equilibrium to the right by efficiently reducing Y_Z^+ or by direct reduction of P_{680}^+ by DPC. Because the EPR spectrum of Y_Z is unchanged by the mutations, it is unlikely that D1-His^{190} contributes significantly to the environment of Y_Z. This is in stark contrast to the results with the corresponding histidine of D2 in *Synechocystis* PCC6803, mutation of which cause significant changes in the Y_D spectrum [68,69]. Both of these observations are consistent with the structural model of PSII based principally on the PbRC structure [70], in which D2-H190 should be closer to Y_D than D1-H190 is to Y_Z. The fact that Tang et al. [71] saw a disappearance of the 5-MHz ESEEM modulation in the S2 multiline signal of *Synechocystis* PSII labeled with ^{15}N-His indicates a histidine ligand to the Mn-cluster. Thus, it is possible that His^{190} is this ligand.

Roffey et al. [66] were successful in making a more subtle mutant, PsbA-H195D, which appears to change the equilibrium constant for the electron transfer reaction (Y_Z $P_{680}^+ \leftrightarrow Y_Z^+$ P_{680}) such that re-reduction of P_{680}^+ is 50-fold slower in the absence of the Mn-cluster. They interpreted this to signify a shift in the midpoint potential of Y_Z, as there is no evidence for a shift of the midpoint potential of P_{680}. PsbA-H195Y and PsbA-H195N resemble wild-type. His^{195} is three residues from His^{198}, the proposed axial ligand to one of the chlorophylls of P_{680}, and should be close to both Y_Z and P_{680}.

The consequences of mutating Y_Z itself have been explored by Minigawa et al. [72], who converted Tyr^{161} of D1 to phenylalanine. As expected from results on the analogous mutant in *Synechocystis* PCC6803 [73], P_{680}^+ is no longer re-reduced with rapid kinetics (<1 μs in wild-type) in the PsbA-Y161F mutant. However, flash-induced fluorescence changes are consistent with the use of slower donors to P_{680}^+. At least some of these are endogenous cofactors, as illumination of thylakoids from the mutant causes irreversible bleaching of absorption bands corresponding to chlorophylls and carotenoids. Bleaching of the carotenoid bands can be inhibited by artificial

donors (hydroquinone) or DCMU, indicating a requirement for multiple formations of P_{680}^{+}, and by anerobiosis or scavenging enzymes (superoxide dismutase or catalase). These latter results implicate reactive oxygen species in the photodestructive process, but the fact that the addition of ferricyanide (as an electron acceptor) under anaerobic conditions allows photobleaching to proceed, indicates that reduction of O_2 is not obligatory. Rather, Minagawa et al. [72] hypothesized that P_{680}^{+} first oxidizes a nearby carotenoid, and after a second photooxidation P_{680}^{+} oxidizes a water molecule. This would lead to the eventual production of hydroxyl radical, which would attack the oxidized carotenoid.

The D1 protein in all organisms studied to date, with the exception of *Euglena gracilis* [74], is synthesized as a precursor with a carboxy-terminal extension [75]. As there is no obvious sequence similarity between the C-termini of various D1 proteins beyond the site of proteolytic cleavage, the role of the extension is unclear, but failure to remove it has dramatic consequences. The LF-1 mutant of the alga *Scenesdesmus obliquus* cannot process D1, with the result that its PSII is defective for oxygen evolution. Although it is able to assemble the PSII RC, it is unable to assemble a functional OEC [76], presumably because the longer C-terminus, which should be located in the lumen, interferes with the assembly process. Two groups have tested the requirement for the C-terminal extension in *C. reinhardtii* by changing the codon corresponding to the first residue of the extension to a stop codon [77,78]. Schrader and Johanningmeier [77] noticed that the loss of the extension does not have a significant effect, but analysis was complicated by the combination of the deletion with the S264A/S266T mutations, which result in herbicide resistance. Lers et al. [78] performed a much more extensive analysis on D1 mutants modified only at the C-terminus, but they reached the same conclusion: under all light regimes, there is no observable difference between the wild-type and the mutant strain in terms of photosynthetic growth or in O_2 evolution. Thus, the only known role for the C-terminal extension is its elimination.

4.3.3. Oxygen evolving complex

The OEC of green plants is protected by three extrinsic proteins, OEE1, OEE2, and OEE3, corresponding to proteins whose apparent molecular weights are usually close to 33, 24, and 17 kDa (reviewed in [79,80]). Only the 33-kDa protein is conserved in cyanobacterial PSII, pointing to its central importance. Although early reports that removal of OEE1 resulted in loss of the Mn-cluster indicated that it might play a direct role in Mn binding, the fact that it can be removed from the PSII core without extraction of Mn under certain conditions has cast doubt on this view. However, the requirement for elevated Ca^{2+} and Cl^{-} levels in these OEE1-less PSII RCs suggests that the extrinsic proteins might stabilize these essential ions in the OEC [79,80].

The FuD44 mutant has a 5 kb insertion in the 5′ region of the *psbO* gene, which results in the absence of both the OEE1 mRNA and protein [81]. While the FuD44 mutant can accumulate OEE2 and OEE3, it contains very little D1, D2, P5, or P6. Their loss appears to be due to rapid turnover. The loss of O_2 evolution in this strain suggests an absolute in vivo requirement for OEE1, although this interpretation is complicated by the apparent requirement for OEE1 during assembly of the PSII RC. Later, several laboratories were able to delete the *psbO* gene in two species of cyanobacteria [82–85]. Interestingly, these cyanobacterial mutants are able to assemble significant amounts of PSII and evolve O_2 at 30–80% the rate of wild-type, but only if thylakoid membranes are isolated in the presence of excess $CaCl_2$ and $MnCl_2$. It has been suggested that cyanobacteria contain higher concentrations of Ca^{2+} and Cl^{-} than chloroplasts [86], which may explain the in vivo differences. However, a comparison with the *C. reinhardtii* PsbA-H190F mutant [65–67], which accumulates 90% of the PSII RC in the absence of a Mn-cluster, suggests that the lack of assembly in the FuD44 mutant might be due to structural constraints rather than a deficiency in Mn-cluster formation.

The BF25 and FUD39 mutants lack the OEE2 protein, which is encoded by the *psbP* gene and is 23 kDa in *C. reinhardtii* [87,88]. Although these mutants accumulated normal levels of D1 and the PSII RC, O_2 evolution was 5% of the wild-type level in whole cells [88]. Wild-type levels of OEE1 are present [89], indicating that the donor side is not completely disrupted. Interestingly, PSII from FuD39 evolves O_2 in vitro at 60% the wild-type rate at saturating Cl^{-} concentrations and at 100% the wild-type rate when

DPC, which can bypass the OEC, is used as a donor. However, the mutant PSII requires much more Cl^- for maximal O_2 evolution (K_d is ca. 4 mM vs. 30 μM for wild-type [87]). The fact that high levels of Cl^- are required for protection against rapid light-dependent inhibition of PSII activity in FUD39 also indicates that this mutant is impaired in chloride binding. Photoactivation of the mutant PSII was found to be submaximal at all light intensities tested and slower than in wild-type, which typically achieves half-maximal activation in 1 min at intensities as low as 1 μmol photons m^{-2} s^{-1} and 90% within 10–15 min. Although enhanced irreversible photoinhibition was observed after prolonged illumination at higher intensities, this could not explain the low activity of OEE2-less PSII after short illumination times at such intensities [90]. Photoactivation involves ligation of a Mn^{2+} ion to the PSII core and its subsequent photooxidation to Mn^{3+}. This occurs twice in two sequential steps to make the relatively stable (Mn^{3+}–Mn^{3+}) binuclear state. Between the two photooxidations is an intervening 'dark' step, which may simply represent binding of the second Mn^{2+} or may also involve a conformational change required to reveal the second Mn-binding site. After the ligation of the second Mn^{3+}, subsequent binding of two Mn^{2+} ions complete the assembly of the tetranuclear cluster [79]. Although the first two intermediates (i.e. after the first photoact and after the dark step) are unstable, the results with the FUD39 mutant are not consistent with the lack of OEE2 decreasing the stability of one of the intermediates. In such a case, higher rather than lower activation would be expected at higher light fluences, as this would lessen the interval between the two photooxidations. Rather, Rova et al. hypothesized that at least one step during the dark rearrangement requires binding of Cl^-, and that this step would require more time in the OEE2-less mutant PSII, as its affinity for Cl^- is much lower; they further postulated that photooxidation of the Cl^--less intermediate would produce a reversible non-productive state liable to photoinhibition if further photooxidized [90]. This model would explain inefficient activation at both low intensities, in which the Cl^--stabilized intermediate state would be inabundant and unlikely to be further photooxidized before relaxation, and high intensities, in which the second photoact would be more likely to produce the non-productive state. Prolonged illumination at higher intensities would most likely lead eventually to photoinhibition. Thus, the use of *C. reinhardtii* mutants that lack OEE2, a protein that has no analog in cyanobacterial PSII, has shed light upon the role of Cl^- ions in the photoactivation process.

4.3.4. Small subunits

The PSII RC preparation [43] was later shown to contain the *psbI* gene product in addition to D1/D2 and cyt b_{559} [91,92]. However, PsbI does not appear to be involved in binding cofactors in the electron transport chain, as one can obtain a D1/D2 core that contains all cofactors (except that it has one instead of two carotenoids [93]). The PsbI polypeptide is only 37 amino acid residues long in *C. reinhardtii*, is 76% identical to its homolog in land plants, and has one 21-residue stretch of predominantly hydrophobic amino acids that could serve as a transmembrane domain [94]. Künstner et al. [95] deleted the *psbI* gene from the chloroplast genome, and found that the transformants can still grow photosynthetically under low light (<100 μmol photons m^{-2} s^{-1}), albeit slowly. This phenotype seems to be due to lowered PSII accumulation, as the level of D1 protein (10–20% of wild-type) is similar to the level of residual oxygen evolution (10–20%). Thus, the major role of PsbI would appear to be in either assembly and/or stability of the PSII RC.

PsbK is another PSII-associated, low molecular weight polypeptide with a single potential transmembrane α-helix. In *C. reinhardtii*, PsbK is 37 residues long, is 80–85% identical to PsbK from land plants, and is encoded on the chloroplast genome [96]. Although it does not always appear to copurify with highly purified PSII particles [97], it is found in very pure preparations of PSII particles from *C. reinhardtii* [50]. Takahashi et al. [98] deleted the *psbK* gene, and found that *psbK*Δ transformants were unable to grow phototrophically, yet were not especially light-sensitive (up to 40 μmol photons/m^2/s). The lack of variable fluorescence and O_2 evolution in this mutant is consistent with the very low amounts of D1 detected (less than 10%). As pulse-labeling of the transformants demonstrated a normal rate of D1 synthesis, the phenotype of *psbK*Δ is presumably due to decreased assembly and/or stability

of PSII. Interestingly, deletion of the *psbK* gene did not have such a drastic effect in the cyanobacterium *Synechocystis* PCC6803 [99]. Analysis of *psbK*Δ mutants in *Synechocystis* was complicated, however, by the fact that these mutants grow at half the wild-type rate even in the presence of glucose. Thus, PsbK may have role outside of PSII in cyanobacteria. However, we can conclude that PsbK is not required for PSII activity, as was already seen by biochemical purification in other species [100,101].

While the above two polypeptides were first identified biochemically and then the phenotype of their ablation was determined, characterization of the *ycf8* gene product took a different route. The *ycf8* gene (for 'hypothetical chloroplast open reading frame 8') was identified by sequencing of chloroplast genomes. It is conserved between *C. reinhardtii* and several land plants, and encodes a potential polypeptide of 31 residues with a significant hydrophobic stretch [102]. Using antibodies raised against recombinant Ycf8, Monod et al. [103] demonstrated that the Ycf8 polypeptide is part of the PSII complex. It not only fractionates as a thylakoid membrane protein, but it copurifies with PSII. Moreover, Ycf8 is reduced in mutants that fail to accumulate PSII. The *ycf8* gene was deleted by biolistic transformation [103]. The resulting transformants are sensitive to high light, although PSII appears to accumulate normally. Additionally, the loss of Ycf8 has a significant effect on the level of variable fluorescence and O_2 evolution (decrease of 10–30%). Thus, the Ycf8 polypeptide appears to be required for full activity of PSII, but not for its assembly or stability; it may function to conserve PSII activity during adverse conditions.

The *psbH* gene product is a 9-kDa phosphopeptide associated with PSII. It has one potential transmembrane α-helix, and the site of phosphorylation at the N-terminus (Thr^3) is presumed to be stromal [104]. Not only is it the most conspicuous non-LHC phosphopeptide in the thylakoid during ^{32}P-labeling experiments [105], but it is also phosphorylated in cyanobacterial PSII [106]. The *psbH* gene was inactivated by Summer et al. [107] in such a way as not to affect the expression the *psbB* and *psbN* genes, which are in the same transcriptional unit [103]. The *psbH*Δ half mutants are non-photosynthetic and do not contain PSII [107]. Interestingly, the core subunits of PSII (PsbA/B/C/D) are translated in the absence of PsbH, but are degraded. Although the rate of degradation is slower than that seen in mutants lacking core PSII subunits, it must be fast enough to account for the fact that no core PSII polypeptides are observed at steady state. Similar results were obtained by O'Connor et al. [108], although they also succeeded in making a more subtle mutation that simply changes the phosphorylation site. The PsbH-T3A mutant grows photoautotrophically and harbors normal PSII activity. The only change in PSII activity observed in this mutant is a 35% decrease in steady-state O_2 evolution. Unfortunately, it was not verified that PsbH is non-phosphorylated in the PsbH-T3A mutant. PsbH is another example of a small polypeptide required for assembly and/or stability of the eukaryotic PSII complex. However, the purpose of its phosphorylation remains unclear.

4.4. Assembly of photosystem II

The assembly of PSII is a complicated process. The core of D1/D2 must not only self-associate and bind the cofactors of the internal electron transfer pathway, but must also associate with cyt b_{559} and the core antenna components CP47 and CP43. To this must be added the Mn-cluster, the extrinsic lumenal proteins with associated ions in addition to the plethora of small hydrophobic polypeptides that are affiliated with PSII. Once PSII is assembled, the story is not over; it has been long known that the D1 protein is degraded at a faster rate than the rest of the core components of PSII. The degradation of D1 appears to be linked in some way to the process of photoinhibition, in which PSII activity is lost in a light-dependent manner (reviewed in [109,110]). It is not clear to what level the PSII complex is disassembled during the recovery process, in which a new D1 polypeptide is synthesized and reinserted into the complex. Below, we review what is known about this process in *Chlamydomonas*, a system that is uniquely advantageous in terms of ease of manipulation and availability of mutants.

A survey of the effects of various PSII mutants was made by de Vitry et al. [89]. They examined various mutants defective for D1 (FUD7), D2 (FUD47), CP43 (F34 and FUD34), OEEI (FUD44), and OEE2 (FUD39 and BF25). Their

data are consistent with the existence of a D1/D2/CP47 sub-assembly unit. Not only is the rate of synthesis of CP43 unaffected by the absence of either D1 or D2, but significant amounts of it can accumulate in thylakoid membranes. CP47 and D1 do not accumulate in FUD47 (D2-less); CP47 and D2 do not accumulate in FUD7 (D1-less). More importantly, in mutants lacking CP43, there exists a subcomplex containing D1, D2, CP47, and cyt b_{559}. However, in mutants lacking either D1 or D2, no subcomplexes are observed. Interestingly, even in mutants with no PSII, all three extrinsic OEE proteins can accumulate in the thylakoid lumen, but they are lost during thylakoid purification, presumably because they are no longer attached to the membrane. The binding of OEE3 to the thylakoid depends upon the presence of OEE2, indicating that OEE2 is required for efficient binding of OEE3 to the PSII RC. There also seems to be an interaction between CP43 and OEE2, as OEE2 is specifically redistributed from stacked to unstacked thylakoid membranes in mutants lacking CP43. This study is complemented by earlier work by Jensen et al. [111], in which a mutant that fails to synthesize CP47 due to a lack of *psbB* mRNA [112] was examined. In this mutant, D1, D2, and CP43 are unstable; interestingly, D2 seems less stable than D1. With antibodies, Monod et al. [102] observed no accumulation of D2 or CP43 in thylakoids of another mutant that does not synthesize CP47. Unfortunately, no one has yet performed a similar analysis as was done by de Vitry et al. [89] to see if there is a transient PSII subcomplex in mutants that lack CP47.

By now it is fairly clear that in the absence of any one of the major subunits of PSII (D1, D2, CP47, CP43, cyt b_{559}, OEE1), the rest fail to accumulate [13]. In some specific cases, there may even be an inhibition of translation of certain subunits in the absence of specific subunits (i.e. D1 might be synthesized at a lower rate in the absence of D2 [89,113]). The fact that a limited subcomplex of D1/D2/CP47 can form transiently in the absence of CP43 may reflect a feature built into PSII that allows it to partially disassemble after photoinactivation, permitting the specific proteolysis of D1 (see below). It has been proposed that PSII may be arranged similarly to PSI [114–116]. That is, the PsaA and PsaB proteins contain both a PbRC-like part and core antenna part, while in PSII these functions are split into separate proteins: D1/D2 would correspond to the PbRC-like core of a heterodimer of two 5-helix membrane proteins, while CP47 and CP43 would correspond to the outer core. This model predicts that each core antenna protein would be primarily associated with one of the RC core proteins. The data would indicate that CP43 is associated with D1 and that CP47 is associated with D2. This would explain why D2 seems to be less stable than D1 in CP47-less mutants [111], while the converse is usually true. The fact that D1/D2/CP47 can assemble transiently into a subcomplex might reflect the fact that CP43 needs to be first removed before D1 can be removed, proteolyzed, and replaced by a new D1; only then could CP43 be reintegrated into PSII.

Adir et al. [117] observed that under conditions of high light, D1 (along with D2 and CP47) moved into unstacked thylakoid membranes. With a very short pulse-labeling, the D1 precursor is detected in stromal lamellae, mature D1 in granal lamellae, and a mixture in the intermediate membranes. Upon chase, all molecules of D1 become mature and localize to the grana. However, even the newly synthesized D1 precursor appears to be part of the PSII RC complex. Thus, it would appear that PSII, or a subcomplex thereof, moves from granal to stromal lamellae, where D1 is degraded and a newly synthesized D1 (precursor) is inserted; the reinvigorated PSII would then return to the granal regions. This sort of scenario is similar to the one envisaged in land plants, although Barbato et al. [118] observed a more complicated maneuver in Tris-washed spinach thylakoid membranes. Upon, illumination with bright light, PSII seems to break down into monomers (from a dimeric state) and then into a subcomplex lacking CP43; subsequently, both the PSII subcomplex and CP43 move independently into the stromal lamellae.

4.5. Photoinhibition

It has been long known that illumination with intense light can cause a loss of PSII activity with a concomitant degradation of the D1 subunit [110]. This has been examined in great detail by several laboratories using *Chlamydomonas*. It is relatively simple to distinguish between the inactivation of PSII and degradation of D1. For example, cells ex-

posed to 3–4 mmol photons m^{-2} s^{-1} for 1.5 h at 2°C lose 80% of PSII activity with only a 20% loss of D1 protein [119]; subsequent incubation at 25°C allows degradation of D1 and replacement by new D1. This latter step can be blocked by inhibitors of chloroplast translation, such as chloramphenicol, with the result that only a small amount of PSII activity is regained [119,120]. Thus, in some way, the D1 protein is 'tagged' for degradation by a process that may or may not have to do with photoinactivation. Unfortunately, few experiments have been designed to distinguish between these different processes.

The process of PSII photoinhibition and subsequent recovery in vivo was examined in detail by van Wijk et al. [119]. There is a measurable amount of PSII activity (25%) that can by restored in the absence of chloroplast translation; this seems to correspond to a fraction of PSII that is only affected in the OEC and is reactivated in the first 2 h of recovery. As synthesis from cytoplasmic ribosomes is not required for reassociation of OEE1 to PSII during recovery [121], this damage of the OEC does not appear to represent irreversible modification of the extrinsic proteins. Recovery of the majority of the cellular PSII activity requires primarily synthesis of new D1 protein, (4.5:1 for D1:D2 and >6:1 for D1:CP43). This ratio drops over time to the steady-state ratios (2:1 for D1:D2 and 3:1 for D1:CP43). By adding translational inhibitors at various times during the recovery process, it could be estimated that it takes approximately 1 h for newly synthesized D1 to be reintegrated into a fully functional PSII complex [119]. This lag may represent the time for rebuilding the OEC, as it appears that newly synthesized D1 is immediately incorporated into complexes [117]. By using DPC to bypass the OEC and by measuring the $Y_Z^{+\bullet}$, $Y_D^{+\bullet}$, and $Q_A^{-\bullet}$ radicals by EPR, it was possible to assess where the damage lay. It appears that about one-third of the protein synthesis-dependent population is damaged at Y_Z, yet still has normal Y_D; it also has functional P_{680} and Q_A, and is capable of charge separation between them. The remaining two-thirds have no detectable Q_A and no photooxidizable Y_Z or Y_D; this population might also be damaged at P_{680}. It may be that the 'Y_Z-less cohort' is an intermediate state that is converted to the second, more damaged, state upon further illumination.

If D1 must be degraded, resynthesized and reincorporated into PSII, the question arises: what happens to the Mn-cluster and extrinsic proteins of the OEC? Eisenberg-Domovich et al. [121] addressed this question in *C. reinhardtii* in vivo. As D1 is degraded during illumination in the presence of chloramphenicol, the extrinsic proteins (OEE1, -2 and -3) lose their association with the membrane, although they are not degraded. There is a very good correlation between the amount of D1 and the amount of thylakoid-attached OEE1. The release of OEE1 requires D1 degradation and not simply photoinactivation, because in mutants blocked in electron transport beyond PSII (see below), the degradation of D1 is inhibited even after loss of 90% of the activity; in this case, OEE1 remains attached to PSII. Reassociation does not require new OEE1 synthesis, but does require assembly of PSII, as was shown using a mutant thermosensitive for PSII assembly. Although this reassociation does not require light, full reactivation of PSII activity does [119,121,122], consistent with the known requirement of light for Mn-cluster activation [79]. These results are similar to those obtained with spinach thylakoids in vitro [123], in which release of the three extrinsic proteins correlated with loss of D1 during photoinhibition. Additionally, after removal of the OEE proteins by 2 M $CaCl_2$ washing, intense illumination results in a progressive loss of Mn that also correlates with D1 degradation (ca. 4 Mn atoms per D1 protein [123]). Thus, before or during D1 degradation the OEC must be disassembled completely, including removal of the Mn atoms, which is not surprising considering the role that D1 plays in Mn-cluster binding [79]. The reintegration of a new D1 into the subcomplex is presumably followed by Mn binding, reassociation of extrinsic proteins with calcium and chloride ions, and then the light-dependent activation of the Mn-cluster for full recovery of PSII activity.

There have been several attempts to understand what controls degradation of D1. In *Chlamydomonas*, as in land plants and cyanobacteria [110,124], the addition of Q_B^- directed herbicides can inhibit the degradation of D1 during photoinhibitory conditions [124,125]. The inhibitor DCMU is capable of inhibiting the slow phase of photoinactivation, and can protect D1 from degradation during intense illumination, but not during the recovery period. Deg-

radation of the 'tagged' D1 can occur in darkness even in the presence of DCMU. Thus, the idea would be that DCMU somehow inhibits the tagging event, but once this occurs degradation is inevitable. The Ohad laboratory has also observed that mutants blocked in electron transport beyond PSII can inhibit the degradation of PSII [120,126]. They examined mutants lacking cyt b_6f (D6), plastocyanin (AC208), and PSI (B4), and found that, although photoinactivation is somewhat slower in the mutants, D1 degradation is much slower. Anaerobic conditions also slow PSII photoinactivation and D1 deg-

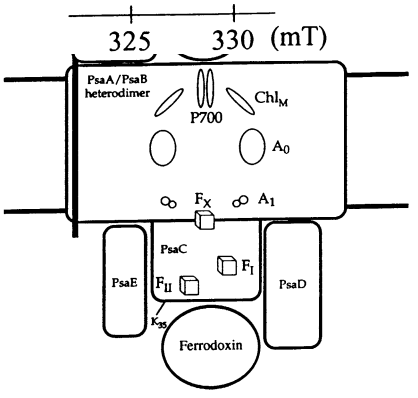

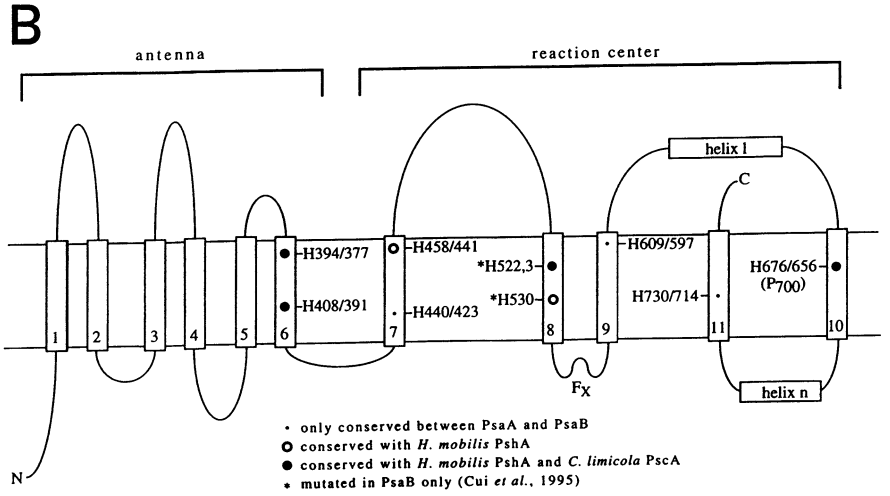

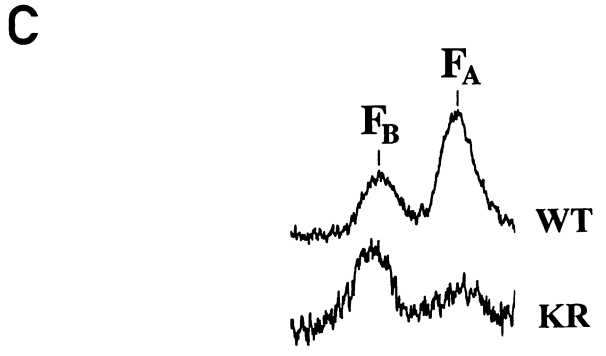

radation. Their explanation for these results is that the PQ/PQH_2 ratio determines the rate of photoinactivation and D1 degradation (i.e. a reduced PQ pool inhibits D1 degradation).

The initial event of photoinhibition in vivo, at least in low light conditions, is now much better understood thanks to an analysis of the quantum efficiency of D1 degradation. Keren et al. [127] found that even low photon fluxes can induce D1 proteolysis. The quantum yield of D1 degradation is very high at 10–50 μmol photons m^{-2} s^{-1}, while photosynthesis saturates at values 20–100-fold higher. An hypothesis to explain this is that the S/Q_B state controls degradation: the S2,3/Q_B^- states can recombine (half-time = 2 s in *C. reinhardtii* cells at 25°C) perhaps generating harmful radicals or triplet states. The efficiency of Q_B^- generation is very high, saturating at 0.5–1 μmol photons m^{-2} s^{-1}, which might explain the high quantum yield of low photon fluxes for D1 degradation: they allow the formation of Q_B^- without providing enough photons to doubly reduce Q_B efficiently before it back-reacts. This hypothesis was tested by a set of courageous experiments. Cultures incubated in the dark with chloramphenicol were given saturating 6-μs flashes every 10 s at 25°C for 4 h, and the amount of D1 remaining was determined by immunoblot. A single-turnover flash would result in formation of Q_B^-, which could then back-react during the 10 s incubation in the dark before the next flash. Consistent with the hypothesis, D1 was degraded significantly more during the flash regime than during 4 h of continuous illumination at 25 μmol photons m^{-2} s^{-1}; note that the total amount of energy delivered by the 1440 flashes would be equivalent to less than 5 s at this intensity. The hypothesis also predicts that a closely spaced series of flashes should produce different results depending on the number of flashes in the series, due to the cycling of the S state. To test this prediction, it was necessary to lower the temperature to 6°C, where S2,3/Q_B^- recombination has a half-time of 30 s. Every 30 s, the cultures were given a series of one to six saturating flashes spaced 300 ms apart. The kinetic model derived by the authors predicts that different steady state levels of Q_B^- will be established after the first 50 flashes by this regime, with an odd number of flashes giving high levels of Q_B^- and an even number giving low levels. Consistent with the model, a series of two flashes resulted in almost no light-dependent D1 degradation, while three flashes gave almost as much as one flash. Beyond this point, the relationship broke down and the data had much higher variability, no doubt due to the unavoidable presence of PSII RCs which were excited either twice or not at all during a flash. Nevertheless, it is striking that a series of single flashes results in D1 degradation equivalent or greater to incubation in low light, while a series of double flashes, which would deliver twice as much energy, results in almost no degradation. That this oscillating pattern has to do with the S cycle was tested by repeating this experiment in *Scenesdesmus* wild-type and LF-1 mutant cells. Although the wild-type cells behave essentially as *C. reinhardtii* (i.e. one flash resulted in more D1 degradation than two), the OEC-less LF-1 cells behaved in the opposite manner (i.e. two flashes resulted in more D1 degradation than one flash).

Note that the experiments described above do not distinguish between photoinactivation (which was not measured), tagging, and degradation. However, it seems most likely that the S2,3/Q_B^- recombination results in damage through generation of the triplet

←

Fig. 3. (A) Schematic model of PSI with emphasis on cofactors. The PsaA/PsaB heterodimer binds the cofactors P_{700} (a pair of Chl *a*), A_0 (monomeric Chl *a*), A_1 (phylloquinone), and F_X (4Fe–4S center), as well as two monomeric chlorophylls (indicated as Chl_M) of unknown function that can be seen in the crystal structure (referred to as 'eC_2' in [130,131]). The PsaC subunit binds the terminal electron acceptors, F_A and F_B (4Fe–4S centers), and, together with the stromal, extrinsic subunits PsaE and PsaD, is involved in binding ferredoxin. The interaction of PsaC residue Lys^{35} with ferredoxin is highlighted. Also emphasized is the electrostatic interaction of lysine residues 16–23 on PsaF with plastocyanin. (B) Topological representation of PsaA/B. The first 6 transmembrane α-helices are thought to bind antenna chlorophylls, while the last five helices would comprise the reaction center of PSI. Conserved histidine residues of the last six helices that have been targeted by Cui et al. [170], Webber et al. [171], and Redding et al. [172] are indicated, as well as their degree of conservation with other type 1 reaction centers from photosynthetic bacteria (see key). The extramembranous helices 'l' and 'n' seen in the crystal structure [130,131] are also indicated. (C) EPR spectra of wild-type PSI and PsaC-K52S/R53A, taken from [137] with permission. The positions of the peaks arising from the reduced F_A or F_B centers are indicated.

state of P_{680}. Chlorophyll triplets are dangerous due to their propensity to react with molecular oxygen and generate singlet oxygen, a highly unstable species that would probably react with the closest possible victim (i.e. P_{680}, Y_Z, the OEC, etc.). Molecular oxygen has been implicated in the process of photoinactivation and D1 degradation [128], and it has been observed that *C. reinhardtii* cells grown anaerobically degrade less D1 than those grown aerobically [126]. Additionally, the $S2,3/Q_B^-$ recombination hypothesis makes sense of previous observations that a reduced plastoquinone pool or the addition of herbicides can protect D1 from degradation, as both these conditions would result in low occupancy of the Q_B site.

However, it is clear that the story is not as simple as we have presented above. Various inhibitors can protect D1 from degradation, probably by inducing a conformational change at the Q_B site. Jansen et al. [124] examined the effects of a large variety of Q_B inhibitors on PSII inhibition and D1 degradation. The 'classical' inhibitors (urea and triazine derivatives) all inhibit D1 degradation to about the same extent (ca. 50%) when applied at their IC_{50} (the concentration at which oxygen evolution is inhibited by 50%), but the 'phenol type' inhibitors (cyanophenols, nitrophenols, and dinitrophenols) can vary dramatically in their ability to inhibit D1 degradation. Systematic variation of the substituent at the R6 position in 2-bromo-4-nitrophenols showed that the bulkier the R6 substituent, the better the inhibition of D1 degradation, although the measured IC_{50} values were all very similar. A fairly good, albeit imperfect, correlation exists between inhibition of D1 degradation in pulse-labeled *Spirodela* cells in vivo and the inhibition of D1 trypsinization (at Arg^{238} in the fourth loop, close to Q_B site residues) in spinach thylakoids in vitro, which suggests the existence of a conformational change caused or inhibited by these compounds. However, DCMU does not protect previously tagged D1 molecules from degradation in the dark, nor does it protect D1 from trypsinization after being previously photoinhibited in *C. reinhardtii* [125]. Thus, the classical inhibitors may act by simply displacing plastoquinone from the Q_B site, while the phenol type may act in another way by altering the site for proteolysis. Finally, the route of photoinhibition may vary depending upon both the quantity and quality of the light. The method of photoinhibition may be different in cells treated with large doses of light compared to those illuminated with low doses. At their IC_{70} (70% inhibition concentrations), different inhibitors can vary widely (1–90%) in how much they inhibit the D1 degradation driven by visible light, but all inhibit by ca. 60–70% the degradation driven by UV-B light [124]. The action spectrum of UV-B-driven degradation resembles that of plastosemiquinone [129], raising the possibilty that the photoreceptor is plastosemiquinone at the Q_B site.

5. Photosystem I

Photosystem 1 (PSI) uses the energy from a photon of visible light to drive the transfer of an electron from plastocyanin or cytochrome c_6 in the lumen of the thylakoid to ferredoxin in the stroma. This process is energetically unfavorable due to the difference in redox potentials between the soluble electron transfer partners and the *trans*-thylakoid electric field. Thus, the energy of a photon of light is used, in much the same manner as in PSII. Upon excitation a dimer of chlorophylls (P_{700}) is able to donate an electron to a nearby chlorophyll (A_0), which serves as a primary acceptor (see Fig. 3A). This electron is then transferred sequentially to a phylloquinone secondary acceptor (A_1), an iron–sulfur center (F_X), and to the terminal acceptors (F_A and F_B), which are also 4Fe–4S centers, before arriving ultimately at a reversibly bound molecule of ferredoxin. The oxidized special pair is then reduced by a lumenal molecule of plastocyanin. The core of the complex is a heterodimer of the polytopic membrane proteins PsaA and PsaB, encoded by the chloroplast genes *psaA* and *psaB*, which bind most of these cofactors. The last two iron–sulfur centers are contained within PsaC, a smaller extrinsic protein bound to the stromal side of the PsaA/PsaB heterodimer. Recently, the structure of a cyanobacterial PSI has been solved to 4 Å resolution [130,131]. The structural model indicates that the last five transmembrane helices of PsaA and PsaB interact to form the reaction center, similar to the way in which the L and M subunits form the purple bacterial RC, while the first 6 transmembrane α-helices are involved in binding many of the 80–100 chlorophylls

of the core antenna (see Fig. 3B). PSI has been reviewed in various degrees of detail [132–134]; thus, this review will focus on work performed on *Chlamydomonas* PSI.

5.1. Purification of the photosystem I complex

Nechustai and Nelson [135,136] reported purification and characterization of a PSI 'reaction center' complex. It contained the PsaA/B heterodimer as well as PsaC, PsaE, and PsaD. It required either divalent cations at low ionic strength or monovalent cations at moderate ionic strength for efficient photooxidation of cytochrome c_{552}, presumably due to the lack of the PsaF subunit (see below). They also observed photooxidation of cytochrome c_{552} by the PsaA/B heterodimer in the absence of the smaller subunits. By treatment with various translational inhibitors, they were able to show that synthesis of PsaA, B, C takes place in the chloroplast, while that of PsaD occurs on cytosolic ribosomes [136]. A more recent protocol for purification of a complete and highly purified PSI complex using β-dodecylmaltoside as the solubilization agent is currently in widespread use [137,138].

Wollman and Bennoun [139] reported the purification of a chlorophyll–protein complex called CP0 as the peripheral antenna complex of PSI. It has a major polypeptide of 27 kDa, 4 minor constituents of 27.5, 25, 23, and 19 kDa, and a Chl *a*/Chl *b* ratio of 6. The complex has an intense fluorescence emission peak at 705 nm at 77 K, which is very similar to the fluorescence peak seen in whole cells lacking PSI. This peak is missing in a double mutant (AC40-14) lacking PSI and LHCI, indicating that it arises from LHCI that is normally quenched by PSI. Bassi et al. [140] performed a more in-depth characterization of LHCI. They obtained N-terminal amino acid sequence from seven of the LHCI apoproteins, and found that they were homologous to *cab* proteins from both land plants and *Chlamydomonas*. Two different LHCI complexes could be separated from PSI: LHCI-680 (fluorescence emission peak at 680 nm) and LHCI-705 (fluorescence emission peak at 705 nm). They differed in their aggregation state and in that LHCI-680 contained the PsaF polypeptide and LHCI-705 did not. LHCI could be further separated by isoelectric focussing into individual chlorophyll-binding proteins and then reconstituted back into a complex that resembled LHCI-705. As many as 10 different chlorophyll-binding proteins are present in LHCI, and immunological analysis indicated that these polypeptides fall into three groups: those resembling high chlorophyll *b*-containing LHCII polypeptides; those resembling CP24; and those resembling the pericentral CP29 and CP26 polypeptides.

5.2. Biophysical analysis of photosystem I

Using single photon counting, Owens et al. [141] examined fluorescence decay in barley PSI core complexes (20–40 Chl/P_{700}) and the *C. reinhardtii* mutant A4D, which lacks PSII and has a 75% reduction in LHCII. The fastest component (20 ps for isolated PSI or 40 ps for A4D cells) accounted for 90% of the amplitude and represents excitations in the core antenna whose lifetime is limited by photochemical quenching at P_{700}. An interesting finding was that the lifetime of the fastest decay correlated linearly with the PSI antenna size (0.63 ps/Chl), giving an intercept at 3.4 ± 0.7 ps for dimeric P_{700}. From this, they estimated trapping and single-step transfer times of 0.2 ps; that is, transfer to P_{700} is not favored over other chlorophylls. With an estimated detrapping rate of 2.4 ps, this results in an average of about 2.4 visits to the trap before trapping, a situation which is nearly diffusion-limited. Another conclusion was that the structure and dynamics of PSI from green plants must be very similar.

In addition, slower decays were observed. The 1.5–2 ns decay representing 4% of the decay in $PSII^-$ $LHCII^-$ cells and 25% in $PSII^-$ cells is likely that from unconnected LHCs as it resembles that from both isolated LHCII and from *C. reinhardtii* mutants that lack both PSI and PSII [142]. An intermediate decay (350–700 ps) accounting for 10% of the amplitude in $PSII^-$ $LHCII^-$ cells and 30% in $PSII^-$ cells probably represents a complex mixture of peripheral and core antenna excitations, and its contribution to the total decay varies highly [142]. The emission spectra for the fast and intermediate components are similar, with the intermediate one being slightly more red-shifted in $PSII^-$ $LHCII^-$ cells. The 1.5–2 ns component is significantly blue-shifted in both strains; its maximum emission is 680 nm compared

to 690–695 nm for the fast and intermediate decays. An in vivo PSI core antenna size of 120 chlorophyll/P_{700} in strains with unaltered antennae was thus estimated.

The fast fluorescence decay in PSII$^-$ LHCII$^-$ cells exhibited a strong temperature-dependence of emission at 720 nm (it decreased 3-fold from 36 to 298 K), but not so strong at 680–710 nm [143]. A similar behavior was seen in PSI particles from these cells, although there was a stronger temperature-dependence of emission at 710 nm. From this, the authors concluded that there are 1–2 low-energy pigments ('red chlorophylls') that are close to P_{700}. It would also appear that peripheral antenna pigments absorb at lower wavelengths than the core antenna. Transfer from the peripheral to core antenna as well as spectral equilibration within the core antenna takes less than 5 ps. Modelling of the excitation movement is more consistent with a 'random walk' rather than a 'funnel' model. These researchers concluded that excitations are twice as likely to be localized on the low-energy pigments than on other pigments. Thus, the red chlorophylls could exert a focussing effect; and transfer from them to nearby P_{700} would occur via a low energy pathway, giving rise to the observed temperature-dependence.

Hastings et al. [144] examined PSI particles from *Synechocystis* PCC6803, *C. reinhardtii*, and spinach using ultra-fast absorption spectroscopy. They were able to calculate two decay-associated spectra (DAS) from all three species. A fast decay (3.7–7.5 ps; 4.6 ps in *Chlamydomonas*) was associated with equilibration of excitations in the core antenna (i.e. from shorter to longer absorption wavelengths). Note that this result is quite complementary to the fluorescence decay kinetics observed both by these same researchers in *Synechocystis* membranes lacking PSII [145] and by Fleming and co-workers [142,143] in *Chlamydomonas*. The DAS of 19–24 ps (22 ps in *Chlamydomonas*) has contributions both from the trapping-limited decay of excitations and the decay of A_0^-. In order to separate these two processes, they repeated the experiments with and without an intense preflash, which serves to preoxidize P_{700}. The idea is that antenna dynamics alone will be seen with the 'oxidized' PSI, as these are not affected by oxidation of P_{700}. Thus, the 'neutral-oxidized' data should represent changes due solely to photochemistry. This method was put to good use in the analysis of *Synechocystis* membranes lacking PSII [146], where the 21-ps DAS was assigned to the $A_0^- - A_0$ difference spectrum. The $A_0 - A_0^-$ spectra are similar for all three species, with a main bleaching at 683–686 nm. However, there also appear to be contributions from a second pigment, which they called A_0'. The difference spectrum of this pigment is consistent with a chlorophyll *a*, but it is markedly different in the different species examined, with a bleaching maximum at ca. 686 nm in *Synechocystis*, ca. 670 nm in spinach, and even more blue-shifted and diffuse in *Chlamydomonas*. This pigment may be an intermediate electron acceptor or a nearby pigment whose spectrum undergoes electrochromic shift upon reduction of A_0.

5.3. Molecular genetics of photosystem I

There is a huge collection of PSI-deficient mutants in *Chlamydomonas*. Girard et al. [147] used treatment with various mutagens followed by fluorescence screening to isolate 25 PSI-deficient mutants. The mutations are recessive, segregate in a Mendelian fashion, and fall into 13 complementation groups. The fact that several complementation groups have only one or two members indicates that this screen was not saturated. Only two of the groups show tight linkage, indicating that mutations affecting PSI are scattered throughout the genome. The mutants are all missing a subset of thylakoid proteins, most of which are enriched in PSI-110 particles. Thus, these mutations cause a coordinated loss of all PSI polypeptides, suggesting the existence of an organized substructure that requires the presence of all components.

Seven different chloroplast mutations that result in a PSI-deficient phenotype have also been described [148,149]. By linkage analysis, they fall into four groups. Group 1 (C3, g2–3, FUD26) is linked to *rbcL* and thus is probably *psaB*. Group 2 mutants have not yet been characterized. Group 3 mutants are deficient in *tscA* [149,150], a gene that maps close to *chlN* and encodes an RNA required for maturation of *psaA* mRNA (see below). The sole group 4 mutant (C1) is leaky and expresses PSI at 10–15% of the wild-type level [148]. All of the chloroplast mutants fail to accumulate thylakoid polypeptides 2a

and 2b (apparent molecular weight of approximately 60 kDa), although the C1 mutant contains a small amount [151]. By pulse-labeling, polypeptide 2a was seen to be synthesized in all mutants, except those of group 1. In FUD26, this polypeptide was replaced by a new one 10 kDa lower in molecular weight. When the 3′ end of *psaB* was sequenced in the FUD26 mutant, a 4-bp deletion was found that would cause a frameshift and a concomitant loss of about 10 kDa. The g2–3 mutant also has a frameshift in *psaB* [152]. The 2b band is not observable by pulse-chase in any mutant except C1, where it appears normal. From these data, the authors hypothesized that polypeptide 2a corresponds to PsaB and 2b corresponds to PsaA and, furthermore, that synthesis of PsaA is dependent upon synthesis of PsaB, but the converse is not true.

The reason why there is such a plethora of nuclear mutants that fail to express PSI is due to a peculiarity of the *psaA* gene. When Kück et al. [153] sequenced and mapped the *psaA* and *psaB* genes of *C. reinhardtii*, they found that *psaA* is split into three exons that are widely separated and on different strands of the chloroplast genome, leading to the proposal that the *psaA* mRNA is created by *trans*-splicing the transcripts of these separate exons. This hypothesis was tested and confirmed by an analysis of PSI-deficient mutants; a quarter of them were deficient in the maturation of the 2.7 kb *psaA* mRNA, and instead accumulated transcripts of unspliced exons [154]. Further analysis with a larger set of mutants [38] showed that such mutants fell into three classes: class A (exon 2–3 splicing defective), class B (no splicing at all), and class C (exon 1–2 splicing defective). As one might expect, class B mutations are epistatic to both class A and C mutations (i.e. a class B/C double mutant resembles a class B mutant). Five out of 13 complementation groups from Girard-Bascou's original set [147] are in class C. With the addition of the new mutants, there are five class A complementation groups (seven members), two groups for class B (four members), and seven groups for class C (many members). The screen is still not at all saturated. The only chloroplast *trans*-splicing mutants are FUD3, H13, and D42, and all affect *tscA*, a chloroplast gene expressing an RNA required for exon 1–2 splicing [21,155].

5.4. Structure–function analysis

With the advent of biolistic transformation of the chloroplast, it is now possible to specifically delete or mutate genes of the PSI subunits. Takahashi et al. [156] deleted the *psaC* gene after cloning and sequencing it. Null mutants in *psaC* fail to grow phototrophically. Although they accumulate only a small amount ($<10\%$) of the PsaA/B heterodimer due to rapid degradation of those subunits, LHCI is accumulated normally. Later, Fischer et al. [137] were able to generate point mutations in PsaC that cause changes in the iron–sulfur centers contained therein (see below).

Most of the site-directed mutants made so far have been in the large chloroplast-encoded subunits PsaA and PsaB (see Fig. 2B). These proteins are homologous to each other (ca. 50%) and are predicted to each contain 11 transmembrane domains [157]. Lee et al. [158] deleted 5 or 10 amino acid residues from the C-terminus of PsaB in order to determine its functional boundary. Although the five-residue truncation mutant behaves as wild-type, the removal of an additional 10 residues results in the loss of PSI. This result is consistent with the hydropathy analysis indicating that helix 11 should end with these essential five residues. Interestingly, extending PsaB by 27 residues also abolishes accumulation of PSI. When revertants were selected from this mutant, all the fast-growers had a shortened PsaB, with extensions (relative to wild-type) of three, five, six, or 14 residues.

Between the hypothetical transmembrane domains 8 and 9 is a highly conserved sequence (FPCDGPGRGGTC) believed to be involved in the formation of the F_X iron–sulfur center [132]. Webber et al. [159] introduced mutations in this region into the *psaB*-g2–3 frameshift mutant, changing the first cysteine and the proline immediately before it. The PsaB-P560A and PsaB-P560L mutants grow photoautotrophically, accumulate PSI at wild-type levels, and exhibit normal electron transfer rates. However, the PsaB-C561H mutant accumulates no detectable PSI and is non-photosynthetic. This study further confirmed that PsaA is not accumulated in the absence of PsaB. Hallahan et al. [160] made mutations in the same region of PsaA, changing the first cysteine and the aspartate immediately after it. PsaA-

D576L accumulates lowered amounts of PSI (40–50%), and has similar back-reaction kinetics to wild-type, but the F_A/F_B EPR spectrum is altered, indicating that the nearby F_A and F_B centers are sensitive to the loss of Asp^{576}. The PsaA-C575L PSI complex cannot be accumulated, but the PsaA-C575H mutant complex is present at 20–30% the wild-type level. The F_A/F_B EPR spectrum was not detectable in the PsaA-C575H mutant; however, as the authors did not verify that PsaC was still present in their mutant preparations, the significance of this result is unclear. They claimed that, although the F_X EPR spectrum appeared normal in PsaA-D576L, it was undetectable in PsaA-C575H. Thus, as one might expect, the PSI RC is extremely sensitive to mutation of the cysteines that serve as ligands to the iron atoms of F_X, while the residues around them can be changed more freely.

Rodday et al. [161] had suggested, based upon molecular modeling studies, that the interhelical F_X domain was also involved in the binding of the PsaC subunit to the PsaA/B heterodimer. Analysis of the PsaB-R561E mutant in *Synechocystis* gave support to this idea, as it displayed impaired binding of PsaC in vitro, although this could be somewhat alleviated by the presence of divalent cations [162]. However, the corresponding PsaB-R566E mutant of *C. reinhardtii* is unable to accumulate detectable PSI, nor is the PsaB-D562N mutant [163]. The PsaB-P564L mutant accumulates normal levels of PSI and is photoautotrophic, allowing the analysis of this mutant along with the previously constructed mutations in Pro^{560} ([159]; see above). Upon treatment with 6 M urea, PsaC disassociates from the PsaA/B heterodimer, along with the other extrinsic subunits, and the loss of the terminal electron acceptors can be followed by the change in backreaction kinetics, as $P_{700}^+ F_X^-$ (or $P_{700}^+ A_1^-$) recombines much faster than $P_{700}^+ F_{A/B}^-$ [164]. PSI can be reconstituted by addition of recombinant cyanobacterial PsaC in the presence of $FeCl_3$, Na_2S, and 2-mercaptoethanol [165]. However, even in the presence of saturating amounts of PsaC (a 20:1 ratio of PsaC to PSI), the PsaB-P560L and PsaB-P564L mutants are capable of attaining only 16–18% reconstitution [163], with the PsaB-P560A mutant intermediate (37%) between them and wild-type (47%). However, the fact that 30% reconstitution of wild-type PSI could be obtained by incubation with a 1:10 ratio of PsaC/PSI is difficult to explain. An analysis of the loss of slow backreaction kinetics (i.e. loss of PsaC) after incubation with increasing amounts of urea was also consistent with the idea that the interaction of PsaC with PSI was weakened by the proline substitution mutants.

Site-directed mutations that affect the F_A and F_B iron–sulfur centers of PsaC have now been described in *C. reinhardtii*. A model for the structure of PsaC [166], based upon the X-ray crystal structure of the ferredoxin from *Peptococcus aerogenes* and sequence similarities between PsaC and bacterial ferredoxins containing two 4Fe–4S clusters, predicts that the positively charged residues Lys^{52} and Arg^{53} would be close to center F_A. Fischer et al. [137] mutated these residues to determine their effect upon electron transfer. Although the PsaC-K52P/R52D and PsaC-K52S/R52D mutants are unable to assemble PSI, the PsaC-K52S/R53A mutant accumulates PSI to approximately 20–30% the wild-type level. Despite this fact, it is incapable of photoautotrophic growth except under weak illumination (5 μmol photons m^{-2} s^{-1}) or anaerobic conditions. Analysis of ferredoxin

Table 1
Properties of PsaC point mutants[a]

Mutation	Dissociation constant of PSI-ferredoxin interaction (μM)	Half-times of first-order rates of ferredoxin reduction (μs)	Second-order rate constant of ferredoxin reduction (M^{-1} s^{-1})
Wild-type	6.0–9.0	<1, 4–11	$2.3\pm0.5\times10^8$
$K_{52}S/R_{53}A$	7.3	<1, 4–11	5.6×10^8
$K_{35}T$	>300	not observed	4.5×10^7
$K_{35}D$	>300	not observed	6.3×10^6
$K_{35}E$	>300	not observed	2.8×10^6
$K_{35}R$	4.5–6.5	<1, 4–11	$2.3\pm0.5\times10^8$

[a]Taken from Fischer et al. [137,232].

reduction by flash spectroscopy indicated that the PsaC-K52S/R53A mutant is normal in terms of interaction with ferredoxin and kinetics of electron transfer to it (see Table 1). Interestingly, after photoreduction at low temperature (15 K) the F_B center is preferentially reduced in the mutant ($F_B^-/F_A^- = 1.9$) whereas the F_A center predominates in wild-type ($F_B^-/F_A^- = 0.65$) and in PSI from other species (see Fig. 3C). This situation is reminiscent of the RC1 from *Chlorobium limicola*, where F_A has a lower redox potential than F_B, causing F_B to be preferentially reduced [167]. The PsaC-like subunit in this organism has Ser and Ala in the analogous position [168], and thus Fischer et al. [137] suggested that Lys^{52} and Arg^{53} of PsaC may play a role in setting the redox potential of F_A. Thus, the PsaC-K52S/R52A mutant might share properties with bacterial RC1 from obligatory anaerobes, perhaps explaining its difficulty in driving photosynthesis during aerobic conditions.

Recently, the search for mutations affecting cofactors has widened to include P_{700}. The realization that the reactions centers from *Heliobacillus* and *Chlorobium* are similar to PSI prompted a search for residues conserved between these distantly related RCs. These bacteria appear to have a single gene similar to PsaA/B, and thus make a homodimeric RC1. Both of these genes are predicted to encode polypeptides with 11 transmembrane α-helices, as in PsaA/B, but the only obvious similarity between them and PsaA/B is in the F_X region. However, the fact that helix 8, directly before the F_X region, has two conserved histidines led to the suggestion that these might coordinate the chlorophylls of P_{700} or A_0 [168,169]. This was tested by mutating these conserved histidines in PsaB [170]. While mutation of His^{522} or His^{523} to tyrosine abolishes accumulation of the mutants PSIs, substitution of glutamine reduces their accumulation by 25 or 75%, respectively. Likewise, a change of His^{523} or His^{530} to leucine reduces accumulation by 88 or 50%, respectively. However, the biochemical activities of the mutant PSIs are the same as wild-type, nor are there any significant changes in the visible difference, ENDOR, or ESEEM spectra of P_{700}^+ in these mutants. Thus, these histidines do not appear to be ligands to the P_{700} chlorophylls. Their effect upon accumulation is exerted post-translationally, as the level of *psaB* mRNA is unchanged as well as the level of PsaB polypeptide observed in a brief pulse-labeling.

Webber et al. [171] then turned to helix 10, where there is a single conserved histidine. The PsaB-H656N mutant has a noticeably changed visible difference spectrum ($P_{700}^+ - P_{700}$), with a slight blue shifting of the maximal bleaching band from 696 to 693–694 nm and a new bleaching band centered at 667 nm, the origin of which is unknown. The redox potential of the P_{700}/P_{700}^+ couple is shifted up from 447 to 487 mV in the PsaB-H656N mutant. Finally, the P_{700}^+ ENDOR spectrum was changed: the isotropic hyperfine coupling of protons at methyl group 12 is increased (20% in PsaB-H656N and 16% in PsaB-H656S), with no significant changes in hyperfine couplings of methyl protons at positions 2 or 7. These data would seem to indicate that the histidine in helix 10 is the axial ligand to P_{700}, but other possibilities remained. The observed effects are not as dramatic as one might expect from mutation of an axial ligand, and they could merely indicate that the helix 10 histidine is near P_{700} or makes a hydrogen bond to one of the keto or ester groups of a P_{700} chlorophyll. However, a recent analysis by Redding et al. [172] lends support to the idea that the histidines of helix 10 in PsaA and PsaB are the axial ligands to P_{700}. In this study, all histidines conserved both in all PsaA and PsaB polypeptides as well as between PsaA and PsaB in the last 6 transmembrane α-helices were changed to glutamine or leucine: this resulted in 7 sites examined in both PsaA and PsaB (two in helix 6, two in helix 7, and one each in helices 9, 10, and 11). Mutants in which the analogous (symmetry-related) histidines had been simultaneously substituted with glutamine were examined spectroscopically for changes in P_{700}. None of the double mutants presents any changes in the $P_{700}^+ - P_{700}$ visible difference spectrum, FTIR difference spectrum, or P_{700}^+ EPR spectrum, except for the double mutant in helix 10 (PsaA-H676Q/PsaB-H656Q), which showed changes in all three. Examination of the single mutants in helix 10 demonstrated that PsaB-H656Q causes the broadening of the linewidth of the P_{700}^+ EPR signal, while PsaA-H676Q has no effect. However, PsaA-H676Q has a more obvious effect upon the FTIR difference spectrum, with a 5 cm^{-1} upshift of the 1700 cm^{-1} band attributed to vibration of the 13^1 keto group in the ground state. Thus, these two stud-

ies give complementary results in terms of examining the two sides of P_{700}. Mac et al. [173] have presented ESEEM and ENDOR data on cyanobacterial PSI labeled with ^{15}N-histidine and concluded that histidine is one of the axial ligands to P_{700}. The X-ray crystal structure would indicate that the last five transmembrane α-helices form the RC part of PSI, with the first six forming the core antenna [130,131]. As all the conserved histidines in the last six transmembrane α-helices have been mutated, and the only ones that show an effect are those in helix 10, we are left with the conclusion that these histidines are the axial ligands to the chlorophylls of P_{700} (see Fig. 3B for all histidines discussed above).

Considering the above, the kinetic analysis performed on the PsaB-H656N mutant by Melkozernov et al. [174] is especially interesting. The non-decaying difference spectrum they observed, which is attributed to $P_{700}^{+}-P_{700}$, is changed by the mutation, as was previously observed on a much longer time scale [171]. There is no change in the $A_0^{-}-A_0$ difference spectrum, indicating that the mutation has a localized effect. The mutation causes a two-fold increase in the time constant of trapping, indicating that the intrinsic rate of charge separation ($P_{700}{*}A_0 \rightarrow P_{700}^{+} A_0^{-}$) has been decreased by the mutation. This was further confirmed by the increase in the lifetime of the fast decay component in picosecond-resolved fluorescence decay kinetics. These authors estimated an upper limit for the charge separation times to be 1.5 ps for wild-type and 3.5 ps for the PsaB-H656N mutant. This change might well be due to a shift in the redox potential of $P_{700}{*}/P_{700}^{+}$, thus decreasing the driving force of the electron transfer from $P_{700}{*}$ to A_0, although other explanations remain.

5.5. Soluble electron carriers that transfer electrons to photosystem I

In *C. reinhardtii* and some other algae and cyanobacteria, plastocyanin and cytochrome c_6 are functionally interchangeable as soluble electron carriers from reduced cyt *f* of the cyt b_6f complex to P_{700}^{+} in PSI in the lumenal space of the thylakoid membrane. The presence of either plastocyanin or cytochrome c_6 depends on the relative availability of copper and iron in the culture medium [175–178]. The importance of these carriers is revealed by the fact that mutants that lack plastocyanin, like ac208 of *C. reinhardtii* which contains a frame shift mutation in the nuclear gene encoding plastocyanin [179], do not grow photoautotrophically. However, if cytochrome c_6 is expressed under copper deficient conditions in this mutant, it regains its ability to grow photoautotrophically, thus demonstrating that cytochrome c_6 can fully substitute for plastocyanin.

5.5.1. Plastocyanin

Plastocyanin is a small (97–105 amino acids) blue copper protein [180]. It is referred to as a type I copper protein according to its spectroscopic properties ($\varepsilon \sim 4900\ M^{-1}\ cm^{-1}$; reviewed in [181,182]). The three-dimensional structure of plastocyanin determined by X-ray crystallography [183–187] is an eight-stranded, antiparallel β-barrel with a single copper atom that is coordinated to two His, one Cys and one Met, in a hydrophobic region near the 'northern' end of the molecule. Although the amino acid sequences of plastocyanin from *C. reinhardtii* (98 amino acids) and land plants are only 61% conserved, the three dimensional structures are conserved (0.76 Å rms deviation in the Cα positions between the *C. reinhardtii* and poplar proteins [188]). The conserved structural features include the copper binding site, a negative patch and a flat hydrophobic surface. The coordination of the copper is in a distorted tetrahedral arrangement, which is reflected in a relatively high redox midpoint potential of the Cu^{I}/Cu^{II} couple, $E_0' = 370$ mV [180,189,190] compared to other type I copper proteins [191]. The hydrophobic patch is located at the 'north' end of the molecule and consists of about 8 residues that are conserved in *C reinhardtii* and other eukaryotic plastocyanins [191]. The solvent accessible surface area of this hydrophobic face is approximately 580 $Å^2$ for plastocyanin from *C. reinhardtii* [188]. His^{87}, one of the copper ligands, points out of this hydrophobic face into the solvent (Fig. 4). The fact that His^{87} is the only solvent-exposed copper ligand, together with its hydrophobic environment make it a likely site for electron transfer. The negative patch is located at the 'east' side of the molecule. The structural organization of the negative residues make up a distinctive face with a high concentration of negative charges. It is formed by the residues Asp^{42}, Glu^{43}, Asp^{44} and Asp^{53}, Asp^{59}, Glu^{85}, that contribute to a 'southern'

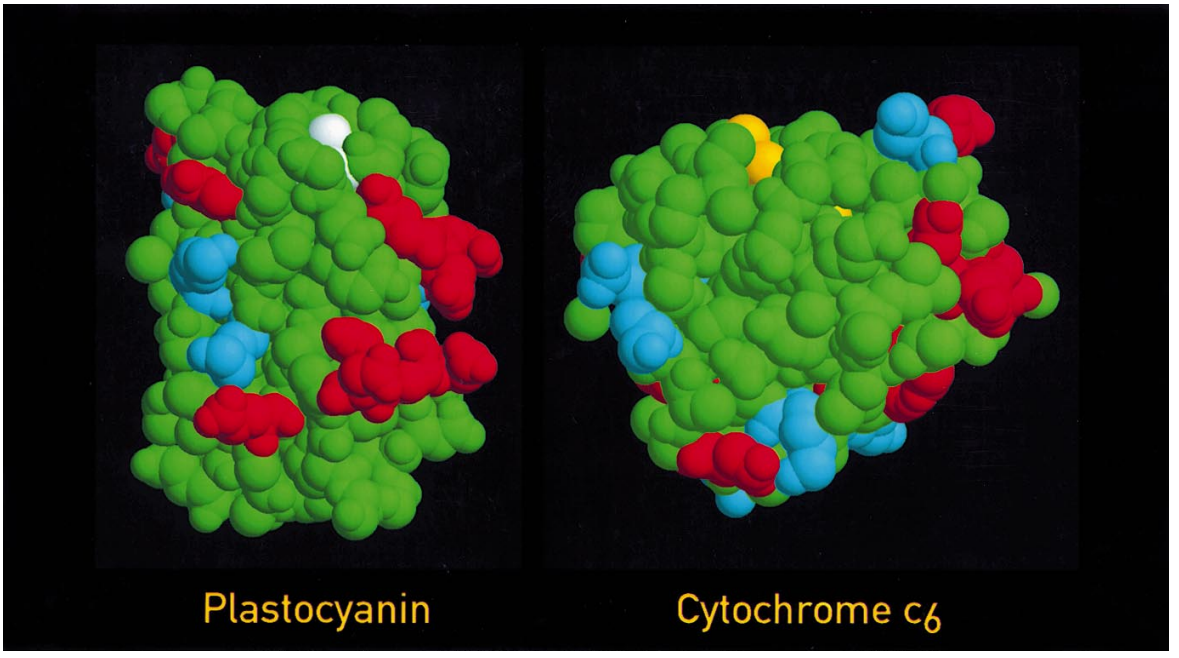

Fig. 4. Distribution of positive (blue) and negative (red) residues on the surface of plastocyanin [186] and cytochrome c_6 [199] from *C. reinhardtii*. Solvent exposed His^{87} of plastocyanin and the heme prosthetic group of cytochrome c_6 are shown in white and yellow, respectively. Rasmol 2.6 was used for graphical presentation of these structures.

and a 'northern' negative patch, respectively (Fig. 4). The former residues are conserved in all known eukaryotic plastocyanin sequences (see [188]), whereas the latter are only conserved in algal plastocyanin structures [185,186,191]. There is strong evidence that the flat hydrophobic surface and the negative patch cooperate to form recognition sites for the interaction with the physiological reaction partners of plastocyanin. Site directed mutagenesis of plastocyanin from land plants [192–195] suggest that binding to PSI is a 'two-step event', including a long-range electrostatic interaction involving the negative patches of plastocyanin and a docking mechanism, which brings the flat hydrophobic surface of plastocyanin in close contact with PSI, thereby allowing efficient electron transfer from copper via His^{87} to P_{700}^{+} [193]. Electrostatic interactions are also important for efficient electron transfer between plastocyanin and cytochrome *f* as shown by studies of site-directed mutants of *C. reinhardtii* (see Section 6).

Plastocyanin is encoded by a single nuclear gene in *C. reinhardtii* containing one intron [179]. The precursor has a two domain transit sequence that is required for correct targeting of plastocyanin to the lumen of the thylakoid membrane. Association of the metal cofactor occurs after the proteolytic processing of the plastocyanin precursor [196,197].

5.5.2. *Cytochrome c_6*

Cytochrome c_6 from *C. reinhardtii* is a small *c*-type cytochrome of 90 amino acids [198], that appears to have an unusually low apparent molecular mass of about 5 kDa on SDS-PAGE [178]. It is the first class-1 *c*-type cytochrome whose molecular structure has been determined to 1.9 Å resolution [199]. The overall structure consists of a series of α-helices and turns that surround the heme prosthetic group. A stretch of highly conserved residues among c_6-type cytochromes form a short two stranded anti-parallel β-sheet in the vicinity of the methionine which acts as axial ligand to the heme. The heme is covalently bound to the protein through thioether linkages between the sulfur atoms of cysteine residues 14 and 17 and the heme prosthetic group. The axial ligands to the heme are His^{18} and Met^{60}. The heme prosthetic group is buried in the protein interior, while the propionate D oxygen atoms are exposed to the solvent (Fig. 4). The area around the heme is almost nonpolar, which results in a hydrophobic 'northern' face of the molecule, comparable to that of plastocyanin

(see above). However, in contrast to plastocyanin, cytochrome c_6 possesses a positively charged Arg residue at position 66, which points out of the 'northern' face into the solvent (Fig. 4). Cytochrome c_6 has a redox potential at 370 mV [200], which is similar to that of plastocyanin, but relatively high compared to that of mitochondrial *c*-type cytochromes [201]. Three negative amino acids at position 69–71 (three Glu in *C. reinhardtii*) are conserved amongst cytochrome c_6 sequences in green algae [199]. These three negative residues are clustered at the 'east' side of the molecule (Fig. 4). Although cytochrome c_6 and plastocyanin have different primary structures and carry distinct redox cofactors, it appears that the distribution of acidic patches and hydrophobic surfaces are similar [186,199]. This may imply that they also interact with their physiological reaction partners in a similar way (see below).

Cytochrome c_6 is encoded by a single nuclear gene in *C. reinhardtii* containing two introns [202]. As for plastocyanin, the precursor protein contains a bipartite transit sequence typical of lumenal proteins [198]. It is thought that holocytochrome c_6 is formed by the ligation of the heme to the cysteinyl thiols after the translocation of apoprecytochrome c_6 into the lumenal space and proteolytic processing of the preprotein [203].

5.5.3. Regulation of the expression of plastocyanin and cytochrome c_6 genes by copper

C. reinhardtii cells respond to the availability of copper in the medium and accumulate either plastocyanin or cytochrome c_6 [178]. The gene encoding plastocyanin is constitutively transcribed independent of the copper concentration in the medium, but apoplastocyanin is rapidly degraded, in the absence of copper [178,204]. Transcription of the gene encoding cytochrome c_6 is initiated below a threshold level of copper and increases as Cu^{2+} decreases such as the total sum of plastocyanin and cytochrome c_6 per cell remains constant [205]. Expression of the cytochrome c_6 gene is maximal when the copper concentration in the medium is lower than 3 nM, but it is totally repressed 3–4 h after addition of copper [206]. The regulation of the copper responsive expression occurs at the level of transcription and the underlying mechanism involves two distinct elements in the 5′ upstream region of the cytochrome c_6 gene. These elements act as targets for transcriptional activators, which induce cytchrome c_6 transcription in the absence of copper [207]. Interestingly, one out of five plastocyanin-deficient mutants obtained after UV-mutagenesis accumulates apoplastocyanin at the expense of holoplastocyanin, indicating the existence of a new locus whose function is required for normal holoplastocyanin accumulation [208].

5.5.4. Electron transfer between plastocyanin/cytochrome c_6 and PSI

Measurements of the second-order electron transfer rate constants between PSI and plastocyanin or cytochrome c_6 from *C. reinhardtii* in vitro revealed values of 6.5×10^7 M^{-1} s^{-1} and 3.5×10^7 M^{-1} s^{-1}, respectively [138]. At high concentrations of both donor proteins, P_{700}^+ is reduced with first-order kinetics and a half-time of 3 μs [138]. In whole cells of the unicellular alga *Chlorella* the half-time of fast electron transfer between plastocyanin and PSI was estimated to be 4 μs [209]. It thus appears that PSI from *C. reinhardtii* allows fast electron transfer from both electron donors, which indicates that they are also interchangeable at the molecular level.

A first-order phase with a half-time of 8 μs was also detected for electron transfer from cytochrome c_6 to P_{700}^+ in the green alga *Monoraphidium braunii*, whereas no first-order μs phase could be detected when plastocyanin was the electron donor [210].

Results of crosslinking, using PSI particles from land plants or cyanobacteria, suggest that the PsaF subunit is involved in docking of plastocyanin and cytochrome c_6 to the PSI complex [211–213]. However, the specific deletion of the *psaF* gene in cyanobacteria did not affect photoautotrophic growth [214] and the in vivo measured electron transfer rate between cytochrome c_6 and PSI was the same as in wild-type [215]. The electron transfer reaction between plastocyanin and P_{700}^+ was shown to be considerably reduced within whole cells of the 3bF strain of *C. reinhardtii* which lacks the *psaF* gene [34]. The second-order rate constants of the electron transfer between PSI isolated from the PsaF-deficient mutant and plastocyanin or cytochrome c_6 are one to two orders of magnitude lower compared to those obtained with PSI from wild-type ([138]; see Fig. 5). Plastocyanin and cytochrome c_6 can be specifically

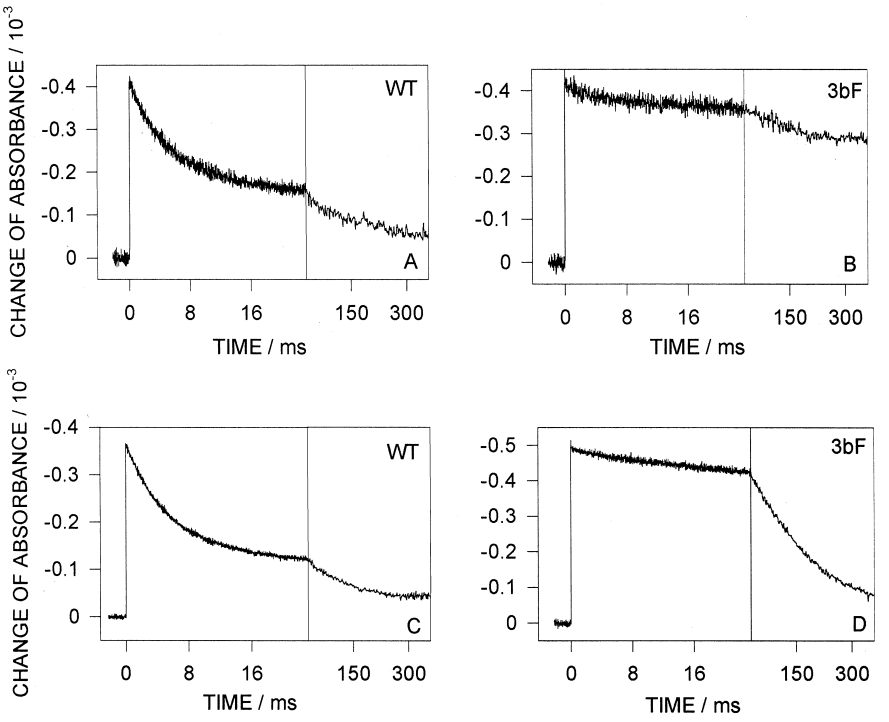

Fig. 5. Electron transfer from plastocyanin or cytochrome c_6 to P_{700}^+ of wild-type or PsaF-deficient PSI. Absorbance transients at 820 nm induced by a laser flash in PSI-particles from wild-type (A,C) or PsaF-deficient mutant (B,D) in the presence of 5 μM plastocyanin (A,B) or 5 μM cytochrome c_6 (C,D). Taken from [138] with permission.

crosslinked to PsaF, using PSI particles isolated from a wild-type strain of *C. reinhardtii*, whereas no crosslinking product is obtained when PSI particles lacking PsaF are used. Furthermore, cytochrome c_6 crosslinked to PSI reduces P_{700}^+ with a half-time of 3 μs, which is similar to the half-time observed with the authentic cytochrome c_6–PSI complex (see above), indicating that crosslinking does not significantly perturb the conformation of the authentic complex [138]. The conformation of the crosslinked and the authentic plastocyanin–PSI complex from spinach appears also to be similar based on the fast kinetics of reduction of $P700^+$ with a half-time of 13–15 μs observed in both cases [213]. These data demonstrate that the PsaF subunit of PSI in *C. reinhardtii* is required for fast electron transfer between plastocanin/cytochrome c_6 and P_{700}^+.

5.5.5. Donor side of photosystem I

According to the three-dimensional structure of PSI from the cyanobacterium *Synechococcus sp.* that has been determined by X-ray crystallography to a resolution of 4 Å [130,131], P_{700} of PSI is localized near the lumenal surface of the thylakoid membrane and is therefore accessible to the lumenal elec-

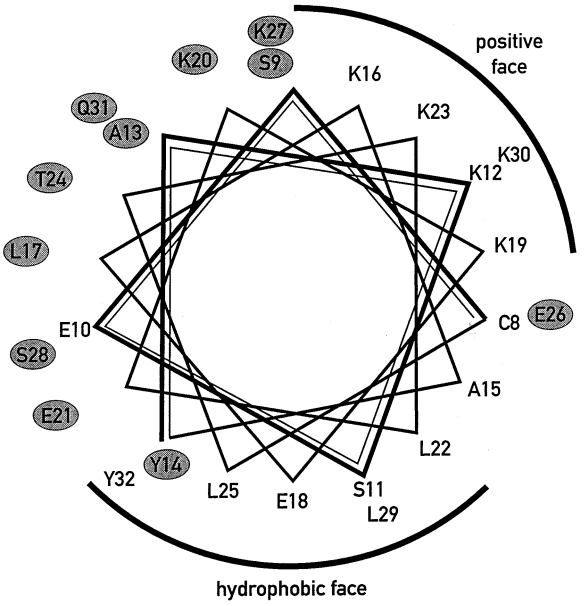

Fig. 6. α-Helical wheel representation of the N-terminal region of the PsaF subunit. Residues conserved between *C. reinhardtii* and *Spinacia oleracea* are shown in unframed letters.

tron donor proteins plastocyanin and cytochrome c_6. A value of 445 mV has been determined for the redox midpoint potential of the couple P_{700}^+/P_{700} in *C. reinhardtii* [216], which is about 30 mV lower than the value determined in spinach [217,218].

The *psaF* gene is nuclear encoded and is interrupted by three introns in *C. reinhardtii* [34]. The precursor has a two-domain transit sequence that directs PsaF to the lumen of the thylakoid membrane [219]. This lumenal subunit at the oxidizing side of PSI is required for efficient electron transfer from plastocyanin and cytochrome c_6 to P_{700}^+ (see Section 5.5.4). Mass-spectroscopic analysis of tryptic peptides of plastocyanin and of the crosslinked product of plastocyanin and PsaF from spinach revealed that the PsaF subunit appears to be crosslinked with one of its N-terminal Lys residues to the conserved acidic amino acids 42–44 and 59–61 of plastocyanin [195]. This region close to the N-terminal end of PsaF could form an amphipathic α-helix, whose positively charged face may interact with plastocyanin ([195], Fig. 6). Since this positively charged N-terminal domain is absent from PsaF of cyanobacteria it was suggested that this motif evolved for binding plastocyanin to PSI in a way which leads to the formation of a stable complex at a low concentration of the electron transfer donor, competent for fast electron transfer. Comparison of the N-terminal amino acid sequence of PsaF from spinach and *C. reinhardtii* reveals that lysines 12, 16, 19, 23 and 30 are conserved between both organisms. Using nuclear transformation of the PsaF-deficient mutant and site directed mutagenesis, modified PsaF was expressed and the PSI particles containing the altered protein were analyzed. Four lysine residues in the N-terminal domain of PsaF were altered to K12P, K16Q, K23Q and K30Q and the interactions between plastocyanin or cytochrome c_6 and PSI isolated from wild-type and the different 3bF transformants were investigated using crosslinking techniques and flash absorption spectroscopy. Whereas the change K12P had almost no effect on binding and electron transfer from plastocyanin or cytochrome c_6 to PSI, the change of K23Q affects crosslinking of plastocyanin to PSI and electron transfer from plastocyanin and cytochrome c_6 to PSI drastically. The corresponding electron transfer rate constants for both donors are reduced by almost one order of magnitude. A less efficient electron transfer was also observed from plastocyanin and cytochrome c_6 to PSI isolated from the 3bF transformants K16Q and K30Q, although these changes were 2- or 3-fold lower, respectively, than with PSI from the K23Q transformant. None of the mutations affected the half-life of the μs electron transfer performed within the intermolecular complex between the donors and PSI. These results indicate that the N-terminal domain of PsaF plays an important role in binding of both electron donors and suggest the existence of a rather precise recognition site for plastocyanin as well as for cytochrome c_6 that allows efficient electron donation to PSI [220].

5.6. *Role of ferredoxin as electron acceptor of photosystem I*

Ferredoxin is an iron–sulfur cluster containing protein that is involved in numerous electron transfer reactions. It plays an important role in photosynthetic organisms since it is involved in NADP photoreduction [221]. In addition, it provides reducing power to several enzymes, such as nitrite reductase, sulfite reductase, glutamate synthase as well as for lipid biosynthesis and for light regulation of chloroplastic enzymes [222]. Ferredoxin from *C. reinhardtii* has a visible spectrum comparable to that of land plants, with maxima at 330, 420 and 465 nm [200,223]. The circular dichroism (CD) spectrum of oxidized ferredoxin [223] and the EPR spectrum of reduced ferredoxin, with *g*-values of 2.060, 1.970 and 1.893, indicate that the *C. reinhardtii* enzyme belongs to (2Fe–2S) plant-type ferredoxin [224]. Measurements of the rate of $NADP^+$ photoreduction with pea thylakoids and ferredoxin from spinach and *C. reinhardtii* revealed that the algal ferredoxin is four times slower than its land plant homolog [223]. The enzymatic activity of isolated ferredoxin-NADP reductase from *C. reinhardtii* or from spinach in the ferredoxin-dependent reduction of cytochrome *c* exhibited similar activities with K_m and k_{cat} values of 0.8 mM and 12–13 s^{-1}, respectively [225]. The interaction between ferredoxin and PSI from *C. reinhardtii* was studied by flash induced spectroscopy. The reduction kinetics of ferredoxin by PSI are complex, with a submicrosecond and milliseconds first-order reduction phase and a following second-order

reduction phase [137], which is comparable to the analogous system in *Synechocystis* 6803 [226].

Ferredoxin is nuclear encoded in *C. reinhardtii*. Its cDNA sequence encodes a 126 amino acid precursor [227], consisting of the mature protein (94 amino acids with a molecular mass of 9908 Da) and a 32-amino acid transit peptide, that directs ferredoxin to the stroma of the chloroplast [223]. *C. reinhardtii* ferredoxin contains six cysteine residues. Four conserved cysteines, 37, 42, 45 and 75, are involved in binding the two iron atoms of the cluster [223,228]. Ferredoxin from *C. reinhardtii* has an excess of 7 negatively charged amino acids and therefore a net charge of −7. Two Glu residues at the C-terminus are conserved in the sequences of land plants, cyanobacteria and other green algae. Site directed mutagenesis and crosslinking results suggest that these residues play an important role in binding and electron transfer to ferredoxin-thioredoxin reductase [229], to FNR [230] and to the PsaD subunit of PSI [231].

Recent work on *C. reinhardtii* indicates that the PsaC subunit of PSI plays a crucial role in the binding of ferredoxin to the stromal side of PSI. In vivo degenerate oligonucleotide-directed mutagenesis of an internal loop of PsaC which is absent from two (4Fe–4S) ferredoxins identified K_{35} as a key interaction site between PSI and ferredoxin [232] (see Fig. 3A). This is based on the observation that the site directed mutations $K_{35}T$, $K_{35}D$ and $K_{35}E$ drastically affect electron transfer from PSI to ferredoxin as measured by flash-absorption spectroscopy, whereas the $K_{35}R$ change has no effect on ferredoxin reduction (see Table 1). Chemical crosslinking experiments show that ferredoxin interacts not only with PsaD and PsaE, but also with the PsaC subunit of PSI. Replacement of K_{35} by T, D, E or R abolishes ferredoxin crosslinking to PsaC and crosslinking to PsaD and PsaE is reduced in the $K_{35}T$, $K_{35}D$ and $K_{35}E$ mutants. The results of [232] show that PsaC provides an important residue for electrostatic interaction with ferredoxin to bring these two proteins in close contact for fast electron transfer between the terminal electron acceptors (F_A; F_B) and the iron–sulfur cluster of ferredoxin.

6. The cytochrome b_6f complex

The cytochrome b_6f complex mediates electron transfer between the PSII and PSI reaction centers in the thylakoid membranes of chloroplasts. It is a large multimeric integral membrane protein complex that oxidizes plastoquinol and reduces plastocyanin or cytochrome c_6 and participates in the establishment of the protonmotive force used for the generation of ATP.

6.1. Structure of the cytochrome b_6f complex

6.1.1. Subunit composition and cofactor binding

Purification and analysis of the b_6f complex from

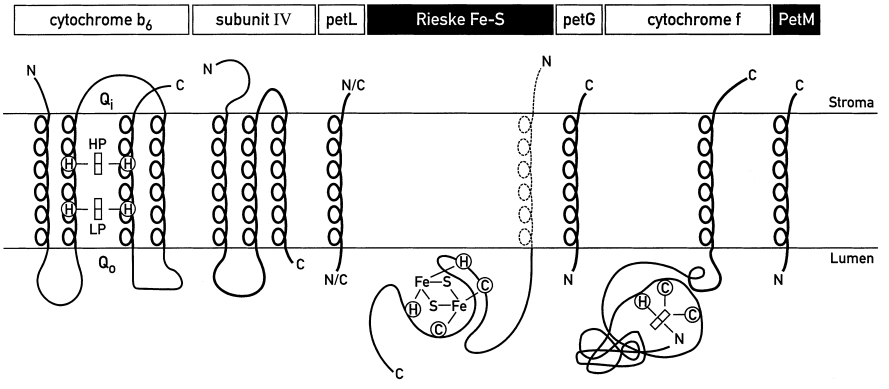

Fig. 7. Topology of the cytochrome b_6f subunits in the thylakoid membrane. N- and C-termini are indicated by N and C, encircled H and C stand for amino acids histidine and cysteine, HP and LP for high-potential and low-potential heme cyt b_6, respectively, and Q_o and Q_i indicate the sites for quinone oxidation and reduction, respectively. The bars stand for heme. The putative transmembrane N-terminal α-helix of the Rieske protein with the N-terminus at the stromal surface of the thylakoid membrane is shown in dashed lines. Chloroplast-encoded subunits are in open rectangles, whereas nucleus-encoded subunits are in shaded rectangles.

C. reinhardtii revealed that its high molecular mass subunits are very similar to their counterparts in land plants [233–235]. More recently, a new purification method of the b_6f complex has revealed the existence of three additional small molecular weight subunits. With a turnover rate of 250–300 s^{-1} the cyt b_6f complex isolated by this method has the highest measured rate of electron transfer from decylplastoquinol to plastocyanin [236]. Its activity is 3–4-fold higher than the electron transfer rates reported for isolated cyt b_6f complexes from spinach [237,238]. N-Terminal amino acid sequencing and Western blot analysis revealed that the purified complex contains seven subunits, which are present in stoichiometric amounts as determined by ^{14}C labeling experiments [236]: cytochrome *f* (*petA* gene product), cytochrome b_6 (*petB* gene product), subunit IV (*petD* gene product) and the Rieske iron sulfur protein (*petC* gene product) and three low molecular weight subunits: PetG (*petG* gene product), PetL (*petL* gene product), and PetM (*petM* gene product). The Rieske iron–sulfur protein and the PetM protein are nuclear-encoded, whereas the other subunits are chloroplast-encoded (Fig. 7).

Cytochrome *f* from *C. reinhardtii* with a molecular mass of 31.8 kDa calculated from its amino acid sequence [239,240] has a redox midpoint potential of 330 mV, slightly lower than that from spinach measured to be 350–370 mV [241,242]. Its α-band absorbance maximum at 554 nm is comparable to that of spinach cytochrome *f* at 554.5 nm [237]. A soluble redox-active 252 residue fragment of cyt *f* from turnip was crystallized and its structure determined at a resolution of 2.3 Å [243]. The polypeptide is organized into a large and small domain in which β structures are dominant. The axial ligands of the heme are His^{25} and the N-terminal amino group of the polypeptide [243]; for review see [244]. The sequence identity between the domains of turnip cyt *f*, seen in the crystal structure, and that of *C. reinhardtii* is 82%. A change of a charged amino acid in the predicted plastocyanin binding region (see [244]) is compensated in the sequence of *C. reinhardtii*, so that the structures of land plant cyt *f* and of *C. reinhardtii* are believed to be very similar. The mature cyt *f* has been proposed to have one transmembrane α-helix [245] with most of the polypeptide and the heme localized in the lumenal space of the thylakoid membrane.

Cyt b_6 with a molecular mass of 25.4 kDa [239] binds two *b*-hemes, b_H and b_L with redox midpoint potentials of −84 mV and −158 mV, respectively. The difference in the α-band maxima of the two *b*-hemes was reported to be 0.6 nm ($b_H = 564$ nm; $b_L = 563.4$ nm) in whole cells of *Chlorella* [246] and 1.8 nm ($b_H = 563.2$ nm; $b_L = 565$ nm) in spinach thylakoids [247]. Cytochrome b_6 from *C. reinhardtii* and tobacco are 89% identical [239]. The bis-histidine coordination of the two hemes is mediated by four His that are conserved in all cytochrome b_6 sequences available in the data bank. The two hemes are bound near each side of the membrane bilayer by the α-helices B and D, that are proposed together with two other α-helices (A and C) to be transmembrane domains (for review see [242]). Transmembrane α-helices bridged by heme have been proposed [248] and documented for mitochondrial cytochrome *b* polypeptides, since the molecular structure of the *bc* complex from beef-heart mitochondria is determined to 2.9 Å [249]. It appears to represent a common structural motif, since the α-hemes within the cytochrome oxidase, whose crystal structure is solved, are bound in a similar way [250,251]. In the FUD2 mutant of *C. reinhardtii*, a 12 amino acid duplication in the cd loop of cyt *b* (due to a 36 base pair duplication in the *petB* gene) leads to less efficient binding of the Rieske protein to the cyt b_6f complex and to increased degradation of the complex in aging cells [252].

The genes for cyt b_6 and subunit IV, *petB* and *petD*, are separated on the chloroplast genome of *C. reinhardtii* [239]. Both proteins appear to have partial homology. The degree of pseudo-identity of 13 b_6 and 16 subunit IV sequences is 79 and 63%, respectively [253]. The partial homology with a stretch of amino acids derived from the C-terminal sequence of cyt *b* from the mitochondrial bc_1 complex [254] was taken as evidence that subunit IV contains three transmembrane α-helices. The amino acid sequence of subunit IV of *C. reinhardtii* is highly conserved when compared with those from land plants (81%, [239]). However, in contrast to land plants it has a 21-residue N-terminal extension, resulting in a molecular mass of 17.4 kDa. Subunit IV from the isolated cyt b_6f complex of spinach could be

photoaffinity-labeled with a quinone derivative, thus suggesting a role in quinone binding [255].

The fourth high molecular weight subunit of the cyt b_6f complex is the Rieske iron–sulfur protein. The sequence of the nuclear gene, *petC* from *C. reinhardtii*, which is interrupted by four introns within the coding sequence, predicts a precursor protein of 206 amino acids with a transit peptide of 29 amino acids, resulting in a molecular mass of 18.6 kDa for the mature protein [256]. In vitro import studies of chimeric Rieske protein constructs into isolated pea chloroplasts indicated that the thylakoid targeting information is located within the N-terminal hydrophobic region of the mature protein [257]. The sequences CTHLGC and CPCHG near the C-terminus, thought to be putative ligands for the iron–sulfur clusters are conserved in other Rieske proteins. The crystal structure of the chloroplast Rieske protein revealed that ligands of the 2Fe–2S cluster are two Cys and two His [258], which was already indicated by spectroscopic data and mutagenesis experiments [259]. *C. reinhardtii* Rieske protein contains a hydrophobic segment of 25 residues near the N-terminus that is followed by a glycine rich-non-polar region, which is conserved along other chloroplast Rieske proteins [256]. The recent crystallization of bc_1 complexes from mitochondria of different species and the determination of its molecular structure indicate that the Rieske protein has a transmembrane segment at its N-terminus [249] [260]. However, biochemical results led to the conclusion that the Rieske protein is an extrinsic subunit of the cyt b_6f complex from *C. reinhardtii,* based on the fact that the Rieske protein can be extracted from the membrane with chaotropic agents and that this protein is unable to interact with detergent micelles as transmembrane protein segments do [261]. Further progress on crystallization and resolution of the structure of the cyt b_6f complex will clarify this issue.

The PetG polypeptide was first reported to copurify with the cyt b_6f complex from spinach [262]. It was also found in preparations of the complex from *C. reinhardtii* [235,236]. The sequence and location of *petG* in the chloroplast genome of *C. reinhardtii* was first reported by Fong and Surzycki [263]. The amino acid sequence identity between PetG from *C. reinhardtii* and land plants is 70% [262,264]. The amino acid sequence predicts a hydrophobic protein with a molecular mass of 4 kDa [264]. Deletion of the *petG* gene in *C. reinhardtii* produced strains that are unable to grow photoautotrophically and accumulate markedly reduced levels of the major cyt b_6f subunits [264], indicating that the protein is either needed for assembly or stability of the cyt b_6f complex in *C. reinhardtii*.

A second small hydrophobic protein PetM has been identified in the purified cyt b_6f complex of *C. reinhardtii* [235,236]. It is encoded by the nuclear gene *petM*, which predicts a polypeptide of 39 amino acids with a molecular mass of 4 kDa [265,266]. The deduced amino acid sequence of the precursor includes an N-terminal transit peptide of 60 amino acids that has stromal targeting features [265]. From proteolytic data and charge distribution of the amino acid sequence it is suggested that the N-terminus of PetM is lumenal [265].

The existence of a third small molecular weight hydrophobic subunit of the cyt b_6f complex, PetL, was derived from chloroplast reverse genetics in *C. reinhardtii* [267]. The 3.4-kDa PetL protein, which contains a potential transmembrane α-helix had escaped biochemical detection in earlier experiments. This protein was shown to copurify with the cyt b_6f complex of *C. reinhardtii* [236–267. The inactivation of the *petL* gene in *C. reinhardtii* revealed: (1) that the Rieske protein is selectively lost after isolation of the cyt b_6f complex from the petL-less mutant; (2) that the in vivo stability of the cyt b_6f complex is impaired; and (3) that the in vivo electron transfer through the complex is slowed, indicating that the *petL* gene product is an authentic subunit of the cyt b_6f complex [267].

An additional polypeptide with an apparent molecular weight of 19.5 kDa was found to copurify with the cyt b_6f complex from *C. reinhardtii* [233]. However, this protein is not present in the highly active cyt b_6f complex purified by Pierre et al. [236]. It is therefore not clear whether the 19.5-kDa protein is a loosely associated authentic subunit of the cyt b_6f complex from *C. reinhardtii*.

The existence of a fifth electron carrier, named 'G', which is in equilibrium with cyt b_H from the cyt b_6f complex has been proposed in unicellular algae such as *Chlorella* and *C. reinhardtii* [268], but not in chloroplasts from land plants [246]. Its difference spectrum, obtained from whole cells of *Chlorella*

suggests that it is a cytochrome *c′* [246]. This protein was not found to copurify with the isolated cyt b_6f complex [233,235,236]. Its possible role is discussed.

6.1.2. Chlorophyll a and carotenoids

The isolated cyt b_6f complex of *C. reinhardtii* was found to contain chlorophyll *a* and carotenoids as revealed by absorbance peaks at 667–668 nm and 460 and 483 nm, respectively [236]. As found for cyt b_6f preparations from *Synechocystis* PCC6803 [269] and spinach [237,270], the molar ratio of Chl *a* to cyt *f* is close to 1 [271]. Further evidence for the presence of a chlorophyll molecule in the cyt b_6f complex came from flash spectroscopy, where a red electrochromic shift (isobestic point around 669 nm) that occurred upon electron transfer at the Q_o site was attributed to a cyt b_6f complex bound chlorophyll molecule [272]. Resonance Raman spectroscopy of the isolated cyt b_6f complex from *C. reinhardtii* revealed that the chlorophyll is bound to the complex at a specific site [273]. Specific binding is also supported by the fact that free ^{3}H/Chl *a* added to *C. reinhardtii* thylakoid membranes at the time of solubilization does not associate with the cyt b_6f complex and that the rate of exchange of Chl bound to the cyt b_6f complex for free ^{3}H/Chl *a* in isolated cyt b_6f complexes is slow [273]. Interestingly, the cyt b_6f complex does not accumulate in a light-grown mutant strain of *C. reinhardtii* deficient in light-independent chlorophyll synthesis [273].

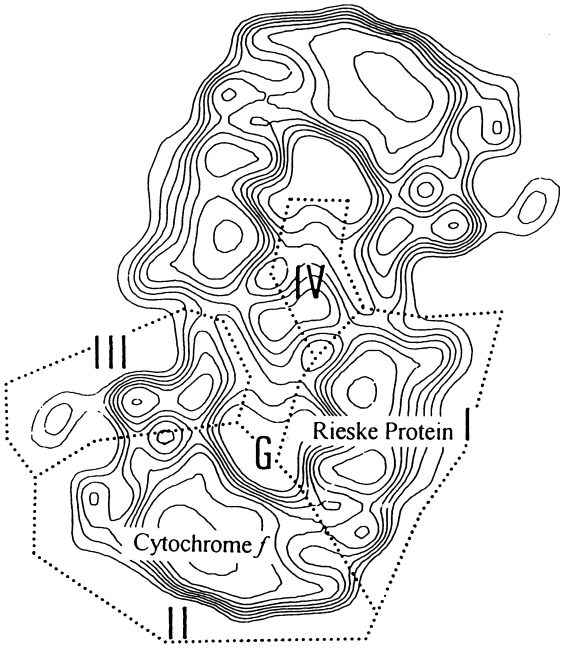

Fig. 8. Calculated projection map at 8 Å resolution derived from electron microscopy and image analysis of two dimensional crystals of the cyt b_6f complex from *C. reinhardtii* support the presence of cyt b_6f dimers. The main densities are numbered from I to IV; G stands for the central groove. The assumed positions of the extramembrane part of cytochrome *f* and the Rieske protein are indicated. Taken from [276] with permission.

6.1.3. Dimeric structure

Molecular weight determination [274] and stoichiometry measurements [236] of the purified cyt b_6f complex from *C. reinhardtii* revealed that it is a dimer with a molecular mass of 310 ± 46 kDa, in agreement with the value of 373 ± 28 kDa calculated for a dimer, taking into account two copies of each subunit, 36 lipids, 260 molecules of detergent and two chlorophylls [275]. Electron microscopy and image analysis of two dimensional crystals of the cyt b_6f complex showed optical diffraction peaks up to 10 Å and a calculated projection map at 8 Å resolution which supported the presence of cyt b_6f dimers [276] (see Fig. 8). PetL appears to be required for dimer formation [275]. The fact that the Rieske protein is lost during preparations of the b_6f complexes from petL-deficient mutants could be explained by monomerization of the b_6f complexes, since dimerization appears to stabilize the Rieske protein through contacts with both cyt *b* subunits in the dimer as revealed by the crystal structure of the cyt bc_1 complex [260].

6.2. Electron transfer and proton translocation in the cyt b_6f complex: Q-cycle versus semiquinone cycle

Electron transfer and proton translocation in the cyt b_6f complex are not fully understood. Two models have been proposed for these processes, the Q-cycle [277], as modified by Crofts et al. [278] and the semiquinone cycle [279]. Both models postulate the existence of two electron transfer chains operating in the cyt b_6f complex: the plastoquinol–Rieske–cyt *f* high potential chain and the plastoquinol cyt b_L–cyt b_H low potential chain (Fig. 9). These models also assume that the cyt b_6f complex contains a site for plastoquinol oxidation, Q_o, near the lumenal side of the thylakoid membrane and a site for plastoqui-

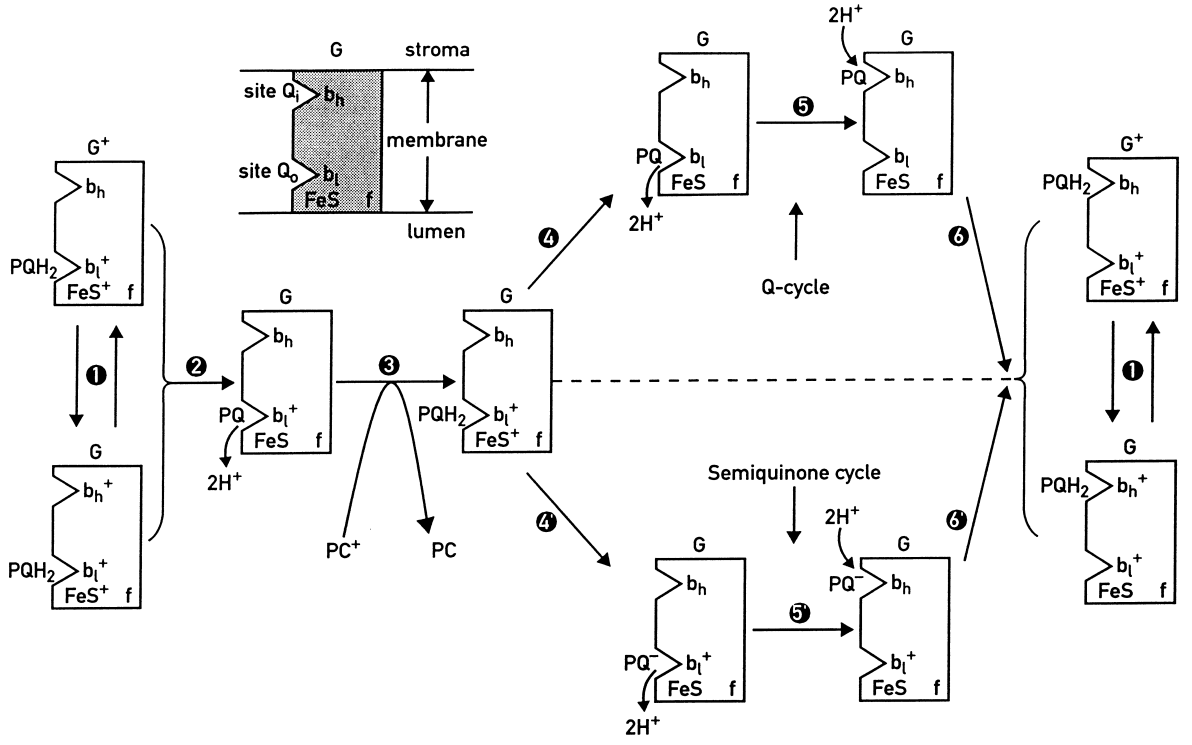

Fig. 9. Comparison of Q-cycle (steps 1–6) and semiquinone-cycle (steps 4′–6′) models as possible mechanism of charge translocation in the b_6f complex. See discussion in text. Adapted from [290].

none reduction, Q_i, near the stromal side of the membrane. In addition a protein factor 'G' has been proposed to be in equilibrium with cytochrome b_H in green algae (see above; Fig. 9, 1, [246]).

According to the Q-cycle model, the oxidation of plastoquinol at the Q_o site occurs through a concerted reduction of cyt b_L and the Rieske Fe–S center and a subsequent rapid reduction of cyt b_H accompanied by the release of two protons on the lumenal side (Fig. 9, 2). Reduction of plastocyanin releases the electron from the high potential chain (Fig. 9, 3). Oxidation of a second plastoquinol at Q_o leads to reduction of both cyt b_L and cyt b_H and the Rieske–cyt f high potential chain (Fig. 9, 4). Plastoquinone is then reduced at the Q_i site by oxidation of cyt b_L and cyt b_H thereby creating an electrogenic electron transfer from Q_o to Q_i (Fig. 9, 5). In this scheme the reduction of plastoquinone at Q_i requires two consecutive turnovers of the cyt b_6f complex.

Support for the Q-cycle has arisen from the study of flash-induced electrochromic absorbance changes at 515 nm in dark-adapted cells, which provide a measure of the thylakoid membrane potential changes [280,281]. Under reducing conditions a short flash induces a fast increase of the membrane potential (phase a, $t_{1/2} < 1$ μs) that is associated with the charge separation within the PSI reaction center and a slow increase in the ms-range (phase b) [281,282]. In isolated chloroplasts, this slow electrogenic phase could be correlated with turnover of the cyt b_6f complex [283,284]). Evidence that it represents an electrogenic electron transfer from Q_o to Q_i is based on the observation that under repetitive-flash illumination in *Chlorella* in the presence of the Q_i inhibitor NQNO, only photoreduction, but not photooxidation of cyt b occurs [285], as also reported for cyt b_6f complexes from land plants [286]. Other inhibitors of Q_o, like DNP-INT, inhibit the electrogenic phase b [287]; see [242], for comparable effects of inhibitors DBMIB, UHDBT, sigmatellin). However, it is not yet clear whether phase b is indeed due to interheme electron transfer or to transfer of protons to the lumenal side of the membrane (see [244]).

The H^+/e^- ratio for cyt b_6f complex in energized thylakoid membrane is a matter of discussion, since the extra redox loop of the Q-cycle should produce a

H^+/e^- ratio greater than one for the electron transfer from PSII to PSI. However, as pointed out by [244] the H^+/e^- ratio is not a proof for an operating Q-cycle, since the mammalian cytochrome *c* oxidase pumps protons and electrons with a H^+/e^- ratio of 2 without a Q-cycle.

The concerted oxidation of a plastoquinol molecule at the Q_o site by oxidized Rieske iron–sulfur center and oxidized cyt *b* could be demonstrated in spinach thylakoids at high ambient redox potential by the fact that the reduction of these two electron carriers occurs with similar kinetics (6–10 ms) after flash excitation [288]. The binding constant of plastoquinol to the Q_o site was estimated at 2×10^4 M^{-1} based on duroquinone/plastoquinone competition experiments with isolated spinach thylakoids [241]. A similar value was estimated under in vivo conditions in *C. reinhardtii* by comparing the measured and calculated oxidation rate at the Q_o site in wild-type and the FUD2 mutant [252]. In the FUD2 mutant, the oxidation rate at the Q_o site was found to be 100 times lower than in wild-type cells, which resulted in an 8-fold reduction of the electron transfer through the cyt b_6f complexes. The equilibrium constant for the concerted oxidation of plastoquinol was calculated and experimentally determined to be 10 in spinach [288]. Similar calculations result in an equilibrium constant that is near unity in *C. reinhardtii*, since the midpoint potentials of the cyt f^+/cyt *f* and cyt b_H^+/cyt b_H couples are found to be 20–30 mV lower in *C. reinhardtii* than in spinach [236,247]. However, since the difference of redox midpoint potential between cyt *f* and plastocyanin ($E_m = 360$ mV, [180]) is 30 mV in *C. reinhardtii* and the in vivo rate of electron transfer between cyt *f* and PSI is much faster than the limiting step of electron transfer between PSII and PSI [282], the driving force for the concerted oxidation of plastoquinol will further increase. In green algae, the hemoprotein 'G' is suggested to be in equilibrium with the low potential chain with a midpoint potential about 20–30 mV higher than that of cyt b_H [246,268]. The electron transfer between 'G' and cyt b_H would further increase the difference in the standard electrochemical potential. This consideration is supported by the fact that the reduction of cyt *b* is faster in the presence of 'G' than in its absence in *Chlorella* [246].

The mechanism of plastoquinone reduction at the Q_i site is unclear. The fact that the rate of cyt *b* oxidation after a single flash is greater than the rate-limiting step of linear electron transfer (reviewed in [244]) led to a model where plastoquinone reduction occurs by a concerted oxidation of both *b*-hemes, assuming that single reduced cyt b_H is stable [288,289].

The semiquinone cycle model [279] proposes that after the first concerted oxidation of plastoquinol at Q_o, the second plastoquinol is oxidized by the high potential chain after oxidation of cyt *f* by plastocyanin (Fig. 9, 4′). The plastosemiquinone radical is then transferred to Q_i, where it oxidizes cyt b_H (Fig. 9, 5′). Interestingly, the crystal structure of the cytochrome bc_1 complex reveals an internal hydrophilic cavity within the dimeric structure [249], which could form a channel for guiding the charged semiquinone from site Q_o to site Q_i. Evidence for the electrogenic transfer of a plastosemiquinone radical is based on the fact that under reducing conditions, when the plastoquinol pool is expected to be fully reduced, the slow electrochromic phase b ($t_{1/2} \sim$ 3 ms) precedes the photooxidation of cyt *b* in *Chlorella* and *C. reinhardtii* [290,291]. In contrast, the Q-cycle model predicts a lag of phase b, because the reduction of cyt b_L has to precede the reduction of plastoquinone at Q_i which gives rise to the electrogenic step. The slow electrogenic phase b becomes biphasic in the presence of NQNO, the fast phase is insensitive to the inhibitor and is associated with cyt *b* reduction, while the second phase is dependent upon the inhibitor concentration and is related to cyt *b* oxidation [285]. Under conditions where a *C. reinhardtii* mutant CC-1729 lacks plastocyanin and cytochrome c_6 (grown at 31°C) only a fast μs electrochromic signal is observed under fully reducing conditions in the presence of HQNO, proving that the slow electrogenic phase originates from the cyt b_6f complex [291]. However, NQNO inhibits phase b by about 60% [290] and diminishes the ratio *R* between the initial rate of phase b and of cyt *b* reduction compared to measurements without inhibitor. This is interpreted in favor for the semiquinone cycle since NQNO binds to site Q_i, which would prevent the transmembrane movement of the plastosemiquinone and therefore diminish phase b that now results exclusively from the reduction of cyt *b*. The SQ-cycle could function as an initiation reaction under highly

reducing conditions to allow a Q-cycle mechanism to continue. Since the isolated cyt b_6f complex is active as a dimer, one could also consider the possibility that two plastosemiquinones are produced at Q_o site of a functional dimer, then disproportionate so that the quinone formed could start a Q-cycle at the Q_i site. However, the fact that the maximum amplitude of phase b is reached under reducing conditions in *Chlorella* when only 10% of PSI centers are hit by a flash does not support a mechanism of this sort [290].

Experimental evidence against the SQ-cycle has arisen from work with spinach thylakoids. Under reducing conditions measurements of fast rereduction of cyt b_H at 563 nm after flashes of low intensities revealed that a significant fraction of cyt b_H was oxidized [292]. The authors propose a 'chain reaction' type model to explain the turnover of the cyt b_6f complex under reducing conditions. In this model a small fraction of cyt b_6f complexes contains cytochromes that are oxidized under these conditions, allowing a normal Q-cycle turnover which produces plastoquinone that in turn will open more centers.

6.3. Site directed mutagenesis of subunits of the cyt b_6f complex

Since deletion mutant strains are available for all five chloroplast-encoded subunits in *C reinhardtii* (see above) expression of modified subunits is feasible. So far, site-directed mutagenesis has been reported for the *petA* gene encoding cytochrome *f* and the *petB* gene encoding cytochrome b_6.

Leu^{204} of cyt b_6 was altered to Pro [293], to mimic the situation found in the *petB* genes of maize and tobacco, in both vascular plants, the proline codon is edited to a leucine codon at the RNA level [294,295]. The L204P change resulted in a non-photosynthetic phenotype with the inability to assemble the cyt b_6f complex [293].

As part of the high potential chain, cyt *f* is oxidized by plastocyanin or cytochrome c_6. At the interface of the large and the small domain of cyt *f* a positively charged motif is formed, including Lys^{58}, Lys^{65} and Lys^{66} (large domain) and Lys^{188} and Lys^{189} (small domain) (see [244]). This interface is believed to interact with the two electron acceptors. Site directed mutagenesis of the three Lys of the large domain to Gln, Ser and Glu, respectively and expression of the altered proteins in *C. reinhardtii* did not drastically change the amplitude and the kinetics of flash-induced photooxidation of cyt *f* in vivo compared to wild-type [296]. The half-time of cyt *f* photooxidation and cyt *f* dark reduction in vivo increased from 0.2 to 0.25 ms and 5–6 to 11–12 ms when comparing wild-type to the quintuple Lys mutant (Lys^{58}Gln-Lys^{65}Ser-Lys^{66}Glu-Lys^{188}-Asn-Lys^{189}Gln) [296]. The rather small effect on the cyt *f* photooxidation is interpreted as a consequence of a relatively high ionic strength environment in the thylakoid lumen, which would weaken the eletrostatical interaction between the negatively charged plastocyanin and the positively charged region in cyt *f* [296]. However, in vitro measurements of cyt *f* photooxidation using plastocyanin as electron acceptor indicate that these basic residues of cyt *f* are implicated in the electrostatic docking at low ionic strength [297].

Change of Tyr^1, whose α-amino group serves as the sixth ligand to the heme, to Pro gave rise to a strain that did not grow photoautotrophically, whereas strains with Tyr^1 changes to Trp, Phe or Ser were comparable to wild-type [298]. The lack of the sixth ligand in the Tyr^1 Pro mutant (since Pro does not posses a free α-amino group) results in the loss of cyt *f* and gives rise to a non-functional cyt b_6f complex [298]. The effect of this mutation is thus similar to that observed for cyt *f* deletion mutants which lack the cyt b_6f complex [299]. The fact that the change of Tyr1 to another aromatic or into a non-aromatic amino acid did not affect the rates of photooxidation and photoreduction of cyt *f* indicates that the side chain of the amino acid providing its α-amino group as the sixth ligand does not play a critical role for electron transfer to the heme [298]. Interestingly the change of Pro^2 to Val had a dramatic effect on the rate of photoreduction of cyt *f* (10-fold reduced), while the rate of photooxidation of cyt *f* was unaffected. This suggests an impaired electron transfer between the Rieske iron–sulfur protein and cyt *f* in the mutant, which is supported by the fact that the electron transfer between these two proteins becomes rate-limiting in overall photosynthetic and growth rates at high light intensities [298].

6.4. Assembly of the cytochrome b_6f complex

The isolation and analysis of numerous mutants deficient in cytochrome b_6f activity has provided important insights into the assembly of this complex. Mutants deficient in the synthesis of the chloroplast-encoded subunits cytochrome *f* and subunit IV were shown to be unable to accumulate the other subunits of the complex [233]. In contrast, in the absence of the Rieske protein, the chloroplast-encoded subunits accumulated to a significant extent in the thylakoid membranes [233]. These results suggest that the chloroplast-encoded subunits form a subcomplex which is deeply embedded in the thylakoid membrane and form an anchor for the Rieske protein which has been proposed to be a peripheral protein in *C. reinhardtii* [256,261].

These studies have been extended by taking advantage of the chloroplast transformation technology to produce deletion strains, each lacking either *petA*, encoding cytochrome *f*, *petB*, encoding cytochrome b_6, or *petD*, encoding subunit IV [299]. In the absence of cytochrome *f* or subunit IV, the transcript levels and the rate of synthesis of cytochrome b_6 were comparable to wild-type, but the protein was highly unstable. Similarly, in the absence of cytochrome *f* or cytochrome b_6, the transcript levels and the rate of synthesis of subunit IV were barely affected as compared to wild-type and the protein was unstable. The half-time of subunit IV in the absence of cytochrome b_6 was considerably shorter than in the absence of cytochrome *f*. This agrees with the finding of a subcomplex between cytochrome b_6 and subunit IV of limited stability in the absence of cytochrome *f*. These results are not unexpected since cytochrome b_6 and subunit IV correspond to the N- and C-terminal parts of the major cytochrome *b* subunit of the cytochrome b_6 complexes in photosynthetic bacteria and mitochondria [300].

In the absence of cytochrome b_6 or subunit IV, cytochrome *f* was found to accumulate to only 10% of wild-type levels [299]. Surprisingly, the rate of synthesis of cytochrome *f* was also markedly reduced under the same conditions, although the *petA* mRNA level was unaffected. Furthermore, the produced cytochrome *f* was stable. Thus the stoichiometric accumulation of the chloroplast-encoded subunits of the cytochrome b_6f complex is controlled by two different mechanisms. A post-translational regulation which involves the proteolytic degradation of unassembled cytochrome b_6 and subunit IV and a co-translational regulation which prevents overproduction of cytochrome *f* in the absence of the other subunits. Thus cytochrome *f* behaves as the core subunit of the cytochrome b_6f complex through which stabilization of its assembly partners occurs. Removal of the C-terminal 35 amino acids of cytochrome *f* containing the membrane-anchoring segment gave rise to a soluble cytochrome *f* which accumulated in the lumen to the same level as wild-type cytochrome *f* [300]. The rate of synthesis of this truncated cytochrome *f* was no longer diminished in the absence of either cytochrome b_6 or subunit IV, suggesting that the C-terminal region of cytochrome *f* deleted in the mutant contains a target site for the control of its translation by subunit IV and cytochrome b_6. Alternatively, there might be an early post-translational stage at which a transient form of membrane-bound cytochrome *f* is highly sensitive to proteolysis.

The synthesis of holocytochrome *f* is a multistep process which requires the translation of the precursor apoprotein and two maturation events, the cleavage of the N-terminal signal peptide and the covalent ligation of the *c*-heme. The crystal structure of a soluble form of cytochrome *f* revealed that these two events may be tightly coupled, since one axial ligand of the *c*-heme is provided by the N-terminus of the mature apoprotein [243]. Site-directed mutagenesis and chloroplast transformation were used to modify the cytochrome *f* processing site. Although this modification delayed the processing of the cytochrome *f* precursor, heme binding to both the precursor and the processed form of cytochrome *f* still occurred [301]. All of these forms were found to be assembled within cytochrome b_6f complexes which were inactive, presumably because of improper orientation of the heme. Furthermore, destruction of the heme-binding site of cytochrome *f* did not affect processing of the precursor, although the protein was highly unstable [301]. This is in marked contrast to other studies which showed that heme attachment to mitochondrial cytochrome c_1 is required for proper processing of this protein [302].

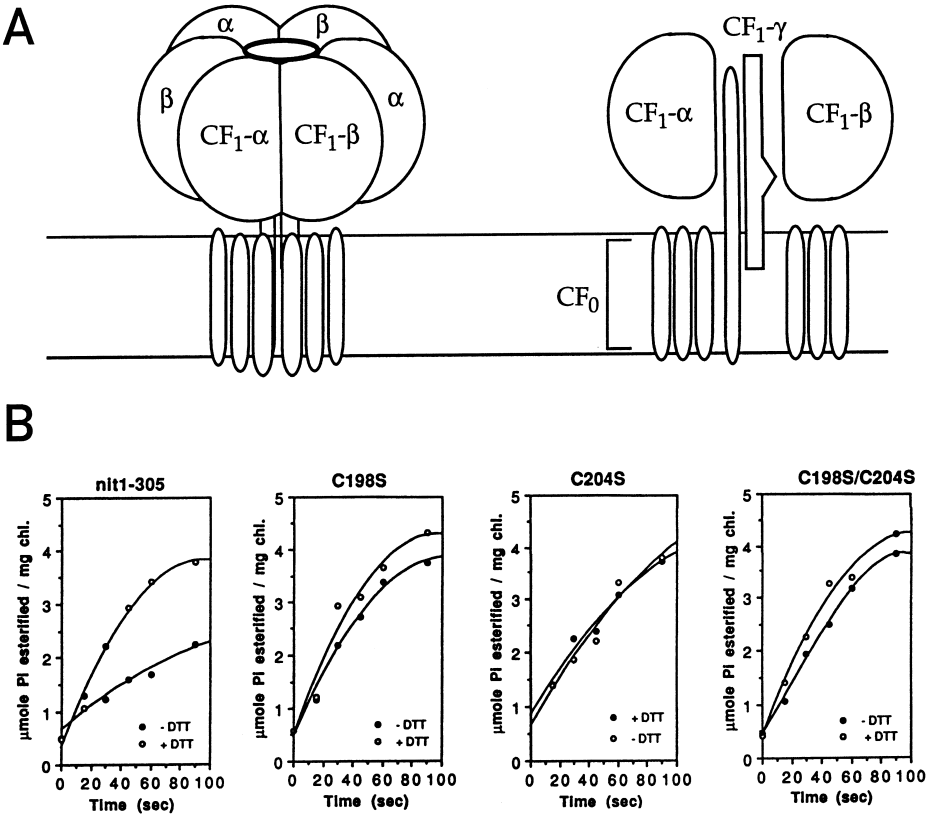

Fig. 10. (A) Schematic model of ATP synthase. As shown on the left, CF_1 is a hexamer of alternating CF_1-α and CF_1-β subunits. CF_0 is embedded in the thylakoid membrane. A cut-away view is shown on the right to highlight the location of CF_1-γ in the axis of CF_1. We have not included other subunits whose positions are unknown. (B) Dithiol regulation of ATP synthesis by thylakoid membranes from wild-type or CF_1-γ mutants. The wild-type enzyme is activated roughly two-fold by DTT, but the Cys→Ser mutants (AtpC-C198S, AtpC-C204S, AtpC-C198S/C204S) do not exhibit this regulation. These cysteine residues form a disulfide bond that attenuates activity; reduction of this bond by thioredoxin is thought to alleviate this inhibition in vivo. Taken with permission from [345].

7. ATP synthase

The chloroplast ATP synthase complex is part of a large family of F_1·F_0 ATPases that are also present in eubacteria and mitochondria. The chloroplast enzyme (CF_1·CF_0), like the other members of this family, has two sectors: the membrane-embedded CF_0 through which protons flow from the thylakoid lumen, and the stromal extrinsic CF_1 where ATP is synthesized or hydrolyzed (see Fig. 10A). CF_1, which is understood much better than CF_0, is composed of five subunits, present with a stoichiometry of $\alpha_3\beta_3\gamma_1\delta_1\varepsilon_1$. These subunits are analogous to the five subunits of the eubacterial ATP synthase. The subunits of the mitochondrial enzyme (MF_1) are not completely analogous: MF_1-δ is equivalent to CF_1-ε, MF_1-ε has no equivalent, and the analogous subunit of CF_1-δ is oscp (oligomycin-sensitivity conferring protein [303,304]).

The mechanism of ATP synthesis has long been postulated to be coupled to the storage of energy in a proton gradient across the thylakoid (or inner mitochondrial or inner eubacterial) membrane [305]. The mechanism of this coupling has not been clearly elucidated, but the generally accepted hypothesis is that the flow of protons through F_0 drives the rotation of an asymmetric subcomplex of subunits relative to the subunits that catalyze ATP synthesis, and that this rotation results in a cyclic change of the conformation of the three catalytic sites where ATP is formed spontaneously (with an equilibrium near unity for the bound substrates and products); energy is required mainly to change the conformation suffi-

ciently to break the tight binding of ATP (reviewed in [306–308]).

The recently solved structure of MF_1 [309] has brought us a long way towards understanding this mechanism in greater detail. MF_1 is in the form of a flattened sphere, the MF_1-α and MF_1-β subunits arranged alternately, like slices in an orange, with an internal shaft filled by the MF_1-γ subunit (see Fig. 10A). As had been previously divined, the nucleotide binding sites are at the interface of adjacent F_1-α and F_1-β subunits, with one subunit providing the vast majority of contacts. As expected from the similarity of their sequences (α and β are 20% identical), the F_1-α and F_1-β subunits have a similar fold, but all three F_1-α subunits bind ATP (in this case, AMP-PNP) in a non-catalytic manner, while the three F_1-β sites are strikingly different: one binds AMP-PNP, the other binds ADP, and the third site is empty because of a large deformation of its structure. The difference in the three sites can be rationalized by their different relationships to the F_1-γ subunit, which forms the axis of the internal shaft with two very long α-helices paired together in a coiled-coil. In the MF_1-β subunit with the empty site, part of the structure is disrupted due to the formation of new hydrogen bonds between MF_1-γ and MF_1-β near the nucleotide-binding site. Note that F_1-γ and the asymmetry that it induces are not strictly necessary for ATPase activity, as $\alpha_3\beta_3$ hexamers retain catalytic potency despite the fact that the F_1-β sites are identical (i.e. the structure has perfect 3-fold symmetry), although catalytic cooperativity is lost [310]. Thus, it is probably closer to the truth to say that F_1-γ (and perhaps other single-copy subunits) drive the interconversion of the catalytic sites in a directional manner ('rotational catalysis').

7.1. Biochemical and molecular analyses of ATP synthase

Selman-Reimer et al. [311] first purified and biochemically characterized *C. reinhardtii* CF_1, extracting it from thylakoid membranes with either EDTA or chloroform. The chloroform-extracted enzyme lacks CF_1-δ but has a higher ATPase specific activity than the EDTA-extracted enzyme. Unlike land plant CF_1, the *Chlamydomonas* enzyme is not activated by heat or proteolysis, is activated only about two-fold by DTT, and prefers Mg^{2+} to Ca^{2+} as the divalent cation. The other characteristics of *Chlamydomonas* CF_1 are more like those of land plants. The activation energy of the ATPase reaction is estimated to be 17 kcal/mol. The apparent K_m for MgATP is 0.2 mM, and the CF_1-ATPase activity is inhibited by free divalent cations. Additionally, an anti-CF_1 (spinach) antibody inhibits both ATP synthesis in thylakoids and ATP hydrolysis in purified CF_1. The subunit stoichiometry of the chloroform-extracted CF_1 is $\alpha_3\beta_3\delta_1\varepsilon_1$ [312]. The lack of a requirement for activation by heat or proteolysis makes *Chlamydomonas* CF_1 an attractive system for structure–function studies.

Piccioni et al. [313] also purified CF_1 by chloroform extraction, and found that the CF_1-α subunit in *C. reinhardtii* is smaller than CF_1-β (54 kDa, compared to 65 kDa in the spinach enzyme [314]). Lemaire and Wollman [315] purified both CF_1 and CF_1·CF_0 from *C. reinhardtii* and were able to identify all nine subunits by either immunological cross-reaction or localization of the site of synthesis (i.e. cytosolic or chloroplastic ribosomes), although the assignment of CF_0-I and CF_0-IV was somewhat arbitrary. Both of these analyses were aided by the availability of mutants that fail to synthesize ATP synthase. For example, they were able to see the loss of polypeptides of the same molecular weight as the subunits of the purified enzyme on SDS-PAGE gels of thylakoid membrane proteins from the FUD50 mutant [315], which fails to accumulate ATP synthase due to a deletion in *atpB*.

As in land plants, all of the ATP synthase subunits are encoded in the *C. reinhardtii* chloroplast genome, except for CF_1-γ, CF_1-δ, and CF_0-II [316]. The genes have been sequenced for CF_1-α (*atpA* [314]), CF_1-β (*atpB* [317]), CF_1-γ (*atpC* [318,319]), and CF_1-ε (*atpE* [316]). Unlike the situation in land plants [320], none of the plastid *atp* genes are organized together into operons in *C. reinhardtii* [316,317]. This has the advantage that mutations in specific structural genes will not have 'polar' effects upon the synthesis of the other structural genes, as often happens in prokaryotic operons.

Fiedler et al. [321] have recently developed new cell wall-less (cw15) strains deleted of the *atpA* or *atpB* genes and characterized them. The *cw15* phenotype allows gentle isolation of thylakoids with a Yeda

press, which tends to preserve photophosphorylation activity. With plasmids containing these genes along with flanking sequences to direct homologous integration and antibiotic-resistance markers (to either spectinomycin or kanamycin) to select for such integrations [322], the production of site-directed mutants in either gene should be facilitated in the future.

7.2. Analysis of random mutants deficient in ATP synthase activity

Woessner et al. [323] analyzed a set of photophosphorylation mutants and organized them into groups based upon complementation and recombination; both methods yielded similar results. The linkage analysis was no doubt aided by the fact that the *atp* genes are not clustered on the plastid genome. Interestingly, the vast majority of the mutants map to the *atpB* gene, which encodes CF_1-β. In a later study, Lemaire and Wollman [324] examined representative mutants from each complementation group. They availed themselves of a useful in vivo technique to assay for ATP synthase: after an actinic flash, an electrochromic shift (475–515 nm) is observed due to the generation of a proton gradient, and its decay (in the ms time scale) is due to the action of ATP synthase. The various mutants were classified according to deficiencies in the synthesis of specific subunits. FUD50, as well as many other mutants, fails to synthesize CF_1-β. FUD16, the only mutant in *atpA*, overproduces CF_1-α and CF_1-β, but assembles $CF_1{\cdot}CF_0$ poorly (see below). FUD17 cannot synthesize CF_1-ε, which was later shown to be due to a frameshift mutation in *atpE* [325]. FUD18 and FUD23 are deficient in CF_0-I or CF_0-IV, respectively (assuming that their arbitrary assignment was correct); as these are chloroplast mutations, they are most likely in the *atpF* or *atpI* genes, respectively. There are also several mutations in nuclear genes that affect the expression of *atp* genes; for example, F54 does not express CF_1-α and ac46 fails to synthesize CF_0-III and IV.

The existence of mutants affected in the expression of specific ATP synthase genes allowed an analysis of the consequence of the absence of particular subunits [324]. CF_1-β can accumulate to a certain extent in the absence of CF_1-α, but it is unable to attach to membranes. CF_1-β is normally synthesized in excess of CF_1-α, but the excess is subsequently degraded. However, CF_1-α is synthesized, but does not accumulate in the absence of CF_1-β or in mutants deficient in other subunits. Likewise, CF_1-ε is poorly synthesized in mutants lacking CF_1-α, CF_1-β, CF_0-I, or CF_0-III. Both CF_1-α and CF_1-β can accumulate to 15–25% in mutants lacking CF_0 subunits, but they are poorly attached to membranes. The smallest effect is observed in CF_0-IV mutants and the largest in ac46 (CF_0-III, IV missing). In the absence of CF_0-I, newly synthesized CF_1-α/β binds transiently to membranes, but does not accumulate there. In the absence of CF_1, the plastid-encoded CF_0 subunits (I, III, and IV) are synthesized and inserted into membranes, but they fail to accumulate [315].

Unfortunately, few point mutants have been found among the collection of photophosphorylation mutants. Robertson et al. [326] found that two mutants in *atpB* (ac-u-c-2-9, 29) had no gross rearrangements, but single nucleotide changes leading to single amino acid substitutions: L47R and K154N (both of these residues are conserved in all F_1-β subunits). The idea that these point mutations were the root cause of the photophosphorylation defect was borne out by the emergence of photosynthetic revertants that had restored the original codons. Both mutants transcribe and translate *atpB*, but accumulate only 3% of the polypeptide; they have no detectable CF_1-α or CF_1-γ. Thus, they are affected in assembly and/or stability of CF_1. FUD16 is the only photophosphorylation mutant with measurable in vivo activity [324], and is the only mutation known in *atpA*. Interestingly, a later study showed that FUD16 has two adjacent point mutations (I184N, N186Y) that caused it to be overproduced [327]. As FUD16 can be complemented by a 1-kb chloroplast DNA fragment in which these were the only changes, it is safe to assume that the phenotype is due to mutation of these two strongly conserved residues (the IXN motif is 7 residues C-terminal of the nucleotide-binding motif, GXXXXGKT, which is conserved in all F_1-α/β subunits). Strangely, FUD16 overaccumulates CF_1-α and CF_1-β, but only a small minority is membrane-associated (10% of CF_1-α and 3% of CF_1-β). This mutant has only a small amount of active CF_1 on the membrane (3% the wild-type level), which evidently is not enough for in vivo needs. Very interestingly, the soluble population of CF_1-α/β behaves as a large

oligomer, and the FUD16 chloroplasts contain amorphous electron-dense bodies that are not surrounded by membranes. By immunolabeling, these structures were shown to contain CF_1-α and CF_1-β, but no CF_1-γ. The formation of these inclusion bodies requires synthesis of CF_1-β, as thm24-FUD16 double mutants cannot accumulate the mutant CF_1-α (the thm24 mutation results in loss of *atpB* mRNA [328]). This was the first demonstration of organellar inclusion bodies.

7.3. Site-directed mutations in the atpB gene

The advent of biolistic transformation has allowed the introduction of site-directed mutations into the ATP synthase genes. The first such mutant was one designed to determine the site of action of tentoxin (Tnt), a cyclic tetrapeptide fungal phytotoxin [329]. Tnt causes chlorosis in germinating seedlings and blocks energy transfer at the photophosphorylation step. It binds to CF_1, but it does not compete with ATP/ADP. Comparison of various Tnt-resistant and Tnt-sensitive *Nicotiana* species revealed a systematic variation at codon 83 of *atpB*: sensitive strains have Asp at this position, and resistant strains have Glu. Interestingly, *C. reinhardtii* CF_1-β has Glu at this position [317] and is Tnt-resistant [311]. Avni et al. [329] transformed the FUD50 mutant, which bears a deletion in *atpB*, with *atpB* genes having either Glu^{83} or Asp^{83} along with four other changes in codons 74–91 to make the surrounding sequence identical to that of *Nicotiana* CF_1-β. Although both genes restore photosynthetic growth, AtpB-E83 was Tnt-resistant and AtpB-E83D was Tnt-sensitive, both in vivo and in vitro. Subsequently, Hu et al. [322] introduced the single change AtpB-E83D without the surrounding mutations and found that the resulting mutant ATP synthase is fully sensitive to the antibiotic, both in the thylakoid membrane and as isolated CF_1. They also made the AtpB-E83K mutant, which is fully active and Tnt-resistant, like the wild-type enzyme [322]. This result indicates that resistance is probably due to a steric blocking of the Tnt binding site due to the larger side chains of Glu or Lys. Thus, *C. reinhardtii* can be used to test specific ideas about ATP synthases of land plants.

Analysis of metal binding to CF_1 had indicated that one of the equatorial metal ligands is a carboxylate group, which is displaced upon activation, when the metal becomes liganded to the phosphate oxygens of ATP [330–332]. Based upon these results and the structure of the MF_1-ATPase [309], Hu et al. [333] constructed the AtpB-E204Q mutant. This mutant is unable to grow photoautotrophically, and its photophosphorylation rate is >100-fold reduced. However, it accumulates normal levels of CF_1 and its thylakoid membranes are not leaky to protons. Interestingly, the CF_1-ATPase reaction is not greatly affected by the mutation (the apparent k_{cat}/K_m actually increases 2-fold), and the mutant $CF_1{\cdot}CF_0$ is able to couple ATP hydrolysis to proton pumping. The mutation has no effect upon either activation by Mg^{2+} or Mn^{2+} or inhibition by an excess of these divalent cations. Moreover, the EPR spectra of VO^{2+} bound at catalytic site 3 gives no indication of a change in coordination to the metal. Taken together, these data disprove the hypothesis that Glu^{204} serves as a ligand to the metal (usually Mg^{2+}) present in the nucleotide binding site. Moreover, the AtpB-E204Q mutation causes a large decrease in the ratio of 'metal-nucleotide' form (where the ATP phosphate oxygens are ligands to the metal) to 'free-metal-inhibited' form (where the nucleotide does not ligate the metal) [333]. From these data, it was argued that Glu^{204} serves as a proton donor during the ADP phosphorylation reaction. This would explain why AtpB-E204Q has such a drastic effect on ATP synthesis, during which protons are limiting, but not on ATP hydrolysis, during which the substrate (water) is abundant. The release of products is the rate-limiting step in the ATPase reaction; since the AtpB-E204Q mutation makes hydrolysis effectively irreversible, the apparent k_{cat}/K_m for the ATPase reaction would be increased, as was seen.

7.4. CF_1-γ: rotational catalysis and redox regulation

One of the most interesting and provocative features of the cyclical interconversion mechanism proposed for ATP synthesis is the requirement for an intersubunit rotation over a full 360°. Until recently, there was not much experimental support for this idea. However, in a very important experiment by Sabbert et al. [334], rotation of CF_1-γ was observed in immobilized CF_1 using the technique of polarized absorption relaxation after photobleaching. They im-

mobilized CF_1 particles in which Cys^{322} of CF_1-γ (a site near the top of CF_1) was crosslinked to eosin-maleimide, excited the eosin chromophore with a polarized laser flash, and monitored its absorbance with polarized light in the planes parallel and perpendicular to the electric vector of the laser flash. In the presence of ATP but not non-hydrolyzable AMP-PNP, anisotropy of immobilized eosin-CF_1 decays with a time constant (100 ms) on the order of ATP hydrolysis. By analysis of the initial and steady-state anisotropies, it was estimated that CF_1-γ must have at least 200° of rotational freedom around its long axis. More recently, full rotation of MF_1-γ relative to MF_1 was directly observed by attaching fluorescent actin filaments to MF_1-γ [335]. In agreement with this, the crystal structure of MF_1 complexed with the inhibitor efrapeptin reveals that this antibiotic binds in the inner cavity of MF_1, making contacts with both MF_1-γ and the MF_1-β that has an empty site in such a way that rotation of MF_1-γ and the conversion of this MF_1-β subunit from an open to a closed configuration would be blocked!! The antibiotic aurovertin B probably has a similar mode of action, as it binds to two of the three MF_1-β subunits in a mobile cleft below their nucleotide-binding domains [336].

In addition, it is known that the activity of the ATP synthase can be regulated by its redox state. The enzyme can be activated by thiols (usually DTT), and this activation is especially apparent during suboptimal conditions, such as low stromal pH [337,338]. The CF_1-γ subunit harbors an intramolecular disulfide bond that is reduced by treatment with DTT [338,339]. It has been mapped to Cys^{199} and Cys^{205} [340], and these residues are conserved in *C. reinhardtii* CF_1-γ [318]. Reduction of this disulfide followed by alkylation with NEM results in high activity that is resistant to oxidizing agents [338,341]. Heat treatments used to activate ATPase, however, do not cause a reduction of the internal disulfide bond, and the activation by heat and DTT are additive. At the present time, the physiological significance of activation by heat is unknown, but the activation by dithiol reagents is likely to reflect an in vivo regulation mechanism. In the chloroplast, the dithiol reducing agent would most likely be thioredoxin, which accepts electron from ferredoxin. This property of $CF_1{\cdot}CF_0$, which is not shared with the eubacterial or mitochondrial enzymes, allows the enzyme to be activated when electron transport is occurring and to be shut off afterwards to prevent waste of ATP that would otherwise be used to maintain a proton gradient [342]. It is an appealing idea that the point of this regulation would be at the level of the 'coupling axle' of the ATP synthase machine, thus impeding both proton flux and ATP hydrolysis.

Smart and Selman [343] made a mutant in *atpC*, the nuclear gene encoding CF_1-γ, by transformation with heterologous DNA and screening for non-photosynthetic colonies after arsenate enrichment. In this mutant, *atp*C1, the *atpC* locus is disrupted and the CF_1-γ subunit is absent. Although the authors did not back-cross *atp*C1 to see if the *atpC* mutation cosegregated with the non-photosynthetic phenotype, they were later able to restore photosynthetic growth by transformation with a segment of genomic DNA containing the wild-type *atpC* gene [344]. As these transformants show a concomitant reappearance of CF_1-γ and CF_1-ATPase activity, it would appear that the only mutation causing loss of photoautotrophy in *atp*C1 is the one in *atpC*.

Using this transformation system, Selman and coworkers were able to introduce a set of site-directed mutations in CF_1-γ. They first attacked the two cysteines involved in the disulfide bond thought to regulate ATP synthase. Mutation of either Cys^{198}, Cys^{204}, or both cysteines to Ser abrogates the activation of ATPase by DTT [345]. In fact, both ATPase and photophosphorylation activities in the Cys → Ser mutants are at the same high level as those of the DTT-activated wild-type enzyme (see Fig. 10B). This is the first genetic proof that the formation of this specific disulfide bond causes an inactivation of ATP synthase. Note that the presence of these cysteine residues is certainly not required for ATP synthase activity, as the transformants grew photoautotrophically. In fact, Ross et al. [345] used this fact to argue that the reduced form of the enzyme must be the 'in vivo form', and claimed that ATP hydrolysis in the dark cannot be significant, as their cultures grew at the wild-type rate during an 8-h light/16-h dark regime. However, this claim requires further experimental evaluation. Surprisingly, mutation of residues in the 5-residue linker between these two cysteines can have the same effect as mutation of the cysteines

themselves. Ross et al. [346] made the AtpC-D199A and AtpC-D199K/K203D mutants. These mutant CF_1-γs are expressed and restore photosynthetic growth. However, as was seen before for the Cys→Ser mutants, they are unresponsive to DTT and constitutively catalyze ATP hydrolysis and synthesis at the DTT-activated rate. It is not clear whether or not these mutations disallow the formation of the disulfide bond or block its effect. Ross et al. [346] favored the second possibility, because of the following: purified CF_1 contains CF_1-ε if isolated without DTT, but lacks it when isolated with DTT; CF_1 from the AtpC-D199A and AtpC-D199K/K203D mutants still contains CF_1-ε when isolated without DTT, but CF_1 from the AtpC-C198S or AtpC-C204S mutants, which cannot form a disulfide bond, lacks CF_1-ε even when isolated without DTT. Thus, the linker mutants should be able to form the disulfide bond, assuming that its formation is required for association with CF_1-ε.

Recently, a mutation in CF_1-β was created that caused a similar lack of responsiveness to redox regulation [347]. It has been shown that ATP synthase can be inhibited by a tightly bound ADP in one of the catalytic sites [307]. Thus, it has been suggested that oxidation of the enzyme (most likely at CF1-γ, see above) has the effect of enabling the trapping of the inhibitory ADP. Based upon the effect of the analogous mutation in a bacterial TF_1-ATPase [348], Hu et al. constructed the AtpB-T168S mutant [347]. This threonine residue serves as part of the Mg^{2+} binding site in MF1 [309]. The AtpB-T168S enzyme has about 10 times the wild-type ATPase activity under non-activating conditions. Unlike the wild-type ATPase, which is activated 2–3-fold by DTT and 20–40-fold by alcohols or detergent, the mutant enzyme is slightly inhibited by DTT and is only mildly stimulated by alcohols or detergent. The maximal activity levels of both wild-type and mutant enzymes are remarkably similar, suggesting that these various activation processes operate through a common mechanism. Interestingly, the mutant retains 1 mol of tightly bound ADP per mol of enzyme, indicating that this ADP is not by itself inhibitory. It may be that the mutation affects the conversion of the enzyme to the free-metal-inhibited form, but the fact that it displays unchanged sensitivity to excess Mg^{2+} would seem to argue against this (the analogous mutation in TF_1-ATPase alleviated inhibition by excess Mg^{2+} [348]). The Mg-ATPase activity of the AtpB-T168S enzyme is much less sensitive to azide than the wild-type (the IC_{50} is at least 10-fold higher). If azide inhibits by trapping the enzyme in an inactive conformation with Mg-ADP in one of the catalytic sites, then the conversion of Thr^{168} to Ser must somehow change the catalytic site so that such entrapment is no longer possible, even though a tightly bound ADP remains at the site. How the CF1-γ subunit redox state is communicated to the CF1-β catalytic site should prove to be an interesting area of future study.

8. Chlororespiration

8.1. Model of chlororespiration

The model of chlororespiration proposes that a respiratory chain operates in the thylakoid membranes which shares the plastoquinol pool with the photosynthetic electron transport chain. One of the key observations made on intact algal cells, which led to this model is that a fast reoxidation of plastoquinol occurs in the dark which requires the presence of molecular oxygen [349–353]. The initial model proposed that plastoquinone is reduced by an NADPH dehydrogenase and that plastoquinol is oxidized in the dark at the expense of oxygen by an oxidase. It was thought that the resulting electron flow is electrogenic and would give rise to the electrochemical gradient across the thylakoid membrane which is observed in the dark even in the absence of FoF1 ATPase [351]. While the model of chlororespiration is mostly based on studies with intact *C. reinhardtii* cells, attempts to identify the components and associated enzymes have met with little success in this alga.

8.2. Reduction of the chlororespiratory chain

The plastoquinone pool is partly reduced in the dark [351].

NAD(P)H could be responsible for this reduction especially since starch degradation is known to lead to the formation of reduced pyridine nucleotides [354]. In land plants, eleven *ndh* genes encoding sub-

units of NADH dehydrogenase have been identified on the chloroplast genome (see [355]). These *ndh* genes are expressed and some of their products have been found in the thylakoid membranes [356–361]. A high molecular weight complex with NAD(P)H dehydrogenase activity was purified from thylakoid membranes and found to contain at least two or three *ndh* products [360,362]. Disruption of the chloroplast genes *ndhC*, *ndhK* and *ndhJ* in tobacco indicate that a putative complex I is dispensable for plant growth. Chlorophyll fluorescence analysis, however, gives evidence that a Ndh complex is implicated in post-illumination reduction of the plastoquinone pool in vivo. In addition, re-reduction kinetics of P^{+}_{700} in the dark after illumination by far-red light indicate that the Ndh complex participates in cyclic electron transfer around PSI [362]. In striking contrast, none of the *ndh* genes could be found on the chloroplast genome of *C. reinhardtii* and attempts to identify a thylakoid-associated NAD(P)H dehydrogenase have been inconclusive [363,364] mostly because thylakoid membrane preparations from *C. reinhardtii* have been shown to be significantly contaminated by mitochondrial membranes [365]. However, an 18-kDa protein from high salt extract of purified thylakoid membranes of *C. reinhardtii* was identified by N-terminal microsequencing to be identical to the gene product of frxB, a gene present in the chloroplast genome of liverwort, tobacco and wheat [366]. It was suggested that the protein is chloroplast encoded in *C. reinhardtii*, since its expression is inhibited by chloramphenicol [367]. According to its EPR spectrum the purified 18-kDa protein contains two (4Fe–4S) iron–sulfur clusters [366] and is therefore a ferredoxin-like protein. Whether this protein is part of a NAD(P)H plastoquinone-oxidoreductase in the thylakoid membrane of *C. reinhardtii* remains unclear, since it is found to form a stable DNA–protein complex with a cloned chloroplast DNA replicative origin [367]. Possible candidates for reducing the plastoquinone pool include succinate dehydrogenase, which has been found in the chloroplast of *C. reinhardtii* [368].

8.3. Interaction between mitochondrial respiratory and photosynthetic activity

Treatment of a *C. reinhardtii* mutant deficient in Rubisco activity with antimycin A and salicylhydroxamic acid (SHAM) drastically reduces the cellular ATP level, increases the NAD(P)H level and leads to the reduction of the plastoquinone pool [369]. This effect occurs presumably through the stimulation of the glycolytic pathway in the chloroplast by the depletion of ATP [370]. Bennoun [353] further showed, that while reduction of the plastoquinone pool is induced by treatment of wild-type cells with myxothiazol, an inhibitor of the mitochondrial bc_1 complex, this does no longer occur when a mitochondrial myxothiazol-resistant mutant is used. This clearly demonstrates that the myxothiazol effect is mediated solely by the mitochondrial respiratory chain. The rate of respiratory O_2 consumption by a *Chlamydomonas* cell suspension was shown to be greater after a period of photosynthesis than in the preceding dark period [371]. This light-enhanced dark respiration was correlated with the photosynthetic production of malate and phosphoglycerate and was photosynthesis-dependent, suggesting that a malate/oxaloacetate shuttle could be responsible for the transport of photo-generated reducing power from the chloroplasts to the mitochondria (Fig. 11).

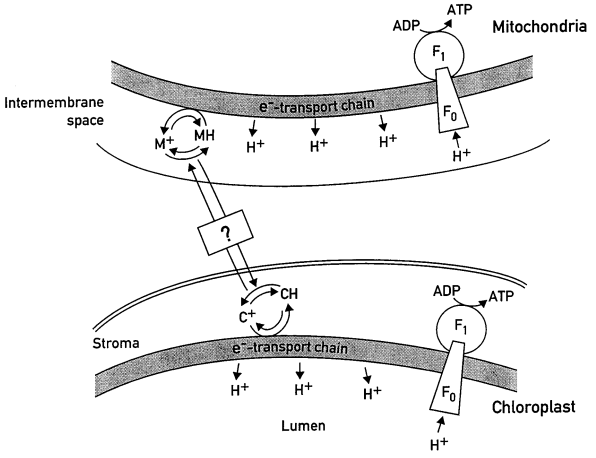

Fig. 11. Communication between chloroplast and mitochondria in *C. reinhardtii*. Mitochondria and chloroplast are shown in the upper and lower parts, respectively. Coupling between electron transfer, proton translocation and ATP synthesis is indicated. A mitochondrial reductant M and a chloroplastic reductant C, both in equilibrium with their electron transfer chains, communicate with each other using an unidentified mechanism symbolized by a question mark (see text for further explanations).

8.4. Where is the oxidase of the chlororespiratory chain?

Oxidation of plastoquinol in the dark requires oxygen, but does not require the presence of the cytochrome b_6f complex, PSI, PSII or the ATP synthase [372]. The original model assumed that the oxidase involved is located in the chloroplast [351]. Peltier et al. [352] noticed a PSI-dependent inhibition of respiratory activity after illumination of dark-adapted wild-type *C. reinhardtii* cells with saturating flashes. Since this inhibition of oxygen uptake was found to be sensitive to cyanide, but not to antimycin A and SHAM, it was concluded that the related respiratory activity occurs inside the chloroplast. The apparent $K_m(O_2)$ value for this phenomenon was measured to be 23 mM, which is much higher that the apparent K_m values of total dark respiration and of the mitochondrial alternative pathway with 0.2 and 5.5 mM, respectively [352]. The rate of chlororespiration was estimated at 10–20% of total respiration [351,352]. However, in a different study it was shown that myxothiazol and antimycin A inhibit the dark reoxidation of the PQ pool [373] as well as a PSII-dependent oxygen uptake [374]. At this time it is not known whether the oxidase of the chlororespiratory chain is located in the chloroplast or in the mitochondria. No biochemical evidence for a chloroplast oxidase has been reported.

8.5. Oxygen evolution in PSI-deficient mutants

The plastoquinol oxidation in the light could occur through reverse electron flow from a chloroplast NAD(P)H dehydrogenase complex. The reduced pyridine nucleotides could then be exported by the chloroplast and oxidized by the mitochondrial respiratory chain. Oxygen emission could indeed be observed in PSI-deficient mutants [375,376], with an oxygen evolution rate about 4–7% of the maximal net photosynthetic rate measured in wild-type cells. Since no photosynthetic CO_2 fixation was observed under illumination in a PSI-less mutant, it is believed that the reducing power produced by PSII is used to reduce molecular oxygen [376]. This result contradicts those obtained by Greenbaum et al. [377] and Lee et al. [378], who found photosynthetic CO_2 fixation in a *C. reinhardtii* mutant lacking PSI (see Section 5). PSII-dependent electron transfer is also observed in a mutant of *C. reinhardtii* lacking the cyt b_6f complex, indicating that PSI and cyt b_6f are not required for this process [375]. DCMU, an inhibitor of the photosynthetic electron transfer between Q_A and Q_B, inhibits the PSII dependent electron flow [375]. Inhibitors of mitochondrial electron transfer block the PSII-dependent light-induced oxygen evolution by 80%, indicating that the reducing power produced by the chloroplast is used to drive mitochondrial electron transfer towards oxygen [375]. It has been suggested that the PSII-dependent electron transfer produces reducing equivalents like NADPH through a reverse electron transfer and that these reducing equivalents are then transported towards the mitochondria [375]. This interpretation is strongly favored by the fact that the addition of salicylhydroxamic acid and myxothiazol had no effect on either the PSII-dependent electron transfer nor on mitochondrial respiration in the double mutant M46MUD2 of *C. reinhardtii*, deficient in PSI and resistant to myxothiazol due to a single mutation in the mitochondrial *cytb* gene (L. Cournac, K. Redding, P. Bennoun and G. Peltier, unpublished results). A transfer of reducing equivalents from chloroplasts to mitochondria was already proposed for a mutant of *C. reinhardtii* that lacks the chloroplast ATPase, but is still able to grow under photoautotrophic conditions [379].

8.6. Source of the electrochemical gradient in the dark

The occurrence of an electrochemical gradient across the thylakoid membrane in the dark raises questions about its generation. Since this gradient is still produced in mutants lacking the chloroplast ATP synthase, it cannot be generated through reverse functioning of this enzyme. The possibility that it arises through NAD(P)H reduction of plastoquinone and the chlororespiratory pathway is contradicted by the observation that myxothiazol addition in the dark leads to a fast decrease of the electrochemical gradient and a slow reduction of the plastoquinone pool [353]. If the chlororespiratory chain were involved in generating this gradient the opposite would have been expected, i.e. reduction of plastoquinone would enhance electron flow and thereby increase the gradient in the dark. Taken to-

gether the data strongly suggest that ATP plays an important role in the establishment of the electrochemical gradient. It has been postulated that it may be caused by an ATP-driven ion gradient generator of unknown composition in the thylakoid membrane [353].

9. State transitions

The concept of state transitions arose from the studies of Bonaventura and Myers [380] and Murata [381] which showed that redistribution of excitation energy between PSII and PSI occurs when the absorption of light energy by these two photosystems is uneven. This redistribution increases the overall quantum yield by decreasing the transfer of surplus excitation energy to PSII while increasing delivery to PSI (or vice versa). Such a process is termed state I–state II transition (or state II–state I transition) (reviewed in [382]). To explain the phenomenon of state transitions, it has been proposed that excess excitation of PSII leads to reduction of the plastoquinone pool of the electron transport chain and to activation of a thylakoid-associated kinase. This kinase phosphorylates a threonine residue near the amino terminus of LHCP, the major protein of the peripheral antenna complex LHCII (see [383]). It is assumed that this event causes migration of LHCII from the PSII-enriched grana region to the PSI-enriched stroma lamellae region of the thylakoids corresponding to state II, which leads to a significant decrease in room-temperature fluorescence. Inversely, excess excitation of PSI leads to the oxidation of the plastoquinone pool and deactivation of the kinase. LHCP is rapidly dephosphorylated, presumably by a thylakoid-associated phosphatase, an event which is believed to induce the migration of LHCII to the PSII-enriched grana region. While the phosphorylation of LHCP under state II conditions has been clearly demonstrated, it has not yet been conclusively shown that this event is the cause of the migration of LHCP rather than its consequence. Attempts to isolate the LHCP-kinase have not been successful [384].

The plastoquinone pool in the thylakoid membrane is shared by the photosynthetic and the chlororespiratory electron transfer chains [351]. It can thus be reduced by either PSII or NADH, and oxidized by either PSI or O_2. In this respect, *C. reinhardtii* offers distinctive advantages for studying state transitions. Methods have been developed to extensively modify the redox state of the plastoquinone pool in intact cells of *C. reinhardtii* [385,386]. State I can be obtained by illumination in the presence of DCMU and state II by an anaerobic treatment which inhibits the chlororespiratory pathway [385] and which leads to a complete reduction of the plastoquinone pool in the dark [385]. Using these procedures it has been possible to induce state transitions which yield room-temperature fluorescence changes 2–3-fold larger than in land plants [385,386]. The half-times of the kinetics of the fluorescence changes in state I to state II and state II to state I transitions were 120 and 320 s, respectively [386]. The changes in excitation energy distribution have also been estimated by the ratio of the low temperature fluorescence emission peaks of PSII and PSI or by a photoacoustic method which measures the quantum yield of PSI and PSII charge separation [387,388]. Furthermore, several photosynthetic mutants of *C. reinhardtii* have been very useful for assessing the role of the various photosynthetic complexes in state transitions (see below).

9.1. Role of cytochrome b_6f complex in state transitions

The cytochrome b_6f complex appears to play an important role in state transitions since cytochrome b_6f-deficient mutants of land plants and *C. reinhardtii* are unable to activate the LHCP kinase and to perform state transitions [389–391]. Inhibitors of the quinol-oxidizing site of the cytochrome b_6f complex block the LHCII kinase activity [390,391]. It has been proposed that the LHCP kinase is closely associated with the cyt b_6f complex and that the activation of the kinase system is mediated by the redox state of a component of the cyt b_6f complex which is determined by the redox state of the plastoquinone pool [392,393]. Ultrastructural studies have shown that cytochrome b_6f complexes co-migrate with LHCII during state transitions in *C. reinhardtii* [394]. These observations raised the interesting possibility that the increased fraction of cyt b_6f complexes in the unstacked PSI-containing regions in

state 2 could be involved in cyclic electron flow around PSI, thereby enhancing ATP production by cyclic photophosphorylation [394,395]. According to this view, state transitions not only serve as a light-adaptation mechanism, but also for rerouting of photosynthetic electron flow, thus allowing the organism to adapt to changes in cell demand for ATP. Alternatively, the state transition-induced migration of the cyt b_6f complex could be involved in the control of the activity of the LHCP-kinase [395]. State I to state 2 transitions could modulate the activation of the enzyme and its accessibility to LHCP. Indeed, photoacoustic measurements of cyclic electron flow around PSI did not reveal any significant differences in leaves from several plant species adapted either to state 1 or state 2 [396]. It is also possible that there are important differences in the events coupled to state transitions between *C. reinhardtii* and plants.

Mutants of *C. reinhardtii* deficient in state transition have recently been isolated (M. Fleischmann and J.D. Rochaix, unpublished results). The screen employed was to record the differences in fluorescence level between state I and state II. Whereas wild-type cells display a large fluorescence signal difference mutant cells do not exhibit a change in fluorescence between state I and state II. Two mutants were identified using this screen. ST7 is unable to phosphorylate LHCII in state II and has otherwise normal photosynthetic properties. The other mutant ST3 is still able to phosphorylate LHCII but unable to perform state transitions. This screen opens the door for a thorough genetic dissection of state transitions.

9.2. Migration of LHCII during state 1 to state 2 transitions

While the dissociation of the phosphorylated LHCII from PSII in state 2 is well documented, evidence for the association of the phosphorylated antenna with PSI was lacking until recently. Delosme et al. [388] performed a thorough study of changes of light energy distribution upon state transitions in intact *C. reinhardtii* cells using photoacoustic measurements. They established spectra of the quantum yield of charge separation in the wild-type and in mutants lacking the cyt b_6f complex, PSII or PSI cores. The results showed clearly that in the wild-type LHCII is connected to PSI in state 2 and that this connection requires the presence of the cyt b_6f complex. These measurements also revealed that, upon migration of LHCII from the stacked grana to the unstacked lamellae, about 80% of the excitation energy absorbed by LHCII is transferred to PSI. However, although the minor complexes CP26 and CP29 were phosphorylated under state II conditions, CP26 was not displaced [388]. CP29 has also been shown to be reversibly phosphorylated in maize. However, the corresponding kinase does not require an active cyt b_6f complex and is activated by reduction of the plastoquinone pool through a quinonic receptor site distinct from the one controlling LHCII kinase [397].

PSII-deficient mutants are still able to perform state transitions indicating that the PSII center is not required for the plastoquinone-mediated phosphorylation of LHCII [385,388]. In these mutants more than 90% of the excitation energy absorbed by LHCII is transferred to PSI under state 2 conditions [388]. In contrast, state transitions do not occur in PSI-deficient strains although LHCII is phosphorylated upon reduction of the plastoquinone pool. Hence reversible kinase activation still occurs. The spectral dependence of the quantum yield remains undistinguishable under both state 1 and state 2 conditions. It resembles the state 1 spectrum of PSII indicating that a significant proportion of the PSI peripheral antenna is connected with PSII in both states. This improved association of LHCI and LHCII with PSII has been attributed to the super-stacked organization of the thylakoid membranes known to occur in PSI-deficient mutants [398,399].

It is noteworthy that the distribution of excitation energy between the two photosystems is rather different in *C. reinhardtii* and land plants. In *C. reinhardtii*, the distribution is 0.45 for PSII and 0.55 for PSI in state 1 and 0.15 for PSII and 0.85 for PSI in state 2. Hence the absorbance cross-sections are nearly balanced in state 1 and considerably uneven in state 2, whereas the opposite has been reported in leaves. Along these lines state 1 would favor linear electron transfer, while state 2 would favor cyclic electron transfer around PSI in *C. reinhardtii*.

10. Hydrogen metabolism

10.1. Hydrogen uptake: photoreduction and oxyhydron reaction

Hydogen metabolism in algae was studied first by Gaffron [400,401]. He observed that when *C. reinhardtii* cells were adapted to anaerobic conditions and illuminated, CO_2 reduction was accompanied by H_2 uptake, a light driven process that was termed 'photoreduction'. *C. reinhardtii* cells adapted to anaerobiosis can also catalyze the uptake of H_2 in the dark, that is coupled to O_2 consumption [402]. This oxyhydron reaction leads to CO_2 fixation through the Calvin-cycle [403]. Photoreduction, but not the oxyhydron reaction, could be detected in isolated chloroplasts from *C. reinhardtii,* that were anaerobically adapted with H_2 [404]. The photoreduction observed in isolated chloroplasts was about 30% compared to that measured in whole cells [404]. Photoreduction in whole cells or isolated chloroplasts was not inhibited by 10 μM DCMU [404,405], indicating that PSII is not involved in this process. Rotenone, an inhibitor of NADH oxidoreductase, or antimycin A and SHAM, inhibitors of mitochondrial respiration, decreased photoreduction in isolated chloroplasts and whole cells, respectively, by 75 or 80 and 90%, respectively. DBMIB inhibited photoreduction in isolated chloroplasts by 95% [404,405]. The oxyhydron reaction was also inhibited in whole cells of *C. reinhardtii* after the addition of SHAM, antimycin A or DBMIB [405]. These results suggest that mitochondrial respiration is coupled with the chloroplast PQ pool in the oxyhydron reaction. To explain the process of photoreduction Maione and Gibbs [405] have proposed a model in which a chloroplast NADPH oxidoreductase (see also Section 8), that is sensitive to rotenone, is coupled to the photosynthetic PQ pool. However, one has to consider that photoreduction is decreased by 60% in isolated chloroplasts (see above) and that isolated chloroplasts from *C. reinhardtii* used for this study are contaminated with mitochondria, since 12% of the cellular cyt *c* oxidase activity (used as a mitochondrial marker) is associated with the chloroplast fraction [406]. Therefore participation of mitochondrial electron transfer components cannot be excluded in these experiments and photoreduction may therefore also depend on the interactions between chloroplast and mitochondria or other subcellular compartments.

10.2. Hydrogen evolution

Another feature of the hydrogen metabolism of *C. reinhardtii* is hydrogen evolution under anaerobic conditions. Hydrogen evolution was first measured in a green alga *Scenedesmus obliquus* [402]. Its production can be measured in the dark, where it is driven by fermentation [407]. However, much higher rates of hydrogen evolution can be detected in the light. Two mechanisms have been proposed to account for hydrogen release in the light. One involves photochemical water splitting at PSII, together with linear electron transfer from PSII to PSI, that results in simultaneous production of water and hydrogen, with a molar ratio of about 2 [408]. This reaction is inhibited by DCMU [408,409]. When dark-adapted cells of *C. reinhardtii* are transferred to light, a transient surge of hydrogen is observed that peaks and then decreases to zero. This is explained by the fact that in the dark the Calvin–Benson cycle is turned off. Upon illumination all the reducing power is initially released as hydrogen, whereas after activation of the cycle, carbon reduction becomes the sink for the reducing equivalents produced by photosynthesis [410]. These observations suggest that one of the physiological roles of the hydrogenase from *C. reinhardtii* is the dissipation of reducing equivalents under anaerobic stress conditions. However, the alternative pathway to hydrogen evolution couples the metabolic oxidation of organic components to PSI and results in the release of hydrogen and carbon dioxide [411–413]. This process is strongly stimulated by acetate [407,412] and glucose [413]. Whereas DCMU did not affect the increase of hydrogen evolution in *C. moewusii* after addition of acetate [407], it inhibited about 80% of the hydrogen production in the F-60 mutant of *C. reinhardtii* [412]. This mutant lacks ribulose kinase and is therefore deficient in the photosynthetic carbon reduction cycle. However, the differences observed in the inhibition of hydrogen production by DCMU in wild-type and this mutant are not fully understood.

Hydrogenase is highly sensitive to oxygen, which irreversibly inhibits hydrogen evolution within mi-

nutes [414,415]. Using anti-hydrogenase antibodies, neither active nor inactive enzyme could be detected in aerobically grown cells of *C. reinhardtii*. In contrast, 10 min after the onset of anaerobic adaptation, hydrogenase was detected [416]. These results contradict those of Roessler and Lien [417] which indicated that 30% of the maximal hydrogenase activity is due to activation of the enzyme or its precursor. However, it seems to be clear that de novo synthesis of hydrogenase occurs only under anaerobic conditions. The fact that cycloheximide inhibits hydrogen production in *C. reinhardtii* [416,417] is taken as evidence that hydrogenase is synthesized on cytoplasmic ribosomes and therefore nucleus-encoded. As mentioned before hydrogenase activity was detected in isolated chloroplasts [404], indicating that the protein is imported into the chloroplast. This finding is supported by Happe et al. [416], who immunodetected hydrogenase only in isolated chloroplasts and not in other cellular fractions of *C. reinhardtii*.

The in vivo electron donor for hydrogenase is ferredoxin (see Section 5.6) with a K_m value for hydrogen evolution of 10–35 mM [418,419]. Effects of the charge properties of electron mediators on the reaction kinetics of hydrogenase suggest the presence of a cationic region near the active site of hydrogenase [418].

Isolation of hydrogenase from *C. reinhardtii* succeeded under anaerobic conditions. A 2750-fold enrichment of hydrogenase was achieved by Roessler and Lien [420]. The preparation was approximately 40% pure and evolved hydrogen with ferredoxin as mediator. A protein with a molecular mass of 47.5 kDa was identified as hydrogenase. More recently, hydrogenase was purified 6100-fold, resulting into a single band in SDS-PAGE with a similar molecular mass of 48 kDa. The isolated protein evolved hydrogen with methyl viologen and ferredoxin as electron mediator [419]. N-Terminal amino acid sequencing identified 24 amino acids of the protein, but no significant amino acid sequence homologies could be found to any sequences from prokaryotic hydrogenases [419]. The activation energy using ferredoxin as mediator for hydrogen evolution was determined with an enriched hydrogenase fraction to be 55.1 kJ mol^{-1}, a value that is similar to that found with prokaryotic hydrogenases [420]. Measurements with isolated hydrogenase and methyl viologen as mediator revealed that hydrogen evolution has an optimal temperature of 60°C and a pH optimum of 6.9 [419]. Atomic absorption experiments performed with highly purified hydrogenase, revealed that the enzyme contains 12 iron atoms per protein molecule, whereas only 0.05 Ni/protein molecule were found [416]. Therefore it appears that the hydrogenase from *C. reinhardtii* belongs to Fe-hydrogenases rather than to a nickel-containing hydrogenase family. This implies that the enzyme may contain iron–sulfur centers, although this remains to be proven.

11. Oxygenic photoautotrophic growth without PSI?

In 1995, interesting new results by Greenbaum and coworkers [377] questioned the classical Z-scheme of photosynthesis. They reported that a *C. reinhardtii* mutant strain B4, which lacks PSI but contains PSII, is capable of photosynthetic assimilation of atmospheric CO_2 under saturating light and in anaerobic conditions. Under aerobic conditions the mutant strain B4 was unstable and its ability to assimilate carbon dioxide in the light declined within 1 day. Greenbaum et al. [377] concluded from these results that in an anaerobic atmosphere the single light reaction of PSII is sufficient to drive photoreduction of carbon dioxide using water as the source of electrons. However, more recently, the same group reported that the PSI-less *C. reinhardtii* mutants were able to grow photoautotrophically in air (21% oxygen), containing about twice the atmospheric CO_2 concentration as the only carbon source [378]. The mutants used in these studies, B4 and F8, contain nuclear mutations that block the *trans*-splicing of the *psaA* mRNA [38,147]. Whereas under anaerobic conditions hydrogen evolution could be measured after the onset of light in the mutants B4 or F8 as well as in wild-type, no hydrogen evolution could be obtained under aerobic conditions, indicating that hydrogen metabolism is not necessary for the mechanism of carbon dioxide fixation in the PSI deficient mutant [377,378]. Interestingly, Peltier and Thibault [375] as well as Cournac et al. [376] reported that PSI-deficient strains of *C. reinhardtii* were able to evolve oxygen as reported by Greenbaum et al. [377] and Lee et al. [378], but in contrast to the latter no carbon dioxide assimilation (in the presence of

500 ppm CO_2, in nitrogen) could be detected [376] (see Section 8.5). Immunoblot analysis using anti-PsaA antibodies indeed confirmed the presence of PsaA in the mutant strains that were capable of photoautotrophic growth [376]. Thus, it appears that photoautotrophic isolates of B4 or F8 have either reverted or have acquired suppressor mutations. The presence of PSI in the mutant strains B4 and F8 is supported by the observation that they are not light sensitive [378], whereas PSI-deficient strains are highly sensitive to light [137,232,376]. The fact that no CO_2 fixation could be observed in transformants of B4 and F8 in which the *psaA* gene had been deleted argues strongly that photosystem I activity is required to assimilate CO_2 in *C. reinhardtii* [376].

12. Carbon fixation: focus on Rubisco

The enzyme ribulose-1,5-bisphosphate carboxylase/oxygenase (Rubisco) is the key enzyme of carbon fixation. It catalyzes the reaction:

$$\text{ribulose}-1,5-\text{bisphosphate(RuBP)} + CO_2 + H_2O <=> 2,3-\text{phosphoglycerate(3-PGA)}.$$

Rubisco is the only enzyme of the Calvin cycle unique to photosynthetic organisms. The triose (3-PGA) generated by Rubisco can be converted to fructose-6-phosphate in a series of reactions essentially identical to those of gluconeogenesis in animals, the first two of which utilize NADPH and ATP. In each cycle, half of the triose is converted to hexose, a third of which is excess and leaves the cycle as glucose 6-phosphate. The rest is combined with the trioses to make pentoses by a series of carbon-shuffling reactions catalyzed by transketolase and aldolase. The resulting pentose phosphates are converted to ribulose phosphate by epimerase and isomerase enzymes. The action of phosphoribulokinase, using a high-energy phosphate from ATP, regenerates RuBP. Note that energy from the light reactions, in the form of NADPH and ATP, is not used by Rubisco itself, but rather in the enzymatic steps immediately before and after the fixation of CO_2. This mechanism serves to drive the carboxylation reaction by efficiently producing the substrate of Rubisco (RuBP) and removing its products (3-PGA). The only other variable is the concentration of CO_2 and, unfortunately, that of O_2, because Rubisco can also catalyze a competing reaction: RuBP+ O_2 <=> 3-PGA + phosphoglycolate. This oxygenation reaction is the initial reaction of photorespiration, in which the phosphoglycolate is oxidized without return of useful energy, and is thus considered a wasteful process. Much of research on Rubisco has, therefore, concentrated on attempts to understand its catalytic mechanism and to improve upon its specificity.

Rubisco may be the most abundant protein on earth, not only because of its importance in photosynthesis, but because of the difficulty of the reaction it catalyzes. This reaction proceeds through a number of steps, including enolization (resulting in a C2–C3 double bond), carboxylation (or oxygenation) at C2, hydration of the C3 ketone, and cleavage of the C2–C3 bond, leading to release of the two molecules of 3-PGA (or 3-PGA+phosphoglycolate). The enzyme stabilizes the enediol form of RuBP by abstraction of a proton from C3. Then the addition of CO_2 (or O_2) at C2 is essentially irreversible, and the reaction is committed to the hydration and cleavage of the addition product. The specificity of Rubisco is often expressed as a CO_2/O_2 specificity factor (Ω) defined as $\Omega = V_C K_O / V_O K_C$, where K_C and K_O are the Michaelis constants for CO_2 and O_2, and V_C and V_O are the maximal velocities of carboxylation and oxygenation, respectively [421]. Thus, the ratio of carboxylation to oxygenation at any given concentration of CO_2 and O_2 can be written as $v_c/v_O = \Omega \times (CO_2)/(O_2)$. In general, $\Omega = 15$ in photosynthetic bacteria, $\Omega = 50$ in cyanobacteria, $\Omega = 60$ in green algae (such as *C. reinhardtii*), and $\Omega = 80$ in land plants [422]. A lot of effort has gone into understanding how to increase this factor, but the problem has proven to be much more difficult than was previously thought.

In green plants, the holoenzyme is a hexadodecamer made up of 8 large subunits (LS; 55 kDa) and 8 small subunits (SS; 15 kDa). Some photosynthetic bacteria utilize a so-called 'form II Rubisco,' which is a homodimer of large subunits [423], indicating that the small subunits are not involved in catalysis. Indeed, the structure of spinach Rubisco complexed with the transition-state analog 2-carboxyarabinitol-1,5-bisphosphate (CABP) shows quite

clearly that the small subunits are far from the active site [424,425]. However, the small subunits are required for stability and maximal activity of the enzyme; an LS_8 octamer reconstituted from recombinant protein possesses only 1% of the activity of the holoenzyme containing small subunits [426]. The 2.4 Å X-ray crystal structure of spinach Rubisco [424] demonstrated that form I Rubisco has the same general architecture as form II, with large subunits forming tightly associated homodimers. Each LS has a smaller N-terminal domain and a larger C-terminal domain dominated by an eight-stranded parallel α/β-barrel. The active site is found at the interface between the C-terminal side of the α/β-barrel of one subunit and the N-terminal domain of the other partner in the LS homodimer, although the majority of the active site residues are contributed from the C-terminal domain. The homodimeric units associate together as a tetramer (i.e. $(LS_2)_4$) in form II Rubisco. The small subunits associate with the LS_8 octamer at opposite poles, where all eight large subunits can be contacted; each SS makes contacts with three different LS [424].

A specific lysine residue (Lys^{201}) must be carbamylated for the enzyme to be active. This activation process entails the reaction of a molecule of CO_2 to Lys^{201} in a way distinct from the reaction with substrate CO_2 [427], occurs at alkaline pH, and can be catalyzed by the enzyme Rubisco activase [428]. The addition of a Mg^{2+} ion further stabilizes the carbamate [429]. Both the carboxylation and oxygenation reactions require carbamylated Lys^{201} and Mg^{2+} in the active site. According to the CABP-complexed structure, ligands for the Mg^{2+} are provided by oxygens from Lys^{201}-carbamyl, Asp^{203}, and Glu^{204} (see below) from LS and the other three ligands come from the substrate [425]. Andersson [425] has proposed a model in which Lys^{201}-carbamyl abstracts a proton from C3, thereby forming the enediol, which is attacked by CO_2, one of whose oxygens would ligate the Mg^{2+}. The addition product is rapidly hydrated to a gem-diol. Subsequently, a second step of deprotonation from one of the C3 hydoxyls drives cleavage of the C2–C3 bond, forming 3-PGA and the carbanion form of 3-PGA, which must be protonated from the side opposite K201-carbamate to form D-3-PGA.

In all green plants, Rubisco LS is encoded by *rbcL* on the chloroplast genome and SS by a family of *rbcS* genes in the nucleus. The *rbcL* [430] and both *rbcS* [431] genes of *C. reinhardtii* have been sequenced. The identity between Rubisco LS from *C. reinhardtii* and spinach, for which the structure is now known at 1.6 Å resolution [425], is 88% and increases to 93% if one considers conservative substitutions; almost all of the remaining differences are in regions that vary among all chloroplast Rubiscos. As the *Chlamydomonas* enzyme is well-characterized biochemically [432,433], it serves as an excellent system in which to examine structure–function questions.

Indeed, Spreitzer and his colleagues have used several aspects of *Chlamydomonas* genetics to their advantage in the analysis of Rubisco (see Table 2 for all mutants discussed). Starting with a single mutation in the *rbcL* gene, Spreitzer and Ogren [434] were able to isolate more mutations in *rbcL* by screening for non-photosynthetic mutants that failed to recombine with the original mutation. Many of the *rbcL* mu-

Table 2
Properties of Rubisco mutants

Mutation (RbcL-)	Biochemical result	Reference
Q45Stop	no protein	[422]
G54D	no protein	[422]
G54A	–	[440]
G54V	$\downarrow v_c$	[440]
W66Stop	no protein	[433,441,462]
N123G	$\downarrow v_c$, $\downarrow \Omega$	[442]
G171D	$-v_c$	[422] and references therein
T173I	$-v_c$	[463]
R217S	no protein	[439]
R217S/A242V	$-v_c$, $\downarrow \Omega$	[439]
G237S	$\downarrow$protein, $-v_c$	[422]
L290F	$\downarrow$protein, $\downarrow \Omega$	[435,436]
L290F/A222T	$\downarrow$protein	[436]
L290F/V262L	$\downarrow$protein	[436]
L326I	$\downarrow$protein	[443]
L326I/M349L	$\downarrow \Omega$	[443]
V331A	$\downarrow \Omega$	[437,438]
V331A/T342I	$\uparrow \Omega$ of V331A	[437,438]
V331A/G344S	$\uparrow \Omega$ of V331A	[438]
V341I	–	[443]
M349L	–	[443]
S379A	$\downarrow v_c$, $\downarrow \Omega$	[442]
W451Stop	no protein	[433,462]

tants do not accumulate Rubisco [422]. However, Chen et al. [435] were able to identify thermosensitive Rubisco mutants that could grow photosynthetically at 25°C, but not at 35°C, thus ensuring that they could at least assemble and accumulate a partially active enzyme. One such mutant, RbcL-L290F, accumulates Rubisco protein at 36% the wild-type level at 25°C, and the enzyme purified under these conditions has $\Omega = 54$, compared to $\Omega = 62$ for wild-type. Although the enzyme has a slight increase in the specificity of binding CO_2 vs. O_2, this was more than offset by a decrease in V_C/V_O. They were later able to identify two intragenic suppressors (RbcL-V262L and A222T) that restored phototrophic growth at high temperature without greatly increasing accumulation of holoenzyme [436]. Both restored Ω to the wild-type value, although they did so in different ways. Compared to RbcL-L290F, the RbcL-L290F/V262L double mutant had lower Michaelis constants for both O_2 and CO_2, but the K_O/K_C ratio was slightly higher. The main effect of A222T was on kinetics; while V_C and V_O were both increased by the secondary mutation, the ratio of carboxylation to oxygenation was slightly higher in the double mutant.

A further example of the use of suppressor genetics was seen in the case of RbcL-V331A, a mutant Rubisco that accumulates normally yet has only 5% of wild-type activity [437]. This effect is due mainly to a large decrease in the carboxylation rate and a 5-fold decrease in affinity for CO_2. This mutation could be suppressed by an intragenic suppressor mutation, RbcL-T342I [437,438]; the double mutant enzyme has only a modest decrease in specificity ($\Omega = 52$). The secondary mutation RbcL-G344S was also isolated as a suppressor, but it is less effective in improving catalytic efficiency [438]. In both cases, suppression is probably a simple case of filling the volume left by the Val→Ala substitution, as all of these residues (Val^{331}, Thr^{342}, and Gly^{344}) are in the same region in space [424]. While they are not in the active site, they are close to Lys^{334}, a residue in the active site thought to be important for stabilizing the enediol of RuBP [424]. Similarly, the residue affected in the thermosensitive mutant RbcL-L290F is not in the active site, but is four residues from His^{294}, which might play a role in the second deprotonation step [425]. Thus, these mutations probably have an effect by subtly altering the conformation of the active site in such a way that it is more or less conducive to carboxylation/oxygenation.

Similarly, the mutation RbcL-R217S prevents assembly and accumulation of Rubisco [439]. This is not surprising, considering that Arg^{217} is part of an internal salt bridge to Asp^{202}, a residue strategically situated between K201-carbamyl and Asp^{203}/Glu^{204}, all three of which are ligands to the active site Mg^{2+} [424]. What is surprising is that Thow et al. were able to isolate an intragenic suppressor, RbcL-A242V, that does not obviously restore the salt bridge [439]. It might, however, be able to fill some of the volume caused by the RbcL-R217S substitution, as these side chains are close together in space [424]. Although the double mutant enzyme has a two-fold lower specificity ($\Omega = 33$) and 10-fold lower maximal carboxylation rate, it does allow photosynthetic growth and demonstrates that the Asp^{202}-Arg^{217} salt bridge is not an absolute requirement of Rubisco architecture [439]. This might have been expected, considering that these two residues are Asn and Thr, respectively, in form I Rubisco from *Rhodospirillum rubrum* [424].

Not all Rubisco mutations can be suppressed intragenically. For example, a mutation in the N-terminal domain of LS, RbcL-G54D, thwarts accumulation of Rubisco holoenzyme and photosynthetic growth [440]. Out of 18 revertants, all were found to have changed codon 54. In most cases (11/18), the change was a true reversion back to a Gly codon, but two pseudorevertants were also isolated: RbcL-G54A and RbcL-G54V. This result is rationalized by examination of the structure: it would be extremely difficult to compensate the introduction of a large, charged residue in the place of Gly by a second-site substitution. As one might expect, the RbcL-G45V enzyme performs significantly worse than RbcL-G54A, which is almost indistinguishable from wild-type. Interestingly, the G54V enzyme binds RuBP slightly better, CO_2 the same, and O_2 less well than wild-type, but these improvements were more than offset by a significant decrease in the carboxylation rate. An intriguing example of non-intragenic suppression is the case of a nonsense mutant (RbcL-Trp^{66}Amber [422]). A photosynthetic pseudorevertant isolated from this mutant does not change codon 66 but instead has a mutation in the anticodon

of the chloroplast Trp tRNA that would allow it to suppress amber mutations [441]. Since there is only one chloroplast Trp tRNA encoded by chloroplast genome, both the wild-type and amber suppressor alleles must be maintained on the multiple copies of the chloroplast genome (i.e. a 'heteroplasmic' state) during photosynthetic growth, but non-photosynthetic clones can arise during non-selective growth due to loss of the amber suppressor. This sort of instability has been observed in two suppressors of the R217S mutation ([439]; see above), indicating that missense suppression is also possible in the chloroplast. These first examples of information suppression in the chloroplast genome open the door for a new type of genetic analysis in the *C. reinhardtii* chloroplast.

The advent of chloroplast biolistic transformation has allowed the creation of site-directed mutations in the *rbcL* gene. Using the crystal structure [424,425] as a guide, Zhu and Spreitzer [442] made two different mutations of residues in the active site of Rubisco: RbcL-N123G and RbcL-S379A. Although both mutations allow normal accumulation of enzyme, they lower Ω to the lowest values yet seen for *C. reinhardtii* Rubisco (12 and 18, respectively). Their low activities (only 2–4% of wild-type), which preclude photosynthetic growth, are due mainly to a 20–40-fold decrease in V_C and to a modest increase in K_C. As both mutant enzymes exhibit no significant change in RuBP binding ($K_m = 10$ μM in mutants as well as wild-type), yet they bound the transition-state analog CABP less tightly, their defect would appear to be in stabilization of the carboxylation transition state.

In order to make *C. reinhardtii* Rubisco more like land plant Rubiscos, which have higher catalytic specificities, three different substitutions were made in the loop between β-strands 6 and 7 [443]. This region is highly conserved, with the targeted residues being the only differences between the *C. reinhardtii* and land plant enzymes, except for a Glu/Asp polymorphism at position 340. Position 341 is quite divergent among various plants, so it is not surprising that the RbcL-V341I mutation has no discernible effect upon catalytic efficiency or specificity. However, the RbcL-L326I mutation destabilizes Rubisco. In the crystal structure of the spinach enzyme, Ile^{326} is in van der Waals contact with Leu^{349}. The substitution of the methionine at position 349 in *C. reinhardtii* Rubisco with leucine has no effect by itself on catalytic efficiency, and only a slight one upon accumulation. However, the double mutant RbcL-L326I/M349L is significantly more stable than the RbcL-L326I mutant protein; it is expressed at a higher level (50 vs. 15%) and is more thermostable. This stabilization of the protein has an unfortunate impact upon catalysis: the specificity of the double mutant enzyme is lower (Ω = 52) than either single mutant, which are close to wild-type. Thus, even though these substitutions bring the *C. reinhardtii* Rubisco closer in sequence similarity to an enzyme with higher specificity (Ω = 80), they have the effect of lowering catalytic specificity.

As mentioned above, formation of a Mg^{2+}-stabilized carbamate on Lys^{201} is essential for Rubisco activity. Although carbamylation is spontaneous, it cannot occur if the active site is occupied by a sugar phosphate [444]. This difficulty is overcome by another stromal enzyme, Rubisco activase [445]. Rubisco from *Solanaceae* plants (such as tobacco) cannot be activated by activase from non-*Solanaceae* plants (such as spinach and *Chlamydomonas*), and vice versa. In order to identify potential activase contact sites, an examination was made of surface residues that systematically differ between Solanaceae and non-Solanaceae Rubiscos [446]. Attention was focussed on residues 89 and 356, and mutations were made at these sites in *C. reinhardtii rbcL* to convert them to the residues found in tobacco Rubisco. The RbcL-K356Q mutant is indistinguishable from wild-type and it is activated by spinach but not tobacco activase. However, the RbcL-P89R mutant had switched specificity: it was activated by tobacco, but not spinach, activase [446]. Thus, this use of *Chlamydomonas* genetics not only provides good evidence that there is a physical interaction between Rubisco and activase, but identifies where this interaction takes place.

Until recently, there has been little work done on the Rubisco SS in *C. reinhardtii*. Compared to the LS, it has been more difficult to work with, since there are two genes encoding SS and both are in the nucleus [431]. However, as the two *rbcS* genes are located close to each other, it was possible to

isolate an insertion mutant that lacked both [447]. This mutant is non-photosynthetic, but photoautotrophy can be restored by introduction of either *rbcS* gene [447]. This should be expected, as there are only four amino acid residue differences between them [431]. So, it is now finally possible to perform site-directed mutagenesis with a eukaryotic Rubisco SS and express it in a genetic background that lacks any other members of this family, a task that would be impossible in land plants harboring many more *rbcS* family members.

In conclusion, none of the mutants isolated so far in *C. reinhardtii* Rubisco cause an increase in Ω. However, it is not to be expected that simple substitutions would cause such an increase, or they would have already arisen due to the action of natural selection. However, the fact that stability, catalytic rate, and specificity can be increased relative to single substitutions by the introduction of second-site mutations gives reason to hope that this goal is not unattainable. In fact, the experience to date would show that very subtle changes in the conformation of the active site of Rubisco can cause substantial changes in its catalytic parameters. It is to be expected that most mutations will result in a decrease in overall efficiency. Finding those that increase efficiency, if they exist, will take longer.

An interesting question now being addressed in plant physiology is where the fixation of CO_2 is occurring. In electron micrographs of *Chlamydomonas* cells, a very prominent electron-dense region in the stroma is visible. This structure, called the pyrenoid, is, in fact, one of the defining characteristics of the *Chlamydomonas* genus [16]. Mutants that lack Rubisco do not have pyrenoids [448]. Moreover, Rubisco is found localized to the pyrenoid [449,450]. An analysis by Borkhsenious et al. [450] using cells grown in high or low CO_2 demonstrated that the amount of Rubisco localized to the pyrenoid could vary from 40% (5% CO_2) to 90% (air). Thus, the majority of Rubisco is normally localized to the pyrenoid, and it must be utilized by the cell, as the in vivo CO_2 fixation rate corresponds closely to the in vitro carboxylation rate [450]. How this structure contributes to CO_2 fixation and how substrates and products are transported into and out of it will be an interesting topic for future work.

13. Mitochondrial functions

The mitochondria and chloroplast of *C. reinhardtii* occupy 2–4 and 40% of the cell volume, respectively. It has not yet been possible to isolate large amounts of mitochondria from this alga. Isolated mitochondria are usually heavily contaminated with thylakoid membrane fragments. However, it was recently reported that mutants of *C. reinhardtii*, unable to synthesize chlorophyll in the dark, provide a convenient source of mitochondrial membranes suitable for spectroscopic and biochemical characterization [451]. In these yellow mutants grown in the dark, the core polypeptides of the PSII and PSI complexes, as well as the antenna system, do not accumulate appreciably and the thylakoid membranes are considerably reduced. The membrane fractions derived from these etiolated cells contain a mixture of mitochondrial and etioplast membranes which can be further depleted of the cytochrome b_6f complex by crossing in mutations leading to the loss of this complex. Using this system it has been possible to measure the reduced minus oxidized redox difference spectra of several mitochondrial cytochromes such as $a+a_3$ from cytochrome oxidase, cytochrome b and cytochrome c_1+c_2 (redox difference peak at 609, 563 and 551 mn, respectively, [451]). This system opens the possibility to characterize mutants with impaired mitorespiration in *C. reinhardtii*.

The linear 15.8 kbp mitochondrial genome of *C. reinhardtii* contains eight protein genes encoding cytochrome *b*, subunit 1 of cytochrome oxidase, five subunits of NADH dehydrogenase, and a reverse transcriptase-like protein of unknown function [452,453]. It is surprising that subunits II and III of cytochrome oxidase and all of the subunits of the ATP synthase are encoded by the nuclear genome in this alga.

As in many land plants, there are two mitochondrial respiratory chains in *C. reinhardtii*. Besides the usual cytochrome cyanide-sensitive pathway, there is the alternative pathway that branches from the main chain at the level of ubiquinone, and that is insensitive to KCN, but sensitive to SHAM [454]. The isolation of mutants of *C. reinhardtii* impaired in mitochondrial function is possible because respiratory function is dispensable in this alga, provided photosynthetic function is intact. In this way several nu-

clear mutants unable to grow heterotrophically and which survive only under phototrophic conditions were isolated [454]. These obligate photoautotrophic mutants, called dk mutants (dark diers) are deficient in key mitochondrial functions. *C. reinhardtii* is thus the only organism in which mutations affecting photosynthesis and respiration have been isolated. It has also been possible to isolate mutants affected at the level of mitochondrial DNA. The first mutants of this type lacked all of the mitochondrial DNA and gave rise to 'minute' colonies in which the cells died after eight to nine divisions even when grown with light [455,456]. It will be of considerable interest to find out which of the mitochondrial DNA-encoded functions are essential for cell survival. More recently, several respiratory-deficient mutants of *C. reinhardtii* have been isolated after mutagenic treatment with acriflavine or ethidium bromide [457]. Biochemical analysis revealed that these mutants are deficient in the cyanide-sensitive cytochrome pathway of respiration. Several of the mutants had deletions in the terminal end of the mitochondrial genome containing the apocytochrome *b* gene. Another mutation was localized in the gene of subunit I of cytochrome oxidase [458]. Manganese ions which induce mitochondrial mutations in yeast appear to do the same in *C. reinhardtii* and have been used to produce several mitochondrial mutations, conferring resistance to myxothiazol and mucidin [459,460]. These inhibitors specifically block the mitochondrial cytochrome bc_2 complex at the ubiquinone redox site Q_o. Analysis of the mitochondrial drug-resistant mutants revealed point mutations in a highly conserved region of the cytochrome *b* gene which specifies part of the myxothiazol binding niche [459]. It is possible to transfer these mitochondrial mutations through cytoduction to recipient strains with desired nuclear and chloroplast mutations [459].

Together with mutants impaired in photosynthetic function, these mutants constitute important tools for studying the functional interactions between mitochondria and chloroplasts. A nuclear mutant, dk97, deficient in cytochrome oxidase activity, was used to show that glycolate produced during photosynthesis accumulates and is excreted in the presence of SHAM, indicating that oxidation of glycolate is linked to the SHAM-sensitive electron transport rather than to peroxisomal metabolism as in land plants [461]. Studies on the effect of SHAM on respiration revealed that, under photoautotrophic growth conditions, mutants deficient in cyanide-sensitive electron transport and wild-type have the same respiratory rate. Under mixotrophic growth, the respiration rate increased in wild-type, but not in mutant, cells. This indicates that the alternative pathway is sufficient to transfer all the electrons to oxygen in the absence of exogenous carbon source, but not in the presence of acetate [458,461].

Acknowledgements

We thank N. Roggli for drawings and photography, Drs. W. Nitschke and J. Kruip for critical reading the manuscript and W.A. Cramer, G. Peltier and L. Cournac for communicating unpublished results. The work was supported by a grant from the Swiss National Fond. M.H gratefully acknowledges a long-term fellowship from the Human Frontier Science Program. K.R. was supported by a Plant Biology Fellowship from the National Science Foundation (USA).

References

[1] R. Sager, Proc. Natl. Acad. Sci. USA 40 (1954) 356–363.
[2] R. Sager, Z. Ramanis, Proc. Natl. Acad. Sci. USA 65 (1970) 593–600.
[3] D.M. Grant, N.W. Gillham, J.E. Boynton, Proc. Natl. Acad. Sci. USA 77 (1980) 6067–6071.
[4] M. Dron, M. Rahire, J.D. Rochaix, L.M. Mets, Plasmid 9 (1983) 321–324.
[5] R.P. Levine, Science 162 (1968) 768–771.
[6] P.J. Hastings, E.E. Levine, E. Cosbey, M.U. Hudock, N.W. Gillham, S.J. Surzycki, R. Loppes, R.P. Levine, Microb. Genet. Bull. 23 (1965) 17–19.
[7] R.P. Levine, D.S. Gorman, Plant Physiol. 41 (1966) 1293–1300.
[8] R. Debuchy, S. Purton, J.D. Rochaix, EMBO J. 8 (1989) 2803–2809.
[9] K.L. Kindle, R.A. Schnell, E. Fernandez, P.A. Lefebvre, J. Cell Biol. 109 (1989) 2589–2601.
[10] S.P. Mayfield, K.L. Kindle, Proc. Natl. Acad. Sci. USA 87 (1990) 2087–2091.
[11] J.E. Boynton, N.W. Gillham, E.H. Harris, J.P. Hosler, A.M. Johnson, A.R. Jones, B.L. Randolph-Anderson, D. Robertson, T.M. Klein, K.B. Shark et al., Science 240 (1988) 1534–1538.

[12] J.D. Rochaix, Annu. Rev. Cell Biol. 8 (1992) 1–28.
[13] J.D. Rochaix, Curr. Opin. Genet. Dev. 2 (1992) 785–791.
[14] N.W. Gillham, J.E. Boynton, C.R. Hauser, Annu. Rev. Genet. 28 (1994) 71–93.
[15] S.P. Mayfield, C.B. Yohn, A. Cohen, A. Danon, Annu. Rev. Plant. Physiol. Plant Mol. Biol. 46 (1995) 147–166.
[16] E.H. Harris, The Chlamydomonas Sourcebook. A Comprehensive Guide to Biology and Laboratory Use, Academic Press, San Diego, 1989.
[17] P. Bennoun, P. Delepelaire, in: M. Edelman, N.H. Chua, R.B. Hallick (Eds.), Methods of Chloroplast Molecular Biology, Elsevier, Amsterdam, pp. 25–38.
[18] J. Fenton, A.R. Crofts, Photosynth. Res. 26 (1990) 58–66.
[19] P. Bennoun, D. Béal, Photosynth. Res. 51 (1997) 161–165.
[20] J.E. Boynton, N.W. Gillham, Methods Enzymol. 217 (1993) 510–536.
[21] M. Goldschmidt-Clermont, Nucleic Acids Res. 19 (1991) 4083–4089.
[22] J.D. Rochaix, Trends Plant Sci. 2 (1997) 419–425.
[23] W. Zerges, J.D. Rochaix, Mol. Cell. Biol. 14 (1994) 5268–5277.
[24] J. Nickelsen, J. van Dillewjin, M. Rahire, J.D. Rochaix, EMBO J. 13 (1994) 3182–3191.
[25] O. Stampacchia, J. Girard-Bascou, J.L. Zanasco, W. Zerges, P. Bennoun, J.D. Rochaix, Plant Cell 9 (1997) 773–782.
[26] W. Zerges, J. Girard-Bascou, J.D. Rochaix, Mol. Cell. Biol. 17 (1997) 3440–3448.
[27] N. Fischer, O. Stampacchia, K. Redding, J.D. Rochaix, Mol. Gen. Genet. 251 (1996) 373–380.
[28] J.A.E. Nelson, P.B. Savereide, P.A. Lefebvre, Mol. Cell. Biol. 14 (1994) 4011–4019.
[29] D. Stevens, J.D. Rochaix, S. Purton, Mol. Gen. Genet. 251 (1996) 23–30.
[30] K.L. Kindle, Proc. Natl. Acad. Sci. USA 87 (1990) 1228–1232.
[31] I. Sizova, T.V. Lapina, O.N. Frolova, N.N. Alexandrova, K.E. Akopiants, V.N. Danilenko, Gene 181 (1996) 13–18.
[32] L.W. Tam, P.A. Lefebvre, Genetics 135 (1993) 375–394.
[33] P.A. Schnell, P.A. Lefebvre, Genetics 134 (1993) 737–747.
[34] J. Farah, F. Rappaport, Y. Choquet, P. Joliot, J.D. Rochaix, EMBO J. 14 (1995) 4976–4984.
[35] S.P. Purton, J.D. Rochaix, Plant Mol. Biol. 24 (1994) 663–672.
[36] H. Zhang, P.L. Herreman, D.P. Weeks, Plant Mol. Biol. 24 (1994) 663–672.
[37] M.R. Kuchka, S.P. Mayfield, J.D. Rochaix, EMBO J. 7 (1988) 319–324.
[38] M. Goldschmidt-Clermont, J. Girard-Bascou, Y. Choquet, J.D. Rochaix, Mol. Gen. Genet. 223 (1990) 417–425.
[39] J.-D. Rochaix, M. Dron, M. Rahire, P.M. Malnoe, Plant Mol. Biol. 3 (1984) 363–370.
[40] R.T. Sayre, B. Andersson, L. Bogorad, Cell 47 (1986) 601–608.
[41] N.H. Chua, P. Bennoun, Proc. Natl. Acad. Sci. USA 72 (1975) 2175–2179.
[42] C.J. Arntzen, K. Pfister, Steinback, K.E., in: H. LeBaron, J. Gressel (Eds.), Herbicide Resistance in Plants, Wiley, New York, 1982, pp. 185–214.
[43] O. Nanba, K. Satoh, Proc. Natl. Acad. Sci. USA 84 (1987) 109–112.
[44] C. de Vitry, F.-A. Wollman, P. Delepelaire, Biochim. Biophys. Acta 767 (1984) 415–422.
[45] J. Deisenhofer, H. Michel, EMBO J. 8 (1989) 2149–2170.
[46] J. Deisenhofer, O. Epp, I. Sinning, H. Michel, J. Mol. Biol. 246 (1995) 429–457.
[47] R.J. Debus, B.A. Barry, I. Sithole, G.T. Babcock, L. McIntosh, Biochemistry 27 (1988) 9071–9074.
[48] J.G. Metz, P.J. Nixon, M. Rögner, G.W. Brudvig, B.A. Diner, Biochemistry 28 (1989) 6960–6969.
[49] B.A. Diner, F.A. Wollman, Eur. J. Biochem. 110 (1980) 521–526.
[50] C. de Vitry, B.A. Diner, J.L. Popo, J. Biol. Chem. 266 (1991) 16614–16621.
[51] D. Bumann, D. Oesterhelt, Biochemistry 33 (1994) 10906–10910.
[52] M. Sugiura, Y. Inoue, J. Minagawa, FEBS Lett. 426 (1998) 140–144.
[53] S.E. Rigby, J.H. Nugent, P.J. O'Malley, Biochemistry 33 (1994) 1734–1742.
[54] J.M. Erickson, M. Rahire, J.-D. Rochaix, L. Mets, Science 228 (1985) 204–207.
[55] J.M. Erickson, K. Pfister, M. Rahire, R.K. Togasaki, L. Mets, J.D. Rochaix, Plant Cell 1 (1989) 361–371.
[56] G.F. Wildner, U. Heisterkamp, A. Trebst, Z. Naturforsch. C 45 (1990) 1142–1150.
[57] C.J. Arntzen, C.L. Ditto, P.E. Brewer, Proc. Natl. Acad. Sci. USA 76 (1979) 278–282.
[58] J. Hirschberg, A. Bleecker, D.J. Kyle, L. McIntosh, C.J. Arntzen, Z. Naturforsch. C 39 (1984) 412–420.
[59] E. Przibilla, S. Heiss, U. Johanningmeier, A. Trebst, Plant Cell 3 (1991) 169–174.
[60] A. Lardans, B. Forster, O. Prasil, P.G. Falkowski, V. Sobolev, M. Edelman, C.B. Osmond, N.W. Gillham, J.E. Boynton, J. Biol. Chem. 273 (1998) 11082–11091.
[61] A. Lardans, N.W. Gillham, J.E. Boynton, J. Biol. Chem. 272 (1997) 210–216.
[62] J. Kim, P.G. Klein, J.E. Mullet, J. Biol. Chem. 266 (1991) 14931–14938.
[63] D. Blubaugh, Govindjee, Photosynth. Res. 19 (1988) 85–128.
[64] R.S. Hutchison, J. Xiong, R.T. Sayre, Govindjee, Biochim. Biophys. Acta 1277 (1996) 83–92.
[65] R.A. Roffey, J.H. Golbeck, C.R. Hille, R.T. Sayre, Proc. Natl. Acad. Sci. USA 88 (1991) 9122–9126.
[66] R.A. Roffey, D.M. Kramer, Govindjee, R.T. Sayre, Biochim. Biophys. Acta 1185 (1994) 257–270.
[67] R.A. Roffey, K.J. van Wijk, R.T. Sayre, S. Styring, J. Biol. Chem. 269 (1994) 5115–5121.
[68] C. Tommos, L. Davidsson, B. Svensson, C. Madsen, W. Vermaas, S. Styring, Biochemistry 32 (1993) 5436–5441.
[69] X.S. Tang, D.A. Chisholm, G.C. Dismukes, G.W. Brudvig, B.A. Diner, Biochemistry 32 (1993) 13742–13748.

[70] B. Svensson, C. Etchebest, P. Tuffery, P. van Kan, J. Smith, S. Styring, Biochemistry 35 (1996) 14486–14502.
[71] X.S. Tang, B.A. Diner, B.S. Larsen, M.L. Gilchrist Jr., G.A. Lorigan, R.D. Britt, Proc. Natl. Acad. Sci. USA 91 (1994) 704–708.
[72] J. Minagawa, D.M. Kramer, A. Kanazawa, A.R. Crofts, FEBS Lett. 389 (1996) 199–202.
[73] J.G. Metz, P.J. Nixon, M. Rogner, G.W. Brudvig, B.A. Diner, Biochemistry 28 (1989) 6960–6969.
[74] G.D. Karabin, M. Farley, R.B. Hallick, Nucleic Acids Res. 12 (1984) 5801–5812.
[75] B. Svensson, I. Vass, S. Styring, Z. Naturforsch. C 46 (1991) 765–776.
[76] B.A. Diner, D.F. Ries, B.N. Cohen, J.G. Metz, J. Biol. Chem. 263 (1988) 8972–8980.
[77] S. Schrader, U. Johanningmeier, Plant. Mol. Biol. 19 (1992) 251–256.
[78] A. Lers, P.B. Heifetz, J.E. Boynton, N.W. Gillham, C.B. Osmond, J. Biol. Chem. 267 (1992) 17494–17497.
[79] R.J. Debus, Biochim. Biophys. Acta 1102 (1992) 269–352.
[80] A. Seidler, A.W. Rutherford, Biochemistry 35 (1996) 12104–12110.
[81] S.P. Mayfield, P. Bennoun, J.D. Rochaix, EMBO J. 6 (1987) 313–318.
[82] R.L. Burnap, L.A. Sherman, Biochemistry 30 (1991) 440–446.
[83] J.B. Philbrick, B.A. Diner, B.A. Zilinskas, J. Biol. Chem. 266 (1991) 13370–13376.
[84] S.R. Mayes, K.M. Cook, S.J. Self, Z. Zhang, J. Barber, Biochim. Biophys. Acta 1060 (1991) 1–12.
[85] R. Bockholt, B. Masepohl, E.K. Pistorius, FEBS Lett. 294 (1991) 59–63.
[86] T.M. Bricker, Biochemistry 31 (1992) 4623–4628.
[87] M. Rova, L.-G. Franzén, P.-O. Frederiksson, S. Styring, Photosynth. Res. 39 (1994) 75–83.
[88] S.P. Mayfield, M. Rahire, G. Frank, H. Zuber, J.D. Rochaix, Proc. Natl. Acad. Sci. USA 84 (1987) 749–753.
[89] C. de Vitry, J. Olive, D. Drapier, M. Recouvreur, F.A. Wollman, J. Cell. Biol. 109 (1989) 991–1006.
[90] E.M. Rova, B. Mc Ewen, P.O. Fredriksson, S. Styring, J. Biol. Chem. 271 (1996) 28918–28924.
[91] M. Ikeuchi, Y. Inoue, FEBS Lett. 241 (1988) 99–104.
[92] A.N. Webber, L.C. Packman, D.J. Chapman, J. Barber, J.C. Gray, FEBS Lett. 242 (1989) 259–262.
[93] X.-S. Tang, K. Fushimi, K. Satoh, FEBS Lett. 273 (1990) 257–260.
[94] E. Boudreau, C. Otis, M. Turmel, Plant Mol. Biol. 24 (1994) 585–602.
[95] P. Kunstner, A. Guardiola, Y. Takahashi, J.D. Rochaix, J. Biol. Chem. 270 (1995) 9651–9654.
[96] G.W. Silk, F. de la Cruz, M. Wu, Nucleic Acids Res. 18 (1990) 4930.
[97] N. Murata, M. Miyao, N. Hayashida, T. Hidaka, M. Sugiura, FEBS Lett. 235 (1988) 283–288.
[98] Y. Takahashi, H. Matsumoto, M. Goldschmidt-Clermont, J.D. Rochaix, Plant Mol. Biol. 24 (1994) 779–788.
[99] M. Ikeuchi, B. Eggers, G.Z. Shen, A. Webber, J.J. Yu, A. Hirano, Y. Inoue, W. Vermaas, J. Biol. Chem. 266 (1991) 11111–11115.
[100] M. Ikeuchi, K. Takio, Y. Inoue, FEBS Lett. 242 (1989) 263–269.
[101] H. Koike, K. Mamada, M. Ikeuchi, Y. Inoue, FEBS Lett. 244 (1989) 391–396.
[102] C. Monod, M. Goldschmidt-Clermont, J.D. Rochaix, Mol. Gen. Genet. 231 (1992) 449–459.
[103] C. Monod, Y. Takahashi, M. Goldschmidt-Clermont, J.D. Rochaix, EMBO J. 13 (1994) 2747–2754.
[104] C. Johnson, G. Schmidt, Plant Mol. Biol. 22 (1993) 645–658.
[105] J. Bennett, Annu. Rev. Plant Physiol. Plant Mol. Biol. 42 (1991) 281–311.
[106] H. Race, K. Gounaris, FEBS Lett. 323 (1993) 35–39.
[107] E.J. Summer, V.H. Schmid, B.U. Bruns, G.W. Schmidt, Plant Physiol. 113 (1997) 1359–1368.
[108] H.E. O'Connor, S.V. Ruffle, A.J. Cain, Z. Deak, I. Vass, J.H. Nugent, S. Purton, Biochim. Biophys. Acta 1364 (1998) 63–72.
[109] J. Barber, B. Andersson, Trends Biochem. Sci. 17 (1992) 61–66.
[110] E.M. Aro, I. Virgin, B. Andersson, Biochim. Biophys. Acta 1143 (1993) 113–134.
[111] K.H. Jensen, D.L. Herrin, F.G. Plumley, G.W. Schmidt, J. Cell Biol. 103 (1986) 1315–1325.
[112] L.E. Sieburth, S. Berry-Lowe, G.W. Schmidt, Plant Cell 3 (1991) 175–189.
[113] J.M. Erickson, M. Rahire, P. Malnoë, J. Girard-Bascou, Y. Pierre, P. Bennoun, J.-D. Rochaix, EMBO J. 5 (1986) 1745–1754.
[114] J.H. Golbeck, Proc. Natl. Acad. Sci. USA 90 (1993) 1642–1646.
[115] A.W. Rutherford, W. Nitschke, in: H. Baltscheffsky (Ed.), Origin and Evolution of Biological Energy Conversion, VCH, New York, 1996, pp. 143–175.
[116] W. Nitschke, T. Mattioli, A.W. Rutherford, in: H. Baltscheffsky (Ed.), Origin and Evolution of Biological Energy Conversion, VCH, New York, 1996, pp. 177–203.
[117] N. Adir, S. Shochat, I. Ohad, J. Biol. Chem. 265 (1990) 12563–12568.
[118] R. Barbato, G. Friso, F. Rigoni, F. Dalla Vecchia, G.M. Giacometti, J. Cell Biol. 119 (1992) 325–335.
[119] K.J. van Wijk, L.O. Nilsson, S. Styring, J. Biol. Chem. 269 (1994) 28382–28392.
[120] H. Zer, O. Prasil, I. Ohad, J. Biol. Chem. 269 (1994) 17670–17676.
[121] Y. Eisenberg-Domovich, R. Oelmuller, R.G. Herrmann, I. Ohad, J. Biol. Chem. 270 (1995) 30181–30186.
[122] I. Ohad, H. Koike, S. Shochat, Y. Inoue, Biochim. Biophys. Acta 933 (1988) 288–298.
[123] T. Hundal, I. Virgin, S. Styring, B. Andersson, Biochim. Biophys. Acta 1017 (1990) 235–241.
[124] M.A. Jansen, B. Depka, A. Trebst, M. Edelman, J. Biol. Chem. 268 (1993) 21246–21252.

[125] H. Zer, I. Ohad, Eur. J. Biochem. 231 (1995) 448–453.
[126] H.S. Gong, I. Ohad, J. Biol. Chem. 266 (1991) 21293–21299.
[127] N. Keren, H. Gong, I. Ohad, J. Biol. Chem. 270 (1995) 806–814.
[128] B. Arntz, A. Trebst, FEBS Lett. 194 (1986) 43–51.
[129] B.M. Greenberg, V. Gaba, O. Canaani, S. Malkin, A.K. Mattoo, M. Edelman, Proc. Natl. Acad. Sci. USA 86 (1989) 6617–6620.
[130] W. Schubert, O. Klukas, N. Krauss, W. Saenger, P. Fromme, H. Witt, J. Mol. Biol. 272 (1997) 741–769.
[131] N. Krauss, W.D. Schubert, O. Klukas, P. Fromme, H.T. Witt, W. Saenger, Nat. Struct. Biol. 3 (1996) 965–973.
[132] J.H. Golbeck, D.A. Bryant, in: C.P. Lee (Ed.), Current Topics in Bioenergetics: Light Driven Reactions in Bioenergetics, Vol. 16, Academic Press, New York, 1991, pp. 83–177.
[133] P.R. Chitnis, Plant Physiol. 111 (1996) 661–669.
[134] K. Brettel, Biochim. Biophys. Acta 1318 (1997) 322–373.
[135] R. Nechushtai, N. Nelson, J. Bioenerg. Biomembr. 13 (1981) 295–306.
[136] R. Nechushtai, N. Nelson, J. Biol. Chem. 256 (1981) 11624–11628.
[137] N. Fischer, P. Setif, J.D. Rochaix, Biochemistry 36 (1997) 93–102.
[138] M. Hippler, F. Drepper, J. Farah, J.D. Rochaix, Biochemistry 36 (1997) 6343–6349.
[139] F.-A. Wollman, P. Bennoun, Biochim. Biophys. Acta 680 (1982) 352–360.
[140] R. Bassi, S.Y. Soen, G. Frank, H. Zuber, J.D. Rochaix, J. Biol. Chem. 267 (1992) 25714–25721.
[141] T.G. Owens, S.P. Webb, L. Mets, R.S. Alberte, G.R. Fleming, Proc. Natl. Acad. Sci. USA 84 (1987) 1532–1536.
[142] T.G. Owens, S.P. Webb, L. Mets, R.S. Alberte, G.R. Fleming, Biophys. J. 56 (1989) 95–106.
[143] M. Werst, Y. Jia, L. Mets, G.R. Fleming, Biophys. J. 61 (1992) 868–878.
[144] G. Hastings, S. Hoshina, A.N. Webber, R.E. Blankenship, Biochemistry 34 (1995) 15512–15522.
[145] G. Hastings, F.A. Kleinherenbrink, S. Lin, R.E. Blankenship, Biochemistry 33 (1994) 3185–3192.
[146] G. Hastings, F.A. Kleinherenbrink, S. Lin, T.J. McHugh, R.E. Blankenship, Biochemistry 33 (1994) 3193–3200.
[147] J. Girard, N.H. Chua, P. Bennoun, G. Schmidt, M. Delosme, Curr. Genet. 2 (1980) 215–221.
[148] P. Bennoun, J. Girard, N.-H. Chua, Mol. Gen. Genet. 153 (1977) 343–348.
[149] J. Girard-Bascou, Curr. Genet. 12 (1987) 483–488.
[150] Y. Choquet, M. Rahire, J. Girard-Bascou, J. Erickson, J.D. Rochaix, EMBO J. 11 (1992) 1697–1704.
[151] J. Girard-Bascou, Y. Choquet, M. Schneider, M. Delosme, M. Dron, Curr. Genet. 12 (1987) 489–495.
[152] S.E. Bingham, R.H. Xu, A.N. Webber, FEBS Lett. 292 (1991) 137–140.
[153] U. Kück, Y. Choquet, M. Schneider, M. Dron, P. Bennoun, EMBO J. 6 (1987) 2185–2192.
[154] Y. Choquet, M. Goldschmidt-Clermont, J. Girard-Bascou, U. Kuck, P. Bennoun, J.D. Rochaix, Cell 52 (1988) 903–913.
[155] C. Roitgrund, L.J. Mets, Curr. Genet. 17 (1990) 147–153.
[156] Y. Takahashi, M. Goldschmidt-Clermont, S.Y. Soen, L.G. Franzen, J.D. Rochaix, EMBO J. 10 (1991) 2033–2040.
[157] L.E. Fish, U. Kück, L. Bogorad, in: Molecular Biology of the Photosynthetic Apparatus, Cold Spring Harbor Laboratory Press, Cold Spring Harbor, NY, 1985 pp. 111–120.
[158] H. Lee, S.E. Bingham, A.N. Webber, Photochem. Photobiol. 64 (1996) 46–52.
[159] A.N. Webber, P.B. Gibbs, J.B. Ward, S.E. Bingham, J. Biol. Chem. 268 (1993) 12990–12995.
[160] B.J. Hallahan, S. Purton, A. Ivison, D. Wright, M.C.W. Evans, Photosynth. Res. 46 (1995) 257–264.
[161] S.M. Rodday, S.-S. Jun, J. Biggins, Photosynth. Res. 36 (1993) 1–9.
[162] S.M. Rodday, R. Schulz, L. McIntosh, J. Biggins, Photosynth. Res. 42 (1994) 185–190.
[163] S.M. Rodday, A.N. Webber, S.E. Bingham, J. Biggins, Biochemistry 34 (1995) 6328–6334.
[164] K.G. Parrett, T. Mehari, P.G. Warren, J.H. Golbeck, Biochim. Biophys. Acta 973 (1989) 324–332.
[165] K.G. Parrett, T. Mehari, J.H. Golbeck, Biochim. Biophys. Acta 1015 (1990) 341–352.
[166] P. Dunn, J. Gray, Plant Mol. Biol. 11 (1988) 311–319.
[167] W. Nitschke, U. Feiler, A.W. Rutherford, Biochemistry 29 (1990) 3834–3842.
[168] M. Büttner, D.L. Xie, H. Nelson, W. Pinther, G. Hauska, N. Nelson, Proc. Natl. Acad. Sci. USA 89 (1992) 8135–8139.
[169] U. Liebl, M. Mockensturm-Wilson, J. Trost, D. Brune, R. Blankenship, W. Vermaas, Proc. Natl. Acad. Sci. USA 90 (1993) 7124–7128.
[170] L. Cui, S.E. Bingham, M. Kuhn, H. Kass, W. Lubitz, A.N. Webber, Biochemistry 34 (1995) 1549–1558.
[171] A.N. Webber, H. Su, S.E. Bingham, H. Kass, L. Krabben, M. Kuhn, R. Jordan, E. Schlodder, W. Lubitz, Biochemistry 35 (1996) 12857–12863.
[172] K. Redding, F. MacMillan, W. Leibl, K. Brettel, J. Hanley, A.W. Rutherford, J. Breton, J.-D. Rochaix, EMBO J. 17 (1997) 50–60.
[173] M. Mac, X.S. Tang, B.A. Diner, J. McCracken, G.T. Babcock, Biochemistry 35 (1996) 13288–13293.
[174] A.N. Melkozernov, H. Su, S. Lin, S. Bingham, A.N. Webber, R.E. Blankenship, Biochemistry 36 (1997) 2898–2907.
[175] P.M. Wood, Eur. J. Biochem. 87 (1978) 9–19.
[176] K.K. Ho, D.W. Krogmann, Biochim. Biophys. Acta 766 (1984) 310–316.
[177] G. Sandmann, Arch. Microbiol. 21 (1986) 6366–6375.
[178] S. Merchant, L. Bogorad, Mol. Cell. Biol. 6 (1986) 462–469.
[179] J. Quinn, H.H. Li, J. Singer, B. Morimoto, L. Mets, K. Kindle, S. Merchant, J. Biol. Chem. 268 (1993) 7832–7841.
[180] S. Katoh, I. Shiratori, A. Takamiya, J. Biochem. 51 (1962) 32–40.

[181] A.G. Sykes, Chem. Soc. Rev. 14 (1985) 283–315.
[182] E.T. Adman, Adv. Protein Chem. 42 (1991) 145–197.
[183] J.M. Guss, H.C. Freeman, J. Mol. Biol. 169 (1983) 521–563.
[184] J.M. Guss, P.R. Harrowell, M.A.N.V. Murata, H.C. Freeman, J. Mol. Biol. 192 (1986) 361–387.
[185] C.A. Collyer, J.M. Guss, Y. Sugimura, F. Yoshizaki, H.C. Freeman, J. Mol. Biol. 211 (1990) 617–632.
[186] M.R. Redinbo, D. Cascio, M.K. Choukair, D. Rice, S. Merchant, T.O. Yeates, Biochemistry 32 (1993) 10560–10567.
[187] U. Badsberg, A.M. Jorgensen, H. Gesmar, J.J. Led, J.M. Hammerstad, L.L. Jespersen, J. Ulstrup, Biochemistry 35 (1996) 7021–7031.
[188] M.R. Redinbo, T.O. Yeates, S. Merchant, J. Bioenerg. Biomembr. 26 (1994) 49–66.
[189] D.G. Sanderson, L.B. Anderson, E.L. Gross, Biochim. Biophys. Acta 852 (1986) 269–278.
[190] F.A. Armstrong, H.A.O. Hill, N. Oliver, D. Whitford, J. Am. Chem. Soc. 107 (1985) 1473–1477.
[191] A.G. Sykes, Struct. Bond. 75 (1991) 175–224.
[192] M. Nordling, K. Sigfridsson, S. Young, L.G. Lundberg, O. Hansson, FEBS Lett. 291 (1991) 327–330.
[193] W. Haehnel, T. Jansen, K. Gause, R.B. Klosgen, B. Stahl, D. Michl, B. Huvermann, M. Karas, R.G. Herrmann, EMBO J. 13 (1994) 1028–1038.
[194] B.H. Lee, T. Hibino, T. Takabe, P.J. Weisbeek, T. Takabe, J. Biochem. 117 (1995) 1209–1217.
[195] M. Hippler, J. Reichert, M. Sutter, E. Zak, L. Altschmied, U. Schröer, R.G. Herrmann, W. Haehnel, EMBO J. 15 (1996) 6374–6384.
[196] S. Merchant, L. Bogorad, J. Biol. Chem. 261 (1986) 15850–15853.
[197] H.H. Li, S. Merchant, J. Biol. Chem. 267 (1992) 9368–9375.
[198] S. Merchant, L. Bogorad, J. Biol. Chem. 262 (1987) 9062–9067.
[199] C.A. Kerfeld, H.A. Anwar, R. Interrante, S. Merchant, O.T. Yeates, J. Mol. Biol. 250 (1995) 627–647.
[200] D.S. Gorman, R.P. Levine, Plant Physiol. 41 (1966) 1643–1647.
[201] F.S. Mathews, Prog. Biophys. Mol. Biol. 45 (1985) 1–56.
[202] K.L. Hill, H.H. Li, J. Singer, S. Merchant, J. Biol. Chem. 266 (1991) 15060–15067.
[203] G. Howe, S. Merchant, J. Biol. Chem. 269 (1994) 5824–5832.
[204] H.H. Li, S. Merchant, J. Biol. Chem. 270 (1995) 23504–23510.
[205] S. Merchant, K. Hill, G. Howe, EMBO J. 10 (1991) 1383–1389.
[206] K.L. Hill, S. Merchant, Plant Physiol. 100 (1992) 319–326.
[207] J.M. Quinn, S. Merchant, Plant Cell 7 (1995) 623–628.
[208] H.H. Li, J. Quinn, D. Culler, J. Girard-Bascou, S. Merchant, J. Biol. Chem. 271 (1996) 31283–31289.
[209] R. Delosme, Photosynth. Res. 29 (1991) 45–54.
[210] M. Hervas, J.A. Navarro, A. Diaz, H. Bottin, M.A. De la Rosa, Biochemistry 34 (1995) 11321–11326.
[211] R.M. Wynn, R. Malkin, Biochemistry 27 (1988) 5863–5869.
[212] R.M. Wynn, J. Omaha, R. Malkin, Biochemistry 28 (1989) 5554–5560.
[213] M. Hippler, R. Ratajczak, W. Haehnel, FEBS Lett. 250 (1989) 280–284.
[214] P.R. Chitnis, D. Purvis, N. Nelson, J. Biol. Chem. 266 (1991) 20146–20151.
[215] Q. Xu, L. Yu, V.P. Chitnis, P.R. Chitnis, J. Biol. Chem. 269 (1994) 3205–3211.
[216] L. Krabben, H. Kab, E. Schlodder, M. Kuhn, W. Lubitz, H. Xu, S. Bingham, A. Webber, in: P. Mathis (Ed.), Photosynthesis: from Light to Biosphere, Vol. II, Kluwer Academic Publishers, Dordrecht, 1995, pp. 123–126.
[217] P. Sétif, P. Mathis, Arch. Biochem. Biophys. 204 (1980) 477–485.
[218] F. Drepper, M. Hippler, W. Nitschke, W. Haehnel, Biochemistry 35 (1996) 1282–1295.
[219] L.G. Franzén, G. Frank, H. Zuber, J.-D. Rochaix, Plant Mol. Biol. 12 (1989) 463–474.
[220] M. Hippler, F. Drepper, W. Haehnel, J.D. Rochaix, Proc. Natl. Acad. Sci. USA 95 (1998) 7339–7344.
[221] D.I. Arnon, Science 149 (1965) 1460–1470.
[222] D.B. Knaff, M. Hirasawa, Biochim. Biophys. Acta 1056 (1991) 93–125.
[223] J.M. Schmitter, J.P. Jacquot, F. Lamotte, C. Beauvallet, S. Dutka, P. Gadal, P. Decottignies, Eur. J. Biochem. 172 (1988) 405–412.
[224] J.W. Rogers, M. Hodges, P. Decottignies, J.M. Schmitter, P. Gadal, J.P. Jacquot, FEBS Lett. 310 (1992) 240–245.
[225] P. Decottignies, P. LeMarechal, J.P. Jacquot, J.M. Schmitter, P. Gadal, Arch. Biochem. Biophys. 316 (1995) 249–259.
[226] P. Setif, H. Bottin, Biochemistry 34 (1994) 8495–8504.
[227] M. Stein, J.P. Jacquot, M. Migniac-Maslow, Plant Physiol. 102 (1993) 1349–1350.
[228] H. Matsubara, H. Hase, in: U. Jensen, D.E. Fairbrothers (Eds.), Proteins and Nucleic Acids in Plant Systematics, Springer, Berlin, 1983, pp. 168–181.
[229] J.P. Jacquot, M. Stein, A. Suzuki, S. Liottet, G. Sandoz, M. Miginiac-Maslow, FEBS Lett. 400 (1997) 293–296.
[230] L. Piubelli, A. Aliverti, F. Bellintani, G. Zanetti, Eur. J. Biochem. 236 (1996) 465–469.
[231] C. Lelong, P. Setif, B. Lagoutte, H. Bottin, J. Biol. Chem. 269 (1994) 10034–10039.
[232] N. Fischer, M. Hippler, P. Setif, J.P. Jacquot, J.D. Rochaix, EMBO J. 17 (1998) 849–858.
[233] C. Lemaire, J. Girad-Bascou, F.A. Wollman, P. Bennoun, Biochim. Biophys. Acta 851 (1986) 229–238.
[234] R.M. Wynn, J. Bertsch, B.D. Bruce, R. Malkin, Biochim. Biophys. Acta 935 (1988) 115–122.
[235] C.L. Schmidt, R. Malkin, Photosynth. Res. 38 (1993) 73–81.
[236] Y. Pierre, C. Breyton, D. Kramer, J.L. Popot, J. Biol. Chem. 270 (1995) 29342–29349.
[237] D. Huang, R.M. Everly, R.H. Cheng, J.B. Heymann, H. Schagger, V. Sled, T. Ohnishi, T.S. Baker, W.A. Cramer, Biochemistry 33 (1994) 4401–4409.

[238] M.T. Black, W.R. Widger, W.A. Cramer, Arch. Biochem. Biophys. 252 (1987) 655–661.
[239] S. Buschlen, Y. Choquet, R. Kuras, F.A. Wollman, FEBS Lett. 284 (1991) 257–262.
[240] J.A. Bretsch, R. Malkin, Plant Mol. Biol. 17 (1991) 131–133.
[241] D.M. Kramer, A.R. Crofts, Biochim. Biophys. Acta 1184 (1994) 193–201.
[242] A.B. Hope, Biochim. Biophys. Acta 1143 (1993) 1–22.
[243] S.E. Martinez, D. Huang, A. Szczepaniak, W.A. Cramer, J.L. Smith, Structure 2 (1994) 95–105.
[244] W.A. Cramer, G.M. Soriano, M. Ponomarev, D. Huang, H. Zhang, S.E. Martinez, J.L. Smith, Annu. Rev. Plant Physiol. Plant Mol. Biol. 47 (1996) 477–508.
[245] D.M. Willey, A.D. Auffret, J.C. Gray, Cell 36 (1984) 555–562.
[246] P. Joliot, A. Joliot, Biochim. Biophys. Acta 933 (1988) 319–333.
[247] D.M. Kramer, A.R. Crofts, Biochim. Biophys. Acta 1183 (1993) 72–84.
[248] M. Degli Esposti, S. De Vries, M.A.G. Crimi, T. Patarnello, A. Meyer, Biochim. Biophys. Acta 1143 (1993) 243–271.
[249] D. Xia, C.A. Yu, H. Kim, J.Z. Xia, A.M. Kachurin, L. Zhang, L. Yu, J. Deisenhofer, Science 277 (1997) 60–66.
[250] S.C.O. Iwata, B. Ludwig, H. Michel, Nature 376 (1995) 660–669.
[251] T. Tsukihara, H. Aoyama, E. Yamashita, T. Tomizaki, T.H. Yamaguchi et al., Science 269 (1995) 1069–1074.
[252] G. Finazzi, S. Buschlen, C. de Vitry, F. Rappaport, P. Joliot, F.A. Wollman, Biochemistry 36 (1997) 2867–2874.
[253] W.A. Cramer, S.E. Martinez, D. Huang, G.S. Tae, R.M. Everly, J.B. Heymann, R.H. Cheng, T.S. Baker, J.L. Smith, J. Bioenerg. Biomembr. 26 (1994) 31–47.
[254] G. Hauska, W. Nitschke, R.G. Herrmann, J. Bioenerg. Biomem. 20 (1988) 211–228.
[255] M.P. Doyle, L.B. Li, L. Yu, C.A. Yu, J. Biol. Chem. 264 (1989) 1387–1392.
[256] C. de Vitry, J. Biol. Chem. 269 (1994) 7603–7609.
[257] F. Madueno, J.A. Napier, F.J. Cejudo, J.C. Gray, Plant Mol. Biol. 20 (1992) 289–299.
[258] C.J. Carell, H. Zhang, W.A. Cramer, J.L. Smith, Structure 5 (1997) 1613–1625.
[259] E. Davidson, T. Ohnishi, E. Atta-Adjei, F. Daldal, Biochemistry 31 (1992) 3342–3351.
[260] Z. Zhang, L. Huang, V.M. Shulmeister, Y.-I. Chi, K.K. Kim, L.-W. Hung, A. Crofts, A.E. Berry, S.-H. Kim, Nature 392 (1998) 677–684.
[261] C. Breyton, C. de Vitry, J.L. Popot, J. Biol. Chem. 269 (1994) 7597–7602.
[262] J. Haley, L. Bogorad, Proc. Natl. Acad. Sci. USA 86 (1989) 1534–1538.
[263] S.E. Fong, S.J. Surzycki, Curr. Genet. 21 (1992) 527–530.
[264] D.A. Berthold, C.L. Schmidt, R. Malkin, J. Biol. Chem. 270 (1995) 29293–29298.
[265] C. de Vitry, C. Breyton, Y. Pierre, J.L. Popot, J. Biol. Chem. 271 (1996) 10667–10671.
[266] S.L. Ketchner, R. Malkin, Biochim. Biophys. Acta 1273 (1996) 195–197.
[267] Y. Takahashi, M. Rahire, C. Breyton, J.L. Popot, P. Joliot, J.D. Rochaix, EMBO J. 15 (1996) 3498–3506.
[268] J. Lavergne, Biochim. Biophys. Acta 725 (1983) 25–33.
[269] D. Bald, J. Kruip, E.J. Boekema, M. Rogner, in: N. Murata (Ed.), Research in Photosynthesis. Proceedings of the IXth International Congress on Photosynthesis, Kluwer, Nagoya, 1992, pp. 629–632.
[270] E. Hurt, G. Hauska, Eur. J. Biochem. 117 (1981) 591–599.
[271] J.L. Popot, Y. Pierre, C. Breyton, Y. Lemoine, Y. Takahashi, J.D. Rochaix, in: P. Mathis (Ed.), Photosynthesis. From Light to Biosphere. Proceedings of the Xth International Congress on Photosynthesis, Kluwer, Montpellier, 1995, pp. 507–512.
[272] A. Joliot, P. Joliot, in: P. Mathis (Ed.), Photosynthesis. From Light to Biosphere. Proceedings of the Xth International Congress on Photosynthesis, Vol. 2, Kluwer, Montpellier, 1995, pp. 615–618.
[273] Y. Pierre, C. Breyton, Y. Lemoine, B. Robert, C. Vernotte, J.L. Popot, J. Biol. Chem. 272 (1997) 21901–21908.
[274] C. Breyton, C. Tribet, J. Olive, M. Recouvreur, J.L. Popot, in: P. Mathis (Ed.), Photosynthesis. From Light to Biosphere. Proceedings of the Xth International Congress on Photosynthesis Kluwer, Montpellier, 1995, pp. 591–594.
[275] C. Breyton, C. Tribet, J. Olive, J.P. Dubacq, J.L. Popot, J. Biol. Chem. 272 (1997) 21892–21900.
[276] G. Mosser, C. Breyton, A. Olofsson, J.L. Popot, J.L. Rigaud, J. Biol. Chem. 272 (1997) 20263–20268.
[277] P. Mitchell, J. Theor. Biol. 62 (1976) 327–367.
[278] A.R. Crofts, S.W. Meinhardt, K.R. Jones, M. Snozzi, Biochim. Biophys. Acta 723 (1983) 202–218.
[279] M. Wikstrom, K. Krab, J. Bioenerg. Biomembr. 18 (1986) 181–193.
[280] W. Junge, H.T. Witt, Z. Naturforsch. 23b (1968) 244–255.
[281] P. Joliot, D. Delosme, Biochim. Biophys. Acta 357 (1974) 267–284.
[282] B. Bouges-Bocquet, Biochim. Biophys. Acta 462 (1977) 362–370.
[283] B. Velthuys, Proc. Natl. Acad. Sci. USA 75 (1978) 6031–6034.
[284] B.R. Velthuys, Proc. Natl. Acad. Sci. USA 76 (1979) 2765–2769.
[285] P. Joliot, A. Joliot, Biochim. Biophys. Acta 849 (1986) 211–222.
[286] M.A. Selak, J. Withmarsh, FEBS Lett. 150 (1982) 286–292.
[287] R. Delosme, P. Joliot, A. Trebst, Biochim. Biophys. Acta 893 (1987) 1–6.
[288] D.M. Kramer, A.R. Crofts, in: N. Murata (Ed.), Research in Photosynthesis. Proceedings of the IXth International Congress on Photosynthesis, Vol. 2, Kluwer Acdemic Publishers, Nagoya, 1992, pp. 491–494.
[289] P.R. Rich, S.A. Madgwick, S. Brown, G. von Jagow, U. Brandt, Photosynth. Res. 34 (1992) 465–477.
[290] P. Joliot, A. Joliot, Proc. Natl. Acad. Sci USA 91 (1994) 1034–1038.

[291] J.G. Fernandez-Velasco, D.A. Berthold, R. Malkin, in: P. Mathis (Ed.), Photosynthesis. From light to Biosphere. Proceedings of the Xth International Congress on Photosynthesis, Vol. 2, Kluwer, Montpellier, 1995, pp. 555–558.
[292] D.M. Kramer, A.R. Croft, in: P. Mathis (Ed.), Photosynthesis. From Light to Biosphere. Proceedings of the Xth International Congress on Photosynthesis, Vol. 2, Kluwer, 1995, Montpellier, pp. 575–578.
[293] F. Zito, R. Kuras, Y. Choquet, H. Kossel, F.A. Wollman, Plant Mol. Biol. 33 (1997) 79–86.
[294] R. Freyer, B. Hoch, K. Neckermann, R.M. Maier, H. Kossel, Plant J. 4 (1993) 621–629.
[295] T. Hirose, T. Wakasugi, M. Sugiura, Plant Mol. Biol. 26 (1994) 509–513.
[296] G.M. Soriano, G.-S. Ponamarev, G.-S. Tae, W.A. Cramer, Biochemistry 35 (1996) 14590–14598.
[297] G.M. Soriano, M.V. Ponamarev, R. Piskorowski, W.A. Cramer, submitted for publication.
[298] J. Zhou, J.G. Fernandez-Velasco, R. Malkin, J. Biol. Chem. 271 (1996) 6225–6232.
[299] R. Kuras, F.A. Wollman, EMBO J. 13 (1994) 1019–1027.
[300] R. Kuras, F.A. Wollman, P. Joliot, Biochemistry 34 (1995) 7468–7475.
[301] R. Kuras, S. Büschlen, F.-A. Wollman, J. Biol. Chem. 270 (1995) 27797–27803.
[302] D.W. Nicholson, R.A. Stuart, W. Neupert, J. Biol. Chem. 264 (1989) 10156–10168.
[303] J.E. Walker, M.J. Runswick, M. Saraste, FEBS Lett. 146 (1982) 393–396.
[304] J.E. Walker, I.M. Fearnley, N.J. Gay, B.W. Gibson, F.D. Northrop, S.J. Powell, M.J. Runswick, M. Saraste, V.L. Tybulewicz, J. Mol. Biol. 184 (1985) 677–701.
[305] P. Mitchell, Nature 191 (1961) 144–148.
[306] L.M. Amzel, P.L. Pedersen, Annu. Rev. Biochem. 52 (1983) 801–824.
[307] P.D. Boyer, Biochim. Biophys. Acta 1140 (1993) 215–250.
[308] W.D. Frasch, in: D.A. Bryant (Ed.), The Molecular Biology of Cyanobacteria, Kluwer, Dordrecht, 1994, pp. 361–380.
[309] J.P. Abrahams, A.G. Leslie, R. Lutter, J.E. Walker, Nature 370 (1994) 621–628.
[310] Y. Shirakihara, A.G. Leslie, J.P. Abrahams, J.E. Walker, T. Ueda, Y. Sekimoto, M. Kambara, K. Saika, Y. Kagawa, M. Yoshida, Structure 5 (1997) 825–836.
[311] S. Selman-Reimer, S. Merchant, B.R. Selman, Biochemistry 20 (1981) 5476–5482.
[312] S. Merchant, S.L. Shaner, B.R. Selman, J. Biol. Chem. 258 (1983) 1026–1031.
[313] R.G. Piccioni, P. Bennoun, N.H. Chua, Eur. J. Biochem. 117 (1981) 93–102.
[314] S. Leu, J. Schlesinger, A. Michaels, N. Shavit, Plant Mol. Biol. 18 (1992) 613–616.
[315] C. Lemaire, F.-A. Wollman, J. Biol. Chem. 264 (1989) 10228–10234.
[316] J.P. Woessner, N.W. Gilham, J.E. Boynton, Plant Mol. Biol. 8 (1987) 151–158.
[317] J.P. Woessner, N.W. Gillham, J.E. Boynton, Gene 44 (1986) 17–28.
[318] L.M. Yu, B.R. Selman, J. Biol. Chem. 263 (1988) 19342–19345.
[319] E. Smart, B.R. Selman, Plant Physiol. 97 (1991) 1596–1598.
[320] J. Hennig, R.G. Herrmann, Mol. Gen. Genet. 203 (1986) 117–128.
[321] H. Fiedler, J. Schlesinger, H. Strotmann, N. Shavit, S. Leu, Biochim. Biophys. Acta 1319 (1997) 109–118.
[322] D. Hu, H. Fiedler, T. Golan, M. Edelman, H. Strotman, N. Shavit, S. Leu, J. Biol. Chem. 272 (1997) 5457–5463.
[323] J.P. Woessner, A. Masson, E.A. Harris, P. Bennoun, N.W. Gilham, J.E. Boynton, Plant Mol. Biol. 3 (1984) 177–190.
[324] C. Lemaire, F.-A. Wollman, J. Biol. Chem. 264 (1989) 10235–10242.
[325] D. Robertson, J.E. Boynton, N.W. Gillham, Mol. Gen. Genet. 221 (1990) 155–163.
[326] D. Robertson, J.P. Woessner, N.W. Gillham, J.E. Boynton, J. Biol. Chem. 264 (1989) 2331–2337.
[327] S.L. Ketchner, D. Drapier, J. Olive, S. Gaudriault, J. Girard-Bascou, F.A. Wollman, J. Biol. Chem. 270 (1995) 15299–15306.
[328] D. Draper, J. Girard-Bascou, F.-A. Wollman, Plant Cell 4 (1992) 283–295.
[329] A. Avni, J.D. Anderson, N. Holland, J.D. Rochaix, Z. Gromet-Elhanan, M. Edelman, Science 257 (1992) 1245–1247.
[330] A.L. Houseman, R. LoBrutto, W.D. Frasch, Biochemistry 33 (1994) 10000–10006.
[331] A.L. Houseman, L. Morgan, R. LoBrutto, W.D. Frasch, Biochemistry 33 (1994) 4910–4917.
[332] A.L. Houseman, R. LoBrutto, W.D. Frasch, Biochemistry 34 (1995) 3277–3285.
[333] C.Y. Hu, A.L. Houseman, L. Morgan, A.N. Webber, W.D. Frasch, Biochemistry 35 (1996) 12201–12211.
[334] D. Sabbert, S. Engelbrecht, W. Junge, Nature 381 (1996) 623–625.
[335] H. Noji, R. Yasuda, M. Yoshida, K. Kinosita, Nature 386 (1997) 299–302.
[336] M.J. van Raaij, J.P. Abrahams, A.G. Leslie, J.E. Walker, Proc. Natl. Acad. Sci. USA 93 (1996) 6913–6917.
[337] J.D. Mills, P. Mitchell, Biochim. Biophys. Acta 764 (1984) 93–104.
[338] S.R. Ketcham, J.W. Davenport, K. Warncke, R.E. McCarty, J. Biol. Chem. 259 (1984) 7286–7293.
[339] J.L. Arana, R.H. Vallejos, J. Biol. Chem. 257 (1982) 1125–1127.
[340] J.V. Moroney, C.S. Fullmer, R.E. McCarty, J. Biol. Chem. 259 (1984) 7281–7285.
[341] C.M. Nalin, R.E. McCarty, J. Biol. Chem. 259 (1984) 7275–7280.
[342] J.E. Walker, Curr. Opin. Struct. Biol. 4 (1994) 912–918.
[343] E.J. Smart, B.R. Selman, Mol. Cell. Biol. 11 (1991) 5053–5058.
[344] E.J. Smart, B.R. Selman, J. Bioenerg. Biomembr. 25 (1993) 275–284.

[345] S.A. Ross, M.X. Zhang, B.R. Selman, J. Biol. Chem. 270 (1995) 9813–9818.
[346] S.A. Ross, M.X. Zhang, B.R. Selman, J. Bioenerg. Biomembr. 28 (1996) 49–57.
[347] D. Hu, H. Strotmann, N. Shavit, S. Leu, FEBS Lett. 421 (1998) 65–68.
[348] J.-M. Jault, C. Dou, N. Grodsky, T. Matsui, M. Yoshida, W. Allison, J. Biol. Chem. 271 (1996) 28818–28824.
[349] P. Joliot, Biochim. Biophys. Acta 102 (1965) 116–134.
[350] B. Diner, D. Mauzerall, Biochim. Biophys. Acta 305 (1973) 329–352.
[351] P. Bennoun, Prog. Clin. Biol. Res. 102, (B) (1982) 291–298.
[352] G. Peltier, J. Ravenel, A. Vermeglio, Biochim. Biophys. Acta 893 (1987) 83–90.
[353] P. Bennoun, Biochim. Biophys. Acta 1186 (1994) 59–66.
[354] R.P. Gfeller, M. Gibbs, Plant Physiol. 77 (1985) 509–511.
[355] M. Sugiura, Plant Mol. Biol. 19 (1992) 149–168.
[356] P.J. Nixon, K. Gounaris, S.A. Coomber, C.N. Hunter, T.A. Dyer, J. Barber, J. Biol. Chem. 264 (1989) 14129–14135.
[357] J. Whelan, S. Young, D.A. Day, Plant Mol. Biol. 20 (1992) 887–895.
[358] S. Berger, U. Ellersiek, P. Westhoff, K. Steinmuller, Planta 190 (1993) 25–31.
[359] M. Martin, L.M. Casano, B. Sabater, Plant Cell Physiol. 37 (1996) 293–298.
[360] G. Guedeney, S. Corneille, S. Cuine, G. Peltier, FEBS Lett. 378 (1996) 277–280.
[361] A. Kubicki, E. Funk, P. Westhoff, K. Steinmuller, Planta 199 (1996) 276–281.
[362] P.A. Burrows, L.A. Sazanov, Z. Svab, P. Maliga, P.J. Nixon, EMBO J. 17 (1998) 868–876.
[363] D. Godde, A. Trebst, Arch. Microbiol. 127 (1980) 245–252.
[364] D. Godde, Arch. Microbiol. 131 (1982) 197–202.
[365] A. Atteia, C. de Vitry, Y. Pierre, J.L. Popot, J. Biol. Chem. 267 (1992) 226–234.
[366] M. Wu, Z.Q. Nie, J. Yang, Plant Cell 1 (1989) 551–557.
[367] Z.Q. Nie, D.Y. Chang, M. Wu, Mol. Gen. Genet. 209 (1987) 265–269.
[368] K.O. Willeford, Z. Gombos, M. Gibbs, Plant Physiol. 90 (1989) 1084–1087.
[369] F. Rebeille, G. Gans, Plant Physiol. 88 (1988) 973–975.
[370] P. Gans, F. Rebeille, Biochim. Biophys. Acta 1015 (1990) 150–155.
[371] X. Xue, D.A. Gauthier, D.H. Turpin, H.G. Weger, Plant Physiol. 112 (1996) 1005–1014.
[372] P. Bennoun, FEBS Lett. 156 (1983) 363–365.
[373] J. Ravenel, G. Peltier, Photosynth. Res. 28 (1991) 141–148.
[374] J. Ravenel, G. Peltier, Biochim. Biophys. Acta 1101 (1992) 57–63.
[375] G. Peltier, P. Thibault, Biochim. Biophys. Acta 936 (1988) 319–324.
[376] L. Cournac, K. Redding, P. Bennoun, G. Peltier, FEBS Lett. 416 (1997) 65–68.
[377] E. Greenbaum, J.W. Lee, C.V. Tevault, S.L. Blankinship, L.J. Mets, Nature 376 (1995) 438–441.
[378] J.W. Lee, C.V. Tevault, T.G. Owens, E. Greenbaum, Science 273 (1996) 364–367.
[379] C. Lemaire, F.A. Wollman, P. Bennoun, Proc. Natl. Acad. Sci. USA 85 (1988) 1344–1348.
[380] C. Bonaventura, J. Myers, Biochim. Biophys. Acta 189 (1969) 366–383.
[381] N. Murata, Biochim. Biophys. Acta 172 (1969) 242–251.
[382] J.F. Allen, Biochim. Biophys. Acta 1098 (1992) 275–335.
[383] J. Bennett, Annu. Rev. Plant Physiol. 42 (1991) 281–311.
[384] A. Sokolenko, H. Fulgosi, A. Gal, L. Altschmied, I. Ohad, R.G. Herrmann, FEBS Lett. 371 (1995) 176–180.
[385] F.A. Wollman, P. Delepelaire, J. Cell. Biol. 98 (1984) 1–7.
[386] P. Delepelaire, F.-A. Wollman, Biochim. Biophys. Acta 809 (1985) 277–283.
[387] R. Delosme, D. Béal, P. Joliot, Biochim. Biophys. Acta 1185 (1994) 56–64.
[388] R. Delosme, J. Olive, F.-A. Wollman, Biochim. Biophys. Acta 1273 (1996) 150–158.
[389] J. Bennet, E.K. Shaw, S. Bakr, FEBS Lett. 210 (1987) 22–26.
[390] A. Gal, Y. Shanak, G. Schuster, I. Ohad, FEBS Lett. 221 (1987) 205–210.
[391] F.-A. Wollman, C. Lemaire, Biochim. Biophys. Acta 933 (1988) 85–94.
[392] A. Gal, G. Schuster, D. Frid, O. Canaani, H.G. Schwieger, I. Ohad, J. Biol. Chem. 263 (1988) 7785–7791.
[393] A. Gal, G. Hauska, R. Herrmann, I. Ohad, J. Biol. Chem. 265 (1990) 19742–19749.
[394] O. Vallon, L. Bulte, P. Dainese, J. Olive, R. Bassi, F.A. Wollman, Proc. Natl. Acad. Sci. USA 88 (1991) 8262–8266.
[395] L. Bulte, P. Bennoun, Curr. Genet. 18 (1990) 155–160.
[396] M. Havaux, Plant Cell Physiol. 33 (1992) 799–803.
[397] E. Bergantino, P. Dainese, Z. Cerovic, S. Sechi, R. Bassi, J. Biol. Chem. 270 (1995) 8474–8481.
[398] U. Goodenough, R.P. Levine, Plant Physiol. 44 (1969) 990–1000.
[399] B. Baldan, J. Girard-Bascou, F.-A. Wollman, J. Olive, J. Cell Biol. 114 (1991) 905–915.
[400] H. Gaffron, Nature 143 (1939) 204–205.
[401] H. Gaffron, Am. J. Botany 27 (1940) 273–283.
[402] H. Gaffron, J. Rubin, J. Gen. Physiol. 26 (1942) 219–240.
[403] G.K. Russel, M. Gibbs, Plant Physiol. 43 (1968) 649–652.
[404] T.E. Maione, M. Gibbs, Plant Physiol. 80 (1986) 360–363.
[405] T.E. Maione, M. Gibbs, Plant Physiol. 80 (1986) 364–368.
[406] U. Klein, C. Chen, M. Gibbs, K. Platt-Aloia, Plant Physiol. 72 (1983) 481–487.
[407] F.P. Healy, Plant Physiol. 45 (1970) 153–159.
[408] E. Greenbaum, R.R.L. Guillard, W.G. Sunda, Photochem. Photobiol. 37 (1983) 649–655.
[409] T. Pow, A.I. Krasna, Arch. Biochem. Biophys. 194 (1979) 413–421.
[410] D.A. Graves, C.V. Tevault, E. Greenbaum, Photochem. Photobiol. 50 (1989) 571–576.
[411] N.I. Bishop, Annu. Rev. Plant Physiol. 17 (1966) 185–208.
[412] E.S. Bamberger, D. King, D.L. Erbes, M. Gibbs, Plant Physiol. 69 (1982) 1268–1273.

[413] T.S. Stuart, H. Gaffron, Planta 106 (1972) 101–112.
[414] F.B. Abeles, Plant Physiol. 39 (1964) 169–176.
[415] D.L. Erbes, D. King, M. Gibbs, Plant Physiol. 63 (1979) 1138–1142.
[416] T. Happe, B. Mosler, J.D. Naber, Eur. J. Biochem. 222 (1994) 769–774.
[417] P.G. Roessler, S. Lien, Plant Physiol. 75 (1984) 1086–1089.
[418] P.G. Roessler, S. Lien, Arch. Biochem. Biophys. 230 (1984) 103–109.
[419] T. Happe, J.D. Naber, Eur. J. Biochem. 214 (1993) 475–481.
[420] P.G. Roessler, S. Lien, Plant Physiol. 75 (1984) 705–709.
[421] C.R. Somerville, W.L. Ogren, Trends Biochem. Sci. 7 (1982) 171–174.
[422] R.J. Spreitzer, Ann. Rev. Plant Physiol. Plant Mol. Biol. 44 (1993) 411–434.
[423] C.R. Somerville, S.C. Somerville, Mol. Gen. Genet. 193 (1984) 214–219.
[424] S. Knight, I. Andersson, C.I. Branden, J. Mol. Biol. 215 (1990) 113–160.
[425] I. Andersson, J. Mol. Biol. 259 (1996) 160–174.
[426] T.J. Andrews, J. Biol. Chem. 263 (1988) 12213–12219.
[427] G.H. Lorimer, Biochemistry 20 (1981) 1236–1240.
[428] M.E. Salvucci, A.R. Portis, W.L. Ogren, Photosynth. Res. 7 (1985) 193–201.
[429] J. Pierce, G.S. Reddy, Arch. Biochem. Biophys. 245 (1986) 483–493.
[430] M. Dron, M. Rahire, J.D. Rochaix, J. Mol. Biol. 162 (1982) 775–793.
[431] M. Goldschmidt-Clermont, M. Rahire, J. Mol. Biol. 191 (1986) 421–432.
[432] R.J. Spreitzer, D.B. Jordan, W.L. Ogren, FEBS Lett. 148 (1982) 117–121.
[433] R.J. Spreitzer, C.J. Chastain, Curr. Genet. 11 (1987) 611–616.
[434] R.J. Spreitzer, W.L. Ogren, Proc. Natl. Acad. Sci. USA 80 (1983) 6293–6297.
[435] Z.X. Chen, C.J. Chastain, S.R. Al-Abed, R. Chollet, R.J. Spreitzer, Proc. Natl. Acad. Sci. USA 85 (1988) 4696–4699.
[436] S. Hong, R.J. Spreitzer, J. Biol. Chem. 272 (1997) 11114–11117.
[437] Z.X. Chen, R.J. Spreitzer, J. Biol. Chem. 264 (1989) 3051–3053.
[438] Z.X. Chen, W.Z. Yu, J.H. Lee, R. Diao, R.J. Spreitzer, Biochemistry 30 (1991) 8846–8850.
[439] G. Thow, G. Zhu, R.J. Spreitzer, Biochemistry 33 (1994) 5109–5114.
[440] R.J. Spreitzer, G. Thow, G. Zhu, Plant Physiol. 109 (1995) 681–685.
[441] W. Yu, R.J. Spreitzer, Proc. Natl. Acad. Sci. USA 89 (1992) 3904–3907.
[442] G. Zhu, R.J. Spreitzer, J. Biol. Chem. 269 (1994) 3952–3956.
[443] G. Zhu, R.J. Spreitzer, J. Biol. Chem. 271 (1996) 18494–18498.
[444] D.B. Jordan, R. Chollet, J. Biol. Chem. 258 (1983) 13752–13758.
[445] A.R. Portis Jr., Ann. Rev. Plant Physiol. Plant Mol. Biol. 43 (1992) 415–437.
[446] E.M. Larson, C.M. O'Brien, G. Zhu, R.J. Spreitzer, A.R. Portis Jr., J. Biol. Chem. 272 (1997) 17033–17037.
[447] I. Khrebtukova, R.J. Spreitzer, Proc. Natl. Acad. Sci. USA 93 (1996) 13689–13693.
[448] M. Rawat, M. Henk, L. Lavigne, J. Moroney, Planta 198 (1996) 263–270.
[449] G. Lacoste-Royal, S. Gibbs, Plant Physiol. 83 (1987) 602–606.
[450] O.N. Borkhsenious, C.B. Mason, J.V. Moroney, Plant Physiol. 116 (1998) 1585–1591.
[451] P. Bennoun, A. Atteia, Y. Pierre, M. Delosme, Proc. Natl. Acad. Sci. USA 92 (1995) 10202–10206.
[452] P. Boer, L. Bonen, R.W. Lee, M.W. Gray, Proc. Natl. Acad. Sci. USA 82 (1985) 3340–3344.
[453] P. Boer, M.W. Gray, EMBO J. 7 (1988) 3501–3508.
[454] A. Wiseman, N.W. Gillham, J.E. Boynton, J. Cell Biol. 73 (1977) 56–77.
[455] N.J. Alexander, N.W. Gillham, J.E. Boynton, Mol. Gen. Gent. 130 (1974) 275–280.
[456] N.W. Gillham, J.E. Boynton, E.H. Harris, Curr. Genet. 12 (1987) 41–48.
[457] R.F. Matagne, M.R. Michel-Wolwertz, C. Munant, C. Duyckaerts, F.E. Sluse, J. Cell. Biol. 108 (1980) 1221–1226.
[458] M.P. Dorthu, S. Remy, M.R. Michel-Wolwertz, L. Colleaux, D. Breyer, M.C. Beckers, S. Englebert, C. Duyckaerts, F.E. Sluse, R.F. Matagne, Plant Mol. Biol. 18 (1992) 759–772.
[459] P. Bennoun, M. Delosme, U. Kuck, Genetics 127 (1991) 335–343.
[460] P. Bennoun, M. Delosme, I. Godehardt, U. Kuck, Mol. Gen. Genet. 234 (1992) 147–154.
[461] D.W. Husic, N.E. Tolbert, Proc. Natl. Acad. Sci. USA 84 (1987) 1555–1559.
[462] R. Spreitzer, M. Goldschmidt-Clermont, M. Rahire, J. Rochaix, Proc. Natl. Acad. Sci. USA 82 (1985) 5460–5464.
[463] R. Spreitzer, T. Brown, Z. Chen, D. Zhang, S. Al-Abed, Plant Physiol. 86 (1988) 987–989.